Analysis of a Developmental Gene Regulatory Network in the Sea Urchin Embryo During Normal and Regulative Development

Tara Sharma

Submitted in Partial Fulfillment of the Requirements for the Degree of
Doctor of Philosophy

Department of Biological Sciences
Carnegie Mellon University
Pittsburgh, PA

February 21st, 2011

Thesis Advisor: Charles A. Ettensohn, Ph.D.

Acknowledgements

First, I wish to express my deep appreciation to Dr. Chuck Ettensohn, a gifted teacher and a wonderful advisor, for his help, support, encouragement, and lots of good ideas throughout my graduate career. Working with him has truly been a privilege and a joy. I learned so much.

I thank Dr. Brooke McCartney and Dr. Veronica Hinman for their valuable inputs, feedback, and for making sure things were on track, especially in the last year.

I also wish to thank Dr. Deborah Chapman for agreeing to serve as the outside reader for my dissertation.

Special thanks to Ashrifia Gogo and Kiran Rafiq, my fellow graduate students, for their help and friendship.

Thanks also to my other friends in Mellon Institute, especially Nina Senutovitch, Smita Yadav and Debrup Sengupta, for making my time in Mellon Institute a more enjoyable experience.

I especially wish to thank my parents for their unwavering support, and unconditional love all along the way.

And finally, my love and appreciation to Rakshiet Jain — my husband, my friend, and my happiness. None of this could have happened without him.

Table of Contents

Abstract

Every zygote follows a characteristic developmental path resulting in a complex multicellular organism, with specialized cells performing specialized functions. This developmental path is faithfully inherited over generations, suggesting that the regulatory code is hardwired in the genome. A unifying theme in developmental biology is to decipher this genomic code. Pioneering work in the sea urchin embryo has lead to the detailed understanding of the gene regulatory network (GRN) that underlies the specification of the skeletogenic cells, cells that secrete the larval skeleton. The sea urchin embryo is also known for its regulative properties and a remarkable feature of the skeletogenic network is that can be ectopically activated in any cell of the embryo during regulative development. This presents a unique opportunity to study the reconfiguration of developmental networks in different cellular contexts.

The work presented in this thesis refines our understanding regarding the initial deployment of this GRN during normal development. The activation of this network is thought to be regulated by a derepression mechanism, which is mediated by the products of the *pmar1* and *hesC* genes. Here, we show that the activation of the skeletogenic network occurs by a mechanism that is distinct from the transcriptional repression of *hesC*. We provide evidence that unequal cell division in the vegetal blastomeres is tightly linked to the activation of the early regulatory genes. In addition, our analysis of the upstream regulation of the two key transcription factors, *alx1* and *tbr*, reveal that these genes are controlled by a two-phase regulation that can be divided into an activation phase and a maintenance phase.

Furthermore, to dissect the molecular underpinnings of regulative development we have taken advantage of the rich knowledge of the skeletogenic GRN. We have used two experimental paradigms, first, that induces the activation of the skeletogenic GRN in the cells of the non-skeletogenic mesoderm and second, that activates this network in the endodermal cells. Our findings highlight several interesting and significant differences in the initial deployment of this network during regulative development. We provide evidence that, despite these upstream differences the downstream network is faithfully recapitulated. We also show that the NSM subpopulation that activates the skeletogenic

GRN is the prospective blastocoelar cells. Finally, we show that mitotic cell division does not play a role in lineage reprogramming (both NSM and endoderm) in the sea urchin embryo. These and other findings described in the following chapters further illuminate our understanding of development GRNs and the evolution of cell lineages.

List of Figures *Page*

Chapter 1

Introduction

1.1 The sea urchin embryo

The sea urchin embryo has a long history as a model system for developmental studies. Several features make this embryo an attractive model system, including: (1) a simple tissue architecture, (2) a short embryonic phase (in the species *L. variegatus* the embryonic phase is only two days), (3) the ability to obtain large numbers of synchronously developing embryos, facilitating molecular and biochemical analyses, and (4) optical clarity, enabling the visualization of cell movements in the living embryo. In addition, sea urchins occupy an important phylogenetic position. They belong to the group of basal deuterostomes, and are thus more closely related to humans than most other invertebrate model systems **(Fig. 1.1).** Previously, this embryo was used as a model system to study experimental embryology. In recent times, the development of molecular biology techniques, advanced imaging techniques, use of morpholino antisense oligonucleotides for perturbing gene expression, and modern genomics-related technologies has transformed this model system from a purely embryological system to a system that is extensively being used to study questions related to gene regulation.

The urchin species used for developmental studies are indirect-developers; they develop from an embryo to an adult indirectly via a feeding larval stage. The embryo proceeds through a variety of recognizable embryological stages before it forms the pluteus larva **(Fig. 1.2)**. Early cleavage divisions result in the formation of a simple, spherical blastula surrounding the blastocoel. At the late blastula stage, the embryo hatches from the fertilization envelope and swims freely with the help of cilia. The start of gastrulation is marked by the ingression of the first set of mesenchymal cells, the primary mesenchyme cells (PMCs), and this stage is referred to thereafter as the mesenchyme blastula stage. Soon after PMC ingression, the vegetal plate invaginates and gives rise to the archenteron of the embryo. During gastrulation, the archenteron deepens and extends across the entire blastocoel. The archenteron bends toward the ventral surface of the embryo to fuse with the oral ectoderm, creating the opening of the mouth and completing the digestive tract. Post-gastrular development is associated with the growth and branching of the skeleton and the formation of the feeding pluteus larva.

In the sea urchin embryo, zygotic genome activation begins immediately after fertilization, whereas in most other systems, including amphibians (*X. laevis*), insects (*D. melanogaster*), nematodes (*C. elegans*) and fish (*D. rerio*), zygotic transcription is initiated later during development, a period referred to as the maternal-to-zygotic-transition (MZT) or the mid-blastula transition (reviewed by Tadros and Lipshitz, 2009). Early zygotic genome activation divides the sea urchin embryo into distinct transcriptional domains early during development, and each domain contributes to a specific cell/tissue type of the embryo. One cell lineage that has been extensively studied in the sea urchin embryo is the skeletogenic lineage. The initial specification of this mesodermal cell lineage is autonomous, and it is one of the first cell lineages to be set aside during development.

1.2 The skeletogenic mesoderm

The founder cells of the skeletogenic lineage arise as a result of two unequal cleavage divisions (4^{th} and 5^{th}) at the vegetal end of the embryo. These unequal cell divisions occur as a consequence of an interaction between the mitotic spindle and the vegetal cortex of the four vegetal blastomeres of the 8-cell stage embryo, causing the displacement of the mitotic spindle towards the vegetal pole (Dan and Tanaka, 1990). The 4^{th} unequal cleavage division generates; four small cells called the micromeres and four large cells called the macromeres. The macromeres give rise to a heterogeneous population of cells, collectively referred to as the non-skeletogenic mesoderm (see below) and the endoderm. The micromeres divide more slowly than the rest of the embryo, and at the 5^{th} cleavage division, once again divide unequally, and give rise to four small and four large cells - the small micromeres and large micromeres, respectively. The small micromeres are quiescent cells and contribute to the coelomic sacs of the larvae (Pehrson and Cohen, 1986). Recently, it has been shown that adults developing from small micromere deleted embryos form small gonads that lack gametes (Yajima and Wessel, 2011). The large micromeres are the precursors of the skeletogenic cells. These cells undergo 2-3 more rounds of cell division, and occupy the central region of the vegetal plate surrounding the small micromeres (Ruffins and Ettensohn, 1996). At the onset of

gastrulation, the large micromeres lose their epithelial character, and begin to ingress into the blastocoel as mesenchymal cells, a process referred to as epithelial-to-mesenchymal transition (EMT). After ingression, these cells are referred to as primary mesenchyme cells (PMCs). Once inside the blastocoel, PMCs migrate to specific target sites by means of filopodia, and arrange themselves in a characteristic ring-like pattern around the invaginating archenteron. The PMCs then fuse to form an extensive syncytium, and eventually secrete the larval endoskeleton, which is primarily composed of $CaCO_3$, small amounts of $MgCO_3$ and associated spicule matrix proteins (Okazaki, 1975; Benson et. al, 1986).

In the past, several lines of evidence based on embryonic manipulations demonstrated that the migration and patterning of the PMCs is dependent upon extrinsic, directional cues that are ectodermal in origin, however the molecular nature of these cues was unknown (Gustafson and Wolpert, 1961; Ettensohn and McClay 1986). More recently, it has been shown that VEGF/VEGFR and FGF/FGFR signaling between the PMCs and the ectoderm is critical for the correct migration and differentiation of the PMCs (Duloquin et. al., 2007, Rottinger et. al., 2008).

The large micromeres also act as signaling centers in the embryo. They are required for inducing the overlying cells to produce vegetal structures, which include the NSM and the endoderm. The inductive property of the micromeres was first identified by transplanting micromere to ectopic locations in the embryo, which leads to the development of a secondary archenteron (Horstadius, 1939; Ransick and Davidson, 1993).

In evolutionary terms, the micromeres/early ingressing PMCs are considered to be a recent invention. The ancestral echinoderm embryo lacked micromeres and an embryonic skeleton, but had an adult skeleton. The immediate ancestor of the euechinoids (modern sea urchins) is believed to be a primitive cidaroid sea urchin. The living cidaroids, which are believed to closely resemble the ancestors of modern sea urchins, have variable numbers of micromeres and lack early ingressing PMCs. The skeleton in these embryos forms from a group of late ingressing mesenchyme cells, however, it is unclear whether the late ingressing skeletogenic cells are derived from the micromeres or from the macromeres. Therefore, the evolution of the micromeres and the

early ingressing PMCs, is considered a result of two heterochronic shifts. The first shift, moved the adult skeletogenic program into the late embryo, and created a population of late ingressing skeletogenic cells, whereas the second shift further moved the skeletogenic program to the early cleavage stages. These shifts, coupled with unequal cell divisions, gave rise to large micromeres and an early ingressing skeletogenic mesenchyme (Schroeder, 1981; reviewed by Ettensohn, 2009).

1.3 The non-skeletogenic mesoderm

The NSM is derived from the macromere descendents (the four large cells produced after the first unequal cell division, see above). The NSM encircle the large micromere descendents in the vegetal plate, and during gastrulation gives rise to at least four different cell populations; pigment cells, blastocoelar cells, muscle cells and cells of the coelomic pouches (Ruffins and Ettensohn, 1996). The pigment cells ingress relatively early in gastrulation (Gustafson and Wolpert, 1967; Gibson and Burke, 1985), and migrate into the aboral ectoderm. During the late gastrula stage the pigment cells produce the pigment, called the echinochrome. Studies have suggested that pigment cells play a role in immuno-defense and photoreception (Service and Wardlaw, 1984; Weber and Dambach, 1974). Blastocoelar cells are the second principle NSM population, which ingress later during gastrulation, and form a network of fibroblast-like cells in the blastocoel (Cameron et al., 1991, Tamboline and Burke, 1992). The other two NSM cell populations; the cells of the coelomic pouches and the circumesophageal muscle cells arise at the completion of gastrulation.

The initial specification of the NSM takes place at the late blastula stage, between the 8^{th} and 10^{th} cleavage division, and is dependent on Delta signaling from the large micromeres (Sherwood and McClay, 1999; Sweet et al., 2002). In addition, Nodal and BMP2/4 signaling, that functions in the ventral and dorsal ectoderm respectively, are required for patterning the blastocoelar and pigment cells in the vegetal plate (Duboc et al., 2010).

1.4 Gene regulatory networks

Gene regulatory networks provide a system level explanation of how developmental functions are encoded in the genome. These networks illustrate functional interactions among regulatory genes and signaling components that are required for cell specific gene expression patterns. GRNs are primarily constructed using perturbation and *cis*-regulatory analysis. One of the first such network to be determined is the skeletogenic GRN of the sea urchin embryo **(Fig. 1.3)**. This is currently the most nearly complete GRN (reviewed by, Oliveri and Davidson, 2004, Ettensohn, 2009). More recently, developmental GRNs have also emerged in several other model systems, like the GRNs underlying mesoderm specification in *X. laevis* (reviewed by Koide et al., 2005), zebrafish (Morley et al., 2009), dorsoventral patterning in *D. melanogaster* (reviewed by Stathopoulos and Levine, 2005), and gut and mesoderm specification in *C. elegans* (reviewed by Maduro, 2009).

Comparative analysis between emerging GRNs, reveal a common basic design shared by all developmental networks - initial spatial inputs establish a regulatory state by activating cell specific transcription factors, this regulatory state is then locked down, other regulatory states are excluded, and later downstream differentiation genes are activated. Furthermore, comparative studies also highlight certain differences. For example, in the *Xenopus* and sea urchin embryo, cell signaling is important from the earliest stages to establish differential gene expression patterns, but, in the *Drosophila* embryo, gene expression patterns are established independent of signaling pathways, as the early embryo is a syncytium lacking cell boundaries. Therefore, in the future, as deeper understanding of GRNs underlying the development of phylogenetically related and diverse animal forms become available, widespread evolutionary comparisons can be made to understand the evolution of development.

1.5 The large micromere/PMC GRN

The earliest input that activates the large micromere GRN is dependent on the selective stabilization of the maternally present β-catenin in the nuclei of micromeres at

the 16-cell stage (Wikramanayake et al., 1998; Logan et al., 1999). A direct target of β-catenin is the transcriptional repressor *pmar1* (*paired-class micromere anti-repressor*). *Pmar1* is expressed in the micromeres beginning at the 16-cell stage, and later is expressed in both the large and small micromeres, until the late cleavage stage (Kitamura et al., 2002; Oliveri et al., 2002). Pmar1 is believed to act by repressing a ubiquitously-expressed second repressor, which has recently been identified as *hesC*, a member of the HES (Hairy-Enhancer-of-Split) family (Revilla-i-Domingo et al., 2007). Thus, the repression of *hesC* by Pmar1 activates the first set of regulatory genes; *alx1* (Ettensohn et al., 2003), *ets1* (Kurokawa et al., 1999), and *tbrain* (Fuchikami et al., 2002; Oliveri et al., 2002). These regulatory genes extend the network by making various downstream connections.

In *L. variegatus*, the expression of *alx1* in the large micromeres is detected at the 128-cell stage (early cleavage). Perturbing alx1 function, using a morpholino antisense oligonucleotide, blocks PMC ingression and the embryo fails to form the larval skeleton (Ettensohn et al., 2003). Several genes in the PMC GRN have been identified whose expression is dependent upon *alx1*, including; the transcription factors *dri*, *foxB*, *tgif*, *snail*, and the TGF-β signaling receptors *vegfr-Ig-10* and *fgfr2*. *Dri* has been shown to be required for the process of skeletogenesis (Amore et al., 2003), *snail* for PMC ingression (Wu and McClay, 2007), and the signaling receptors *vegfr-Ig-10* and *fgfr2* for the correct migration and differentiation of the PMCs (Duloquin et al., 2007; Rottinger et al., 2008).

The transcripts of the two other early regulatory genes, *ets1* and *tbr, are* maternally provided and their zygotic activation is detected during the late cleavage stages (Fuchikami et al., 2002; Oliveri et al., 2002; Kurokawa et al., 1999). *Tbr* function is required for skeletogenesis, whereas *ets1* function, like *alx1*, is required for both PMC ingression and skeletogenesis. The Ets1 protein contains a consensus MAP-kinase phosphorylation site (PPTP). Overexpression studies using a constitutively active (T107D) or a kinase-dead (T107A) form of Ets1, confirmed that Ets1 is a direct target of MAP-kinase signaling (Rottinger et al., 2004). MAPK signaling is activated in the PMCs prior to ingression, and blocking MAPK signaling using the MEK inhibitor U0126, like Ets1, blocks PMC ingression and skeletogenesis.

In addition to the early regulatory genes, the double negative gate mediated by

Pmar1 also activates the transcription of the signaling gene *delta* in the large macromeres. Delta/Notch signaling is required for the segregation of the endomesoderm into definitive endoderm and mesoderm (Croce and McClay, 2010). Ectopic activation of Delta/Notch signaling leads to an increase in the number of NSM cells, at the expense of the endoderm cells, while the loss of Delta/Notch signaling results in a reciprocal phenotype (Croce and McClay, 2010; Sherwood and McClay, 1999; Sweet et al., 2002). More recently, Nodal and BMP2/4 signaling has also been shown to have a role in patterning gene expression in the PMCs along the dorsal/ventral axis (Duboc et al., 2010).

The sequential activation of transcription factors culminates in the activation of genes that regulate morphogenetic cell biological functions as well as differentiation genes. The differentiation genes are usually cell type specific. In the PMC GRN, genes like *p16* (Cheers and Ettensohn, 2005), *p58-a*, *p58-b* (Adomako-Ankomah and Ettensohn, 2011), and members of the MSP130 protein family are exclusively expressed in the PMCs, and are required for secreting the skeleton. In contrast to the differentiation genes, some genes expressed in the PMC GRN are also shared by other GRNs in the embryo. For example, genes like *ets1*, *erg*, *snail* and *twist*, that directly or indirectly regulate morphogenetic cell biological functions in the PMCs, are also expressed in cells of the NSM, however, the expression of these genes in the NSM is under the control of a different GRN.

1.6 Developmental Plasticity

A growing body of literature demonstrates that the identity of a cell can be fully reversed. Examples of developmental plasticity have been documented in almost all metazoan embryos that are being used for developmental studies. Furthermore, this phenomena is not only restricted to embryonic cells, but is also frequently observed in terminally differentiated, adult somatic cells (Zhou et al., 2008; Takahashi and Yamanaka, 2006). Most studies aimed at understanding the molecular mechanisms underlying the phenomenon of developmental plasticity, in both embryonic and adult cells, make use of an experimentally-elicited reprogramming response. For example, in adult newts removal of the lens of the eye causes the cells of the dorsal iris to proliferate,

undergo depigmentation and eventually redifferentiate to form a new lens (Tsonis et al., 2004; Yamada and McDevitt, 1984; Wolff, 1985), In *D. melanogaster*, cells of the leg imaginal disc transdetermine to wing cells either by disc fragmentation experiments or by the ectopic expression of *wingless* (Hadorn, 1968; Maves and Schubiger, 1995). In recent years, several examples of cell fate conversions have been documented that occur during normal development or under certain pathological conditions. The best evidence that differentiated cells can change fate during normal development comes from studies on the origin of fetal haematopoietic cells, where a few functionally differentiated embryonic endothelium cells transdifferentiate into erythroid and monocytic cells (Eilken et al., 2009). Therefore, it is highly likely that lineage reprogramming induced experimentally may mimic the molecular mechanisms that leads to cell fate respecification during normal and disease state, unifying the fields of experimental and developmental biology. In addition, a better understanding of the mechanisms that govern lineage reprogramming is an important part of future regenerative medicine, the goal of which is to produce new cells to repair or replace diseased or damaged tissue.

The sea urchin embryo, like other metazoan embryos, exhibits remarkable regulative abilities. Studies related to developmental plasticity in the sea urchin embryo have focused on the respecification of embryonic cells to a skeletogenic fate, in response to certain molecular or surgical manipulations, a process referred to as transfating. For example, during early embryogenesis, the removal of micromeres at the 16-cell stage induces macromere-derived cells to a skeletogenic fate (Horstadius, 1939), or the treatment of animal blastomeres with LiCl redirects the animal blastomeres to a skeletogenic fate (Livingston and Wilt, 1989; Minokawa et al., 1997).

Remarkably, the cells of the NSM and the endoderm retain their regulative property even during gastrulation, when distinct GRNs have already been established in these cell lineages. The microsurgical removal of the PMCs at the mesenchyme blastula stage causes the transformation of a subpopulation of NSM cells to a skeletogenic fate (Ettensohn and McClay, 1988; Ettensohn, 1990) **(Fig. 1.4)**. In addition, a study by Logan and McClay showed that the surgical removal of both the PMCs and the NSM causes the endodermal cells to become skeletogenic at the late gastrula stage (McClay and Logan, 1996) **(Fig. 1.5)**. A careful examination of these surgically manipulated embryos shows

that these embryos give rise to a correctly patterned skeleton.

These studies indicate, that transfating cells undergo extensive epigenetic modifications that lead to the activation of the skeletogenic GRN and the complete erasure of the preexisting GRN. It has been shown that transfated skeletogenic cells activate downstream differentiation genes, namely, *p16*, which is required for skeletal rod elongation; *p58-a*, which is required for biomineralization; and several genes of the *msp130* family. (Ettensohn et al., 2007). In addition, the early regulatory gene *alx1* is activated early during the transfating response, however, unlike normal development, its activation is independent of Pmar1 (Ettensohn et al., 2007).

The work described in following chapters aims at developing a better understanding of the GRN underlying the specification of the skeletogenic cells during normal development. In addition, we take advantage of our findings uncovered in this study, along with the preexisting information about the network, to understand how the skeletogenic GRN reconfigures itself during lineage reprogramming.

As mentioned above, the initial deployment of the skeletogenic GRN is believed to occur by a transcriptional derepression mechanism mediated by the two repressors *pmar1* and *hesC*. Using quantitative fluorescent whole mount in situ hybridization (FWMISH) we show that the early regulatory genes (*alx1* and *delta*) are activated prior to the transcriptional repression of *hesC*. This finding indicates the presence of additional repressors other than *hesC* that are responsible for activating this network. In addition, we show that the expression of early regulatory genes (*alx1* and *tbr*) is controlled by a two-phase regulation that can be divided into an activation phase and a maintenance phase. We find that the activation phase is tightly linked to unequal cleavage division that occurs in the vegetal blastomeres, as experimentally altering unequal cell division prevents the activation of the early genes. The maintenance phase is regulated by MAPK signaling and the transcription factor Ets1.

The work described in chapter 3 takes advantage of the preexisting knowledge of the skeletogenic GRN, and the findings uncovered in this study to understand the mechanisms that establish this network in the transfating cells. We use two experimental paradigms, one that induces transfating in cells within the same germ layer (NSM transfating) and second, that induces transfating across germ layers (endoderm

transfating). We demonstrate that MAPK signaling is essential for activating the PMC GRN during both NSM and endoderm transfating, in contrast to its role during normal development. Our findings reveal several other differences in the upstream circuitry of the skeletogenic GRN during normal and regulative development that are described in detail in chapter 3. Despite these changes in the upstream circuitry of the network, later regulatory layers and key morphoregulatory genes are deployed in a fashion that recapitulates the normal deployment of the network. We demonstrate that this network is activated by presumptive blastocoelar cells, and not by presumptive pigment cells, as was previously proposed. Finally, we show that mitotic cell division is not required for lineage re-programming in the sea urchin embryo.

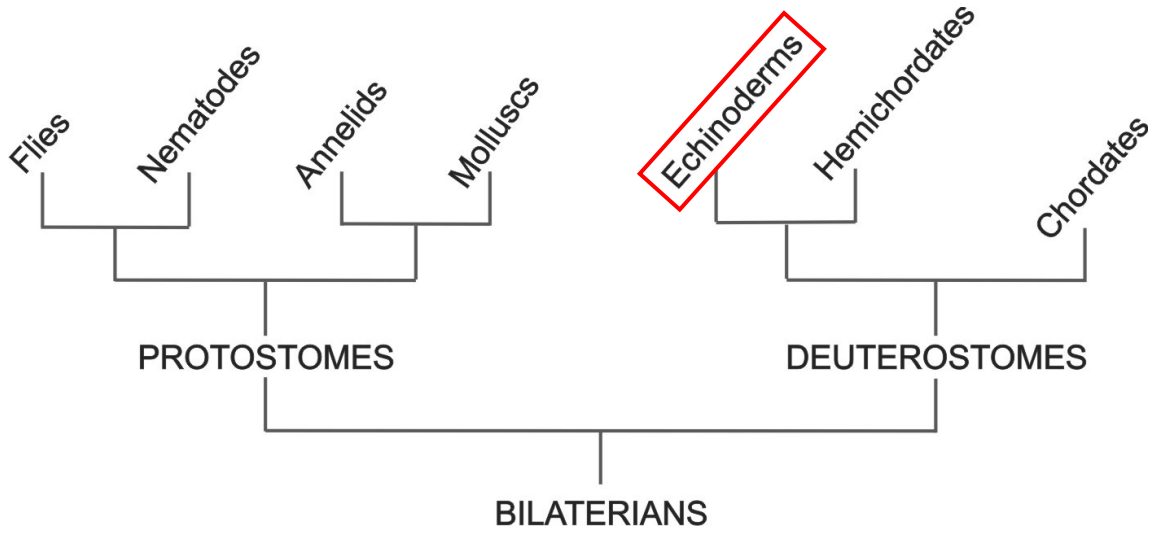

Fig 1.1. Phylogenetic tree. The sea urchins are basal deuterostomes that belong to the phylum Echinodermata.

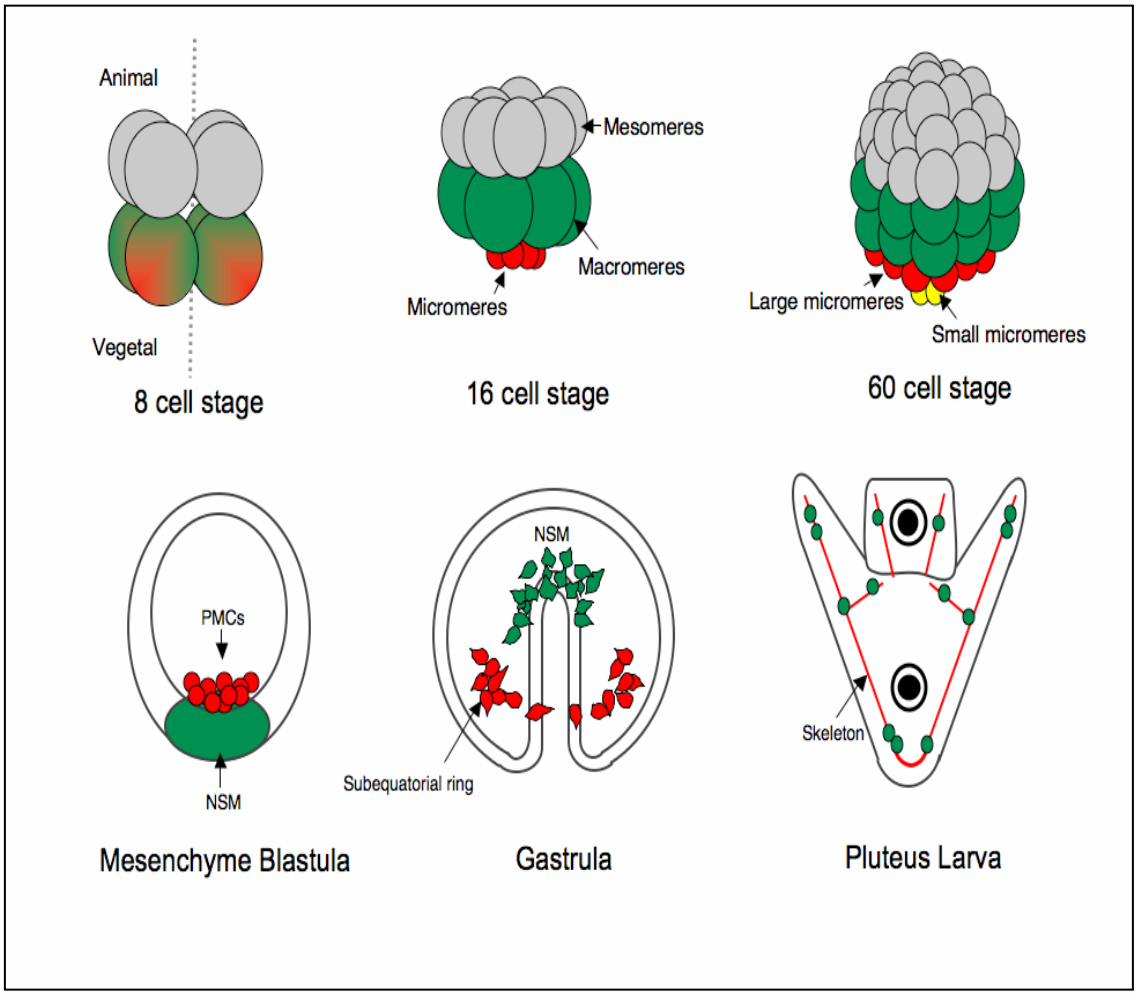

Fig. 1.2. Stages of sea urchin embryonic development.

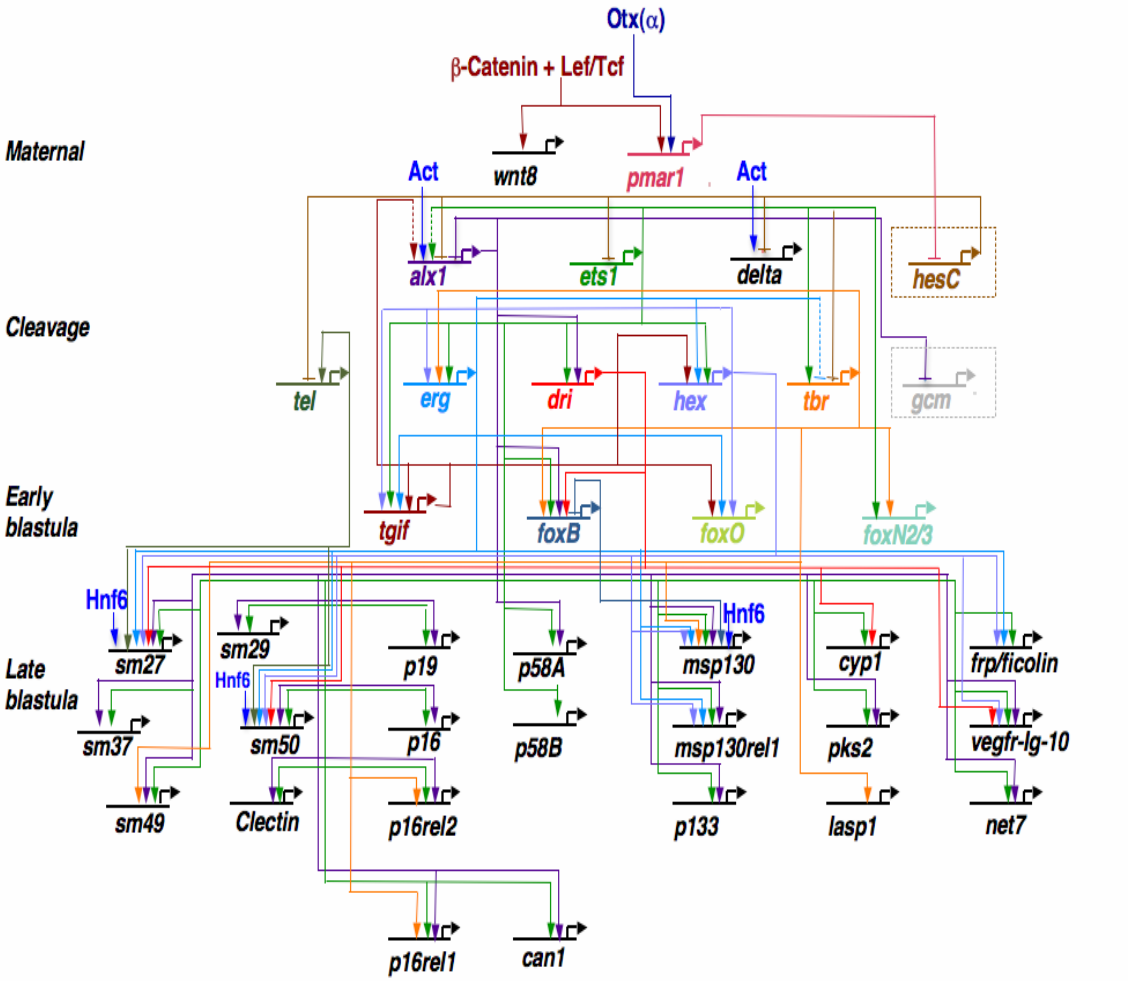

Fig. 1.3. The micromere-PMC GRN.

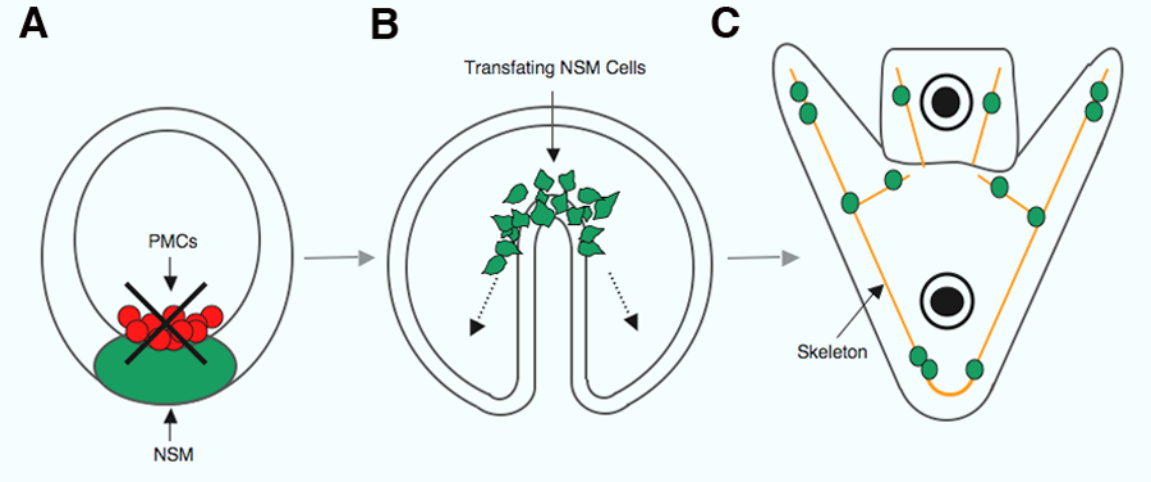

Fig. 1.4. PMC depletion induces the cells of the NSM to adopt a skeletogenic fate. Surgical removal of PMCs at the mesenchyme blastula stage (A) induces a subpopulation of NSM cells to activate the skeletogenic GRN. These cells migrate away from the tip of the archenteron at the late gastrula stage (B) and later secrete a normally patterned skeleton (C). Dotted arrows indicate the migration of transfated NSM cells to PMC-specific target sites.

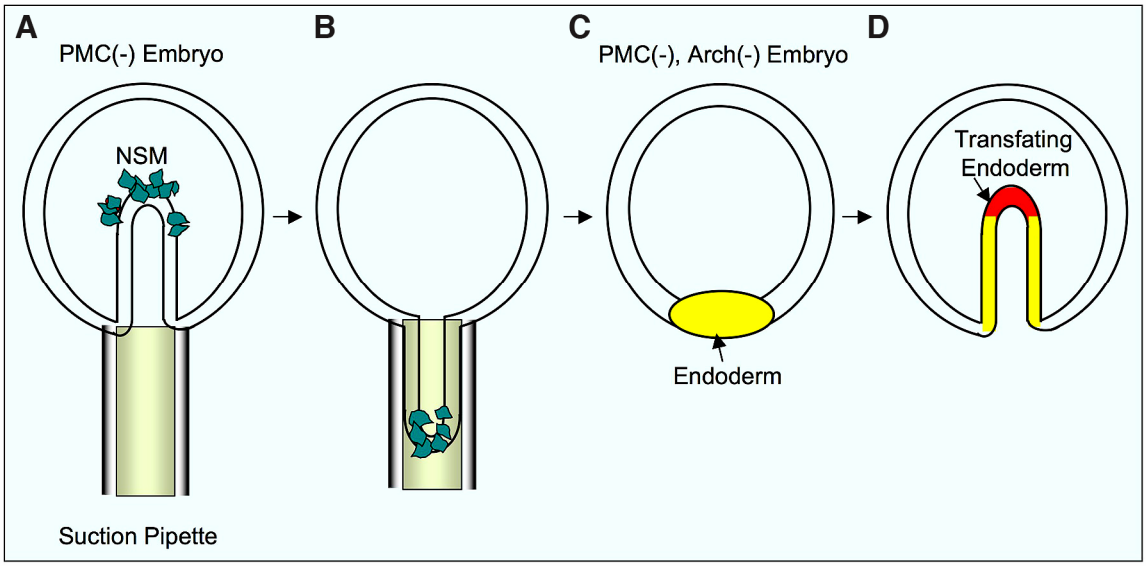

Fig. 1.5. Depletion of both the PMCs and the NSM induces the endoderm cells to adopt a skeletogenic fate. Surgical removal of the regenerating (B) archenteron from a PMC(-) embryo (A), induces the endodermal cells to activate the skeletogenic GRN (D).

Chapter 2

Activation of the Skeletogenic Gene Regulatory Network in the Early Sea Urchin Embryo

2.1 Abstract

The gene regulatory network (GRN) that underlies the development of the embryonic skeleton in sea urchins is an important model for understanding the architecture and evolution of developmental GRNs. The initial deployment of the network is thought to be regulated by a de-repression mechanism, which is mediated by the products of the *pmar1* and *hesC* genes. Here, we show that the activation of the skeletogenic network occurs by a mechanism that is distinct from the transcriptional repression of *hesC.* By means of quantitative, fluorescent whole mount *in situ* hybridization, we find that two pivotal, early genes in the network, *alx1* and *delta*, are activated in prospective skeletogenic cells prior to the down-regulation of *hesC* expression. An analysis of the upstream regulation of *alx1* shows that this gene is regulated by MAPK signaling and by the transcription factor Ets1; however, these inputs influence only the maintenance of *alx1* expression and not its activation, which occurs by a distinct mechanism. By altering normal cleavage patterns, we show that the zygotic activation of *alx1* and *delta*, but not that of *pmar1*, is dependent upon the unequal division of vegetal blastomeres. Based on these findings, we conclude that the widely-accepted double-repression model is insufficient to account for the localized activation of the skeletogenic GRN. We postulate the existence of additional, unidentified repressors that are controlled by *pmar1*, and propose that the ability of *pmar1* to de-repress *alx1* and *delta* is regulated by the unequal division of vegetal blastomeres.

2.2 Introduction

A prominent feature of the embryogenesis of indirectly developing sea urchins is the formation of an elaborate, calcified endoskeleton. Recent studies have revealed a gene regulatory network (GRN) that controls the development of the skeletogenic large micromere-primary mesenchyme cell (PMC) lineage (reviewed by Oliveri et al., 2008; Ettensohn, 2009). The PMC gene network is currently one of the most complete developmental GRNs, and is being used to elucidate GRN architecture, the evolution of developmental programs, and developmental plasticity. For example, recent studies suggest that the evolution of skeletal development in echinoderms involved the co-option by the embryo of an ancestral, adult skeletogenic GRN via the invention of new regulatory connections (Gao and Davidson, 2008; Erwin and Davidson, 2009; Ettensohn, 2009). The regulative deployment of the PMC GRN in non-micromere lineages during gastrulation is a striking example of developmental plasticity, and has been shown to involve novel upstream inputs (Ettensohn et al., 2007). Such studies have focused attention on the molecular mechanisms that activate the skeletogenic GRN, and highlight the need to clarify the initial regulatory inputs into this network.

The activation of the PMC GRN in the large micromere territory is dependent upon the stabilization of β-catenin. One important target of β-catenin is the transcriptional repressor *pmar1,* which is transiently expressed in the micromere lineage beginning at the 16-cell stage (Kitamura et al., 2002; Oliveri et al., 2002). Ectopic expression of Pmar1 causes most cells of the embryo to adopt a PMC-like fate (Oliveri et al., 2002; Oliveri et al., 2008). Because Pmar1 is a transcriptional repressor, it presumably activates the skeletogenic GRN indirectly, by blocking the expression of a second repressor. This second repressor is believed to be HesC, a member of the HES (hairy-enhancer-of-split) family (Revilla-i-Domingo et al., 2007). *HesC* transcripts are ubiquitous in the early embryo, but disappear from the vegetal region (including the presumptive PMCs) at the early blastula stage (Revilla-i-Domingo et al., 2007; Smith and Davidson, 2008). Overexpression of Pmar1 results in a decrease in the level of *hesC* transcripts, while morpholino (MO) knockdown of HesC leads to the ectopic expression of *delta* throughout the embryo and to an increase in the levels of *alx1*, *ets1*, and *tbr*

mRNAs (Revilla-i-Domingo et al., 2007). These findings support the model that the skeletogenic GRN is activated by a Pmar1/HesC double-repression "gate", a model that has been widely accepted (Davidson and Levine, 2008; Oliveri et al., 2008; Ettensohn, 2009).

Alx1 is one of the earliest regulatory genes to be activated specifically in the large micromere lineage, and this gene plays a pivotal role in PMC specification (Ettensohn et al., 2003). Delta is a signaling molecule that mediates an interaction between the large micromere progeny and adjacent, non-skeletogenic mesoderm (NSM) cells (Sweet et al., 2002). The cis-regulatory control of *delta* has been analyzed in considerable detail (Revilla-i-Domingo et al., 2004; Smith and Davidson, 2008). In contrast, little is known concerning the regulation of the *alx1* gene, other than a proposed input from the *pmar1/hesC* double-repression system. A positive regulatory input from *ets1* has been demonstrated by MO knockdown experiments and QPCR studies (Oliveri et al., 2008). Perturbation of Ets1 function by MO knockdown or by overexpression of a dominant negative form of the protein blocks PMC ingression and skeletogenesis, whereas overexpression of Ets1 transforms most cells of the embryo to a mesenchymal fate (Kurokawa et al., 1999; Rottinger et al., 2004; Oliveri et al., 2008). Rottinger et al. (2004) provided evidence that the phosphorylation of Ets1 by MAP kinase is essential for its function and showed that inhibition of MAP kinase signaling down-regulates the expression of *alx1*. Together, these findings suggest that the MAP kinase pathway up-regulates *alx1* expression via the phosphorylation of Ets1.

The micromeres arise as a consequence of an unequal cell division at the vegetal pole. This stereotypical pattern of cleavage plays an important role in PMC specification. The unequal fourth cleavage division is a consequence of the displacement of the nuclei and mitotic spindles of the four vegetal blastomeres of the 8-cell stage embryo toward the vegetal pole (Dan and Tanaka, 1990). These cytological changes may be dependent upon a specialized microtubule attachment site in the vegetal cortex. Pharmacological agents have been used to inhibit the displacement of the mitotic spindles toward the vegetal pole, thereby equalizing cleavage and producing micromere-less embryos (Tanaka, 1976; Dan, 1979; Tanaka, 1979; Langelan and Whiteley, 1985). Micromere-less embryos show a striking reduction in the development of the skeleton. These studies preceded the recent

elucidation of the skeletogenic GRN, and no linkage between unequal cleavage and specific steps in the molecular specification of PMCs has been established.

Here, we focus on the initial deployment of the large micromere-PMC GRN. Our findings lead to a significant revision of the current model of the activation of this GRN. We show that the lineage-specific expression of at least two early genes in the network, *alx1* and *delta*, occurs by a mechanism that is distinct from the transcriptional repression of *hesC*. We confirm that *alx1* is regulated by MAPK signaling and by the transcription factor Ets1, but show that these inputs influence only the maintenance of *alx1* expression, and not its activation, which occurs by a distinct mechanism. By experimentally altering normal cell division patterns, we show that the initial expression of *alx1* and *delta* is linked tightly to the unequal cleavage of vegetal blastomeres. Surprisingly, the activation of *pmar1* is not dependent upon unequal cleavage.

2.3 Materials and Methods

Animals

Adult *Lytechinus variegatus* were obtained from the Duke University Marine Laboratory (Beaufort, NC, USA) and from Reeftopia Inc. (Key West, FL, USA). Adult *Strongylocentrotus purpuratus* were obtained from Patrick Leahy (California Institute of Technology). Embryos were cultured at 23°C (*L. variegatus*) or 15.5°C (*S. purpuratus*) in temperature-controlled incubators.

Constructs and mRNA injections

Capped mRNAs were synthesized using the SP6 mMessage mMachine RNA transcription kit (Ambion) and were microinjected into fertilized eggs as described by Cheers and Ettensohn (2004). A C-terminal, GFP-tagged form of Pmar1 (coding region only) was cloned into the BamHI and XbaI sites of the pCS2+ vector.

Equalization of cleavage

The 4^{th} and 5^{th} cleavage divisions were equalized by treating *L. variegatus* embryos for 1 hour with sodium dodecyl sulfate (SDS) at a concentration of 30 μg/ml, beginning at the 4-cell stage (Langelan and Whiteley, 1985). The embryos were then transferred to ASW (without SDS) and were allowed to continue development.

Polymerase chain reaction (PCR)

Total RNA was isolated using the Nucleospin RNA II kit (Clontech). cDNA synthesis was carried out using the RETROscript kit (Ambion) and HiFi Taq polymerase (Invitrogen). Quantitative PCR (QPCR) was performed using an ABI 7300 real-time PCR system and SYBR-Green/ROX master mix (Bio-Rad). PCR primers are shown in **Table 2.1**.

Whole-mount in-situ hybridization (WMISH)

Conventional WMISH was carried out as described previously (Ettensohn et al., 2007). For single-color, fluorescent WMISH (F-WMISH), embryos were incubated in a

blocking buffer that consisted of 5% lamb serum in phosphate buffered saline containing 0.1% Tween-20 (PBST) for 30 minutes at room temperature (RT), followed by incubation in a 1:1500 dilution of horseradish peroxidase (HRP)-conjugated anti-digoxigenin antibody (Roche) in blocking buffer for 30 minutes at RT. The embryos were then incubated in a 1:100 dilution of FITC-Tyramide Signal Amplification solution (Fluorescein-TSA Plus Fluorescence System, PerkinElmer) in the diluting buffer provided with the kit for 4 minutes at RT. The embryos were counterstained with Hoechst 33342 (0.5 mg/ml) in PBST for 5 minutes, followed by several washes with PBST. For two-color F-WMISH, embryos were incubated overnight with a mixture of a (DIG)-11-UTP-labeled probe and a fluorescein-labeled probe. After incubating the embryos in blocking buffer as described above, the embryos were incubated in a 1:750 dilution of HRP-conjugated anti-fluorescein antibody in PBST for 2 hours, followed by a 4 minute incubation (RT) with a 1:100 dilution of Cy3-TSA in diluting buffer provided with the kit (Cy3-TSA Plus Fluorescence System, PerkinElmer). Peroxidase activity was quenched by incubating the embryos in 5% (vol/vol) H_2O_2 in PBS-T for 30 minutes. The transcripts for the second gene were then detected using the HRP-conjugated anti-digoxigenin antibody and the fluorescein-TSA Plus Fluorescence System, as described above.

Microscopy and quantitative image analysis

Embryos labeled by F-WMISH were examined using a Zeiss LSM 510 metal/UV DuoScan spectral confocal microscope and a 40X oil immersion lens. Embryos that had been double-labeled with *hesC* and *alx1* probes were used to measure the levels of *hesC* mRNA in the large micromere territory and in the remainder of the embryo. ImageJ was used to generate two-dimensional projections of small stacks (3-5 images with a 1 mm spacing) of confocal sections that approximately bisected the region of *alx1* expression (the large micromere territory). For each projection, we used ImageJ to calculate the average pixel intensity of *hesC* signal in a) the cells that also expressed *alx1* and b) the remainder of the embryo. These two values were obtained from a total of 6-12 confocal image stacks, each of which was collected from a different embryo. We then calculated the mean and standard deviations of the values for the two regions and compared them

using a paired, two-sided t-test. In control experiments using single probes, we confirmed that there was no detectable spill-over between the *alx1* and *hesC* channels. In addition, controls processed in the absence of probe indicated that there was no detectable background signal in either channel. In all experiments, pixel intensities were below saturation.

2.4 Results

2.4.1 The activation of *alx1* and *delta* precedes the clearing of *hesC* transcripts from the large micromere territory

Several early genes in the skeletogenic GRN, including *alx1*, *tbr*, *delta*, and *ets*, are thought to be activated via the transcriptional repression of *hesC* (Oliveri et al., 2008). *Tbr* and *ets* mRNAs are abundant maternally and are ubiquitous in the early embryo, making it difficult to pinpoint the time at which these genes are first activated in the large micromere territory. *Alx1* and *delta*, in contrast, are expressed only zygotically. We reported previously that *Spalx1* mRNA accumulates in the four large micromeres in the first cell cycle after these cells are born (Ettensohn et al., 2003). This early onset of expression suggested to us that the activation of *alx1* transcription might precede the loss of *hesC* mRNA from vegetal blastomeres.

To compare directly the dynamic patterns of *Spalx1* and *SphesC* expression in the same embryo, we used two-color F-WMISH. The domain of *Spalx1* expression served as an unambiguous marker of the large micromere territory. Quantification of the F-WMISH signals confirmed that when *Spalx1* mRNA was first detectable at the 56-cell stage (8 hours post-fertilization, or hpf), the level of *SphesC* mRNA in the large micromere territory was equivalent to that in the other cells of the embryo **(Fig. 2.1.A,A',F).** At the mid-blastula stage (10-12 hpf), *SphesC* transcripts were down-regulated in the central region of the vegetal plate; i.e., in a region that contained the large micromere, as shown by a decrease in the average pixel intensity of the F-WMISH signal **(Fig. 2.1.B,B',F)**.

To determine whether this temporal pattern of gene expression was shared by other sea urchin species, we carried out a similar analysis using *L. variegatus* embryos. *LvhesC* was cloned using degenerate RT-PCR and RACE (random amplification of cDNA ends). A comparison between *SphesC* and *LvhesC* revealed that the two genes were ~80% identical at the nucleotide level **(Fig. 2.2)** and showed that they encoded proteins with ~85% amino acid identity **(Fig. 2.3)**. Phylogenetic analysis using ClustalW and the software "Phylogenetic Analysis Using Parsimony" (PAUP) demonstrated that *LvhesC*

and *SphesC* are orthologous genes **(Fig. 2.4)**. We examined the developmental expression of *LvhesC* by WMISH and found that the pattern was very similar to that of *SphesC* **(Fig. 2.5)**.

F-WMISH confirmed that *Lvalx1* was activated specifically in the eight daughter cells of the large micromeres, beginning at ~5 hpf (7^{th} cleavage), as reported previously (Ettensohn et al., 2003). Quantitative, two-color F-WMISH showed that, at this stage, the level of *LvhesC* mRNA in the large micromere progeny was equivalent to that in the remainder of the embryo **(Fig. 1.1.C,C',F)**. At the hatched blastula stage (8 hpf), *LvhesC* transcripts were down-regulated in the central region of the vegetal plate **(Fig. 2.1.D,D',F)**. *LvhesC* expression also declined in the apical plate region, as has been described in *S. purpuratus* (Smith and Davidson, 2008). These studies confirmed that in *L. variegatus*, as in *S. purpuratus, alx1* was activated selectively in the large micromere progeny prior to the clearing of *hesC* transcripts from these cells.

In *L. variegatus*, expression of *delta* in the large micromere territory begins ~ 5 hpf (Sweet et al., 2002). We carried out two-color F-WMISH analysis of *L. variegatus* embryos labeled with *Lvdelta* and *LvhesC* probes, and found that expression of *LvDelta* in the large micromere territory also preceded the clearing of *LvhesC* transcripts from the vegetal region **(Fig 2.1.E,E')**. Although we did not carry out equivalent, double-label F-WMISH studies of *delta* and *hesC* expression in *S. purpuratus,* it has already been reported that *Spdelta* is first transcribed at the late 5^{th} cleavage stage (8 hr – 8 hr 40 min after fertilization) (Smith and Davidson, 2008). This is the same cleavage division at which we first detect *Spalx1* expression in the large micromeres, and 2-3 hr before *SphesC* mRNA clears from the micromere territory **(Fig. 2.1.A,A',F)**. Therefore, these studies indicate that at least two early genes in the skeletogenic GRN, *alx1* and *delta*, are activated in the large micromeres prior to any measurable decline in *hesC* transcript levels.

In *S. purpuratus*, *hesC* transcripts are present maternally at relatively low levels (~500 transcripts/egg) and increase sharply in abundance beginning at about the 56-cell stage, indicating that zygotic transcription of the gene is taking place by this stage (Revilla-i-Domingo et al., 2007). We used QPCR to compare directly the temporal patterns of *hesC*, *alx1,* and *delta* expression in both *S. purpuratus* and *L. variegatus* **(Fig. 2.1G,H)**. Activation of *alx1* and *hesC* transcription occurred at approximately the same

time in both species, while *delta* lagged slightly behind. Significantly, at the same developmental stages that were used for our quantitative F-WMISH analysis of *hesC* expression prior to vegetal clearing (i.e., at 8 hpf in *S.purpuratus* and 5 hpf in *L. variegatus*), *hesC* transcript levels were more than 10-fold higher than maternal levels. Therefore, these QPCR studies showed that, in both species, *hesC* transcripts that were visualized by F-WMISH at the developmental stages shown in **Fig. 2.1** were predominantly zygotic in origin. We conclude that *hesC* is transiently transcribed in the large micromere territory and that the lineage-specific activation of the skeletogenic GRN occurs at a stage when *hesC* mRNA is uniformly distributed throughout the embryo.

2.4.2 Ets1 is not required for the onset of *Lvalx1* expression, but is required for its maintenance

The observation that *Lvalx1* is activated before the clearing of *LvhesC* transcripts from the large micromere territory prompted us to examine other factor(s) that might trigger the onset of *Lvalx1* expression. Ets1 has been identified as a positive regulator of *alx1* (Rottinger et al., 2004; Oliveri et al., 2008) and the presence of maternal *ets1* transcripts was demonstrated previously in the sea urchin (Kurokawa et al., 2000; Oliveri et al., 2008). To test whether maternal Ets1 protein plays a role in activating *alx1*, we carefully compared the spatial and temporal patterns of expression of the mRNAs and proteins encoded by *Lvets1* and *Lvalx1*. WMISH studies confirmed that *Lvets1* mRNA was expressed ubiquitously in *L. variegatus* embryos until ~6 hpf (mid-blastula stage) **(Fig. 2.6.A)**. At this developmental stage, very strong expression of *Lvalx1* mRNA was apparent in the large micromere territory in sibling embryos **(Fig. 2.6.C)**. At the hatched blastula stage (8 hpf), *Lvets1* mRNA, like *Lvalx1* mRNA, was restricted to the large micromere lineage **(Fig. 2.6.B,D)**.

We used a polyclonal antiserum that recognizes LvEts1 (Ettensohn et al., 2007) to examine the distribution of this protein at different developmental stages. Immunostaining studies showed that LvEts1 was not detectable in nuclei at 6 hpf **(Fig. 2.6.E)**. At 8 hpf, however, the protein was concentrated in the nucleus of every blastomere, and was visibly enriched in the nuclei of the large micromere progeny **(Fig. 2.6.F)**. We do not know whether the expression of LvEts1 protein outside the large micromere territory at this

stage is a consequence of the translation of ubiquitous, maternal transcripts or reflects transient, widespread zygotic transcription of *Lvets1* during early development. If the former is the case, then the reason for the significant lag in the nuclear accumulation of the protein following fertilization is unclear. In any event, the absence of detectable nuclear LvEts1 protein at 6 hpf, when *Lvalx1* transcripts are expressed at very high levels, suggests that LvEts1 does not play a role in the onset of *Lvalx1* transcription.

To test more directly the role of LvEts1 in the onset of *Lvalx1* expression, we over-expressed a dominant negative form of Ets1 that lacked the N-terminal activation domain (dnLvEts1) (Kurokawa et al., 1999). We considered it likely that this dominant negative form would interfere with the function of both maternal and zygotic pools of endogenous LvEts1 protein. Consistent with previous findings in a different species (Kurokawa et al., 1999), embryos injected with mRNA encoding dnLvEts1 failed to form PMCs and completely lacked skeletal elements, even after prolonged periods in culture **(Fig. 2.7.A,B)**. F-WMISH analysis showed, however, that there was no change in *Lvalx1* expression at 6 hpf in dnLvEts1-expressing embryos as compared to sibling, control embryos that had been injected with 20% glycerol **(Fig. 2.7.C,E)**. Soon thereafter, the expression of *Lvalx1* declined markedly in embryos expressing dnLvEts1, and by 8 hpf *Lvalx1* transcripts were no longer detectable by F-WMISH **(Fig. 2.7.D,F)**. These findings indicate that LvEts1 is required for the maintenance, but not for the activation, of *Lvalx1* expression.

Mis-expression of wild-type Ets1 results in the formation of supernumerary mesenchymal cells (Kurokawa et al., 1999; Rottinger et al., 2004). The precise fate of these cells is unclear; it has been reported that they express some skeletogenic genes but not others (Kurokawa et al., 1999). Based on these findings, it seemed possible that mis-expression of Ets1 might be sufficient to activate *alx1* in non-micromere-derived cells. We tested this possibility by injecting mRNA (8 mg/ml) encoding wild-type LvEts1 into fertilized eggs. We chose this concentration because it reliably induced the formation of large numbers of supernumerary mesenchymal cells in ~75-80% of injected embryos. *Lvalx1* expression was analyzed by WMISH at the hatched blastula stage and during the phase of supernumerary mesenchymal cell ingression. These studies showed that there was no expansion of the expression domain of *Lvalx1* at either developmental stage **(Fig.**

2.8.C,D). In contrast, >50% of the injected embryos showed a moderate reduction in the number of cells expressing *Lvalx1* as compared to sibling, uninjected embryos (n =35 at each developmental stage). We also examined skeletogenic specification in these embryos by immunostaining with monoclonal antibody 6a9, an antibody that recognizes MSP130 family proteins. Again, we observed no increase in the numbers of skeletogenic cells (data not shown). These findings indicate that the striking conversion of cells to a mesenchymal phenotype induced by the mis-expression of Ets1 is not accompanied by the ectopic activation of *alx1*. Taken together, our studies suggest that LvEts1 is neither necessary nor sufficient for the initial activation of *Lvalx1*, although the protein plays an important role in maintaining *Lvalx1* expression in the large micromere territory.

2.4.3 MAPK signaling is required for the maintenance, but not for the activation, of *Lvalx1* expression

Rottinger et al., (2004) showed that *alx1* expression was inhibited when embryos were treated with U0126, a MEK inhibitor. They provided evidence that one important role of MAPK signaling is to promote the phosphorylation of Ets1. Previous work showed that U0126 has the same general effects on embryonic development (i.e., a complete inhibition of PMC formation and skeletogenesis) in *L. variegatus* as it does in other species, and is effective at similar concentrations (Ettensohn et al., 2007). We analyzed the effect of U0126 on *alx1* expression in *L. variegatus*, focusing specifically on the initial phase of expression. Embryos treated continuously with 6 μM U0126 from the 2-cell stage exhibited strong *Lvalx1* expression at 7 hpf (late blastula stage) **(Fig. 2.9.C)**. Such embryos were indistinguishable from control embryos treated with DMSO alone **(Fig. 2.9.A)**. In contrast, by 9 hpf (hatched blastula stage), no *Lvalx1* expression was detectable in U0126-treated embryos **(Fig. 2.9.B,D)**. The effects of U0126 on *Lvalx1* expression were therefore very similar to those of dnLvEts1, and reinforced the view that the activation and the maintenance of *Lvalx1* expression are controlled by different mechanisms.

2.4.4 The expression of *Lvalx1*, but not that of *Lvpmar1*, is dependent upon unequal cell division

To determine whether the unequal cleavage divisions that occur at the vegetal pole influence the activation of *alx1* expression, we equalized both the 4th and 5th cleavage divisions using low concentrations of SDS. ~72% of SDS-treated embryos (*L. variegatus*) underwent an equal 4th cleavage division and ~67% of the treated embryos underwent equal divisions at both the 4th and 5th cleavages **(Fig. 2.10.A-D)**. The remaining embryos formed variable numbers of micromeres. As reported by Langelan and Whiteley (1985), SDS-treated embryos lacked PMCs, gastrulated in a delayed fashion, and formed spicules after a considerable delay **(Fig. 2.10.E-H)**. Skeleton formation in these embryos was probably a consequence of the transfating of non-micromere-derived cells. F-WMISH analysis of SDS-treated embryos revealed a striking reduction in *Lvalx1* expression **(Fig. 2.11.D,E)** compared to sibling controls **(Fig. 2.11A,B)** at 8 hpf (hatched blastula stage) and 10 hpf (pre-ingression-blastula stage). Only 30-35% of the SDS-treated embryos exhibited any detectable *Lvalx1* expression at these stages. At 12 hpf, when sibling control embryos were at the mesenchyme blastula stage **(Fig. 2.11.C)**, *Lvalx1* expression was detectable in ~50% of the SDS-treated embryos, but usually in a much smaller number of cells than in control embryos **(Fig. 2.11.F)**. The residual expression of *Lvalx1* at early developmental stages in SDS-treated embryos is probably a consequence of the incomplete effect of the detergent on the pattern of cleavage.

We next asked whether the effect of the cleavage pattern on *Lvalx1* activation might be mediated by *pmar1*. 200 control embryos and 200 sibling, SDS-treated embryos were collected at 6 hpf (mid-blastula stage) and the expression of *Lvpmar1*, *Lvalx1*, and *Lvdelta* was assessed by RT-PCR using equivalent serial dilutions of the cDNA samples. SDS had no effect on *Lvpmar1* expression, but the expression of *Lvalx1* and *Lvdelta* was clearly reduced **(Fig. 2.11.G)**. We also examined *Lvpmar1* expression at earlier developmental stages (3-4 hpf) and found in three independent trials that equal cleavage had no effect on transcript levels (data not shown). The effect of SDS on *Lvpmar1*, *Lvalx1*, and *Lvdelta* expression was confirmed by QPCR **(Fig. 2.11.H)**. These experiments showed that, although *pmar1* is ordinarily expressed specifically in the micromeres immediately after they form, unequal cleavage is not required for the transcriptional activation of *pmar1*. The level of *Lvpmar1* expression on a per embryo basis was not affected by SDS-treatment, but the level of expression per cell may have been altered due

to changes in cell size. Unlike *Lvpmar1*, *Lvalx1* and *Lvdelta* were dependent on unequal cell division for their activation; this might have been a consequence of changes in the level of *pmar1* expression per cell, or could have occurred by other mechanisms

2.4.5 Pmar1 protein is stable in both the large and small micromeres

Pmar1 mRNA is detectable in the micromeres immediately after they are born and continues to be expressed in both the large and small micromeres until the blastula stage (Oliveri et al., 2002). In contrast, *alx1* and *delta* are activated specifically in the large micromeres and are restricted to this lineage throughout later development (Sweet et al., 2002; Ettensohn et al., 2003). Mis-expression studies show that Pmar1 is sufficient to activate the GRN widely throughout the embryo; why then does Pmar1 not ordinarily activate *alx1* and *delta* in the small micromeres? One possibility is that, despite the presence of *pmar1* mRNA in the small micromeres, post-transcriptional mechanisms prevent the accumulation of functional Pmar1 protein in these cells.

First, to further support the idea that *pmar1* provides a positive regulatory input into *alx1*, we used F-WMISH to show that over-expression of *Lvpmar1* was sufficient to activate *Lvalx1* throughout the embryo **(Fig. 2.12.A,B)**. This finding supported earlier studies demonstrating an increase in *alx1* mRNA levels as measured by QPCR (Ettensohn et al., 2003), and experiments showing that mis-expression of *pmar1* induces the ectopic activation of *delta* (Oliveri et al., 2002). Selective protein degradation regulates the expression of other transcription factors in the sea urchin embryo (Weitzel et al., 2004; Angerer et al., 2005). Therefore, to test whether Pmar1 might be selectively degraded in the small micromeres, we microinjected mRNA encoding a GFP-tagged form of LvPmar1 (coding region only) into fertilized eggs and monitored the expression of fluorescent protein in living embryos by confocal microscopy. LvPmar1-GFP was expressed in all cells of the embryo during cleavage, including both the large and small micromere lineages **(Fig. 2.12.C,D)**, and continued to be stably expressed in both territories until at least the blastula stage, after the onset of *Lvalx1* expression. This pattern of protein expression contrasts with that of other GFP-tagged transcriptional regulators: for example, b-catenin-GFP is rapidly degraded in animal blastomeres during early cleavage (Weitzel et al., 2004). These findings argue against the hypothesis that LvPmar1 is degraded

selectively in the small micromeres and indicate that other mechanisms prevent the activation of the GRN in these cells.

2.5 Discussion

Much progress has been made in dissecting the GRN that underlies the development of the skeletogenic primary mesenchyme (Oliveri et al., 2008; Ettensohn, 2009). The identification of Pmar1 as an important early activator of this pathway, combined with evidence that this protein functions as a transcriptional repressor, led to the hypothesis that Pmar1 activates the GRN by blocking the expression of a second repressor. HesC has been identified as this second repressor based on the following criteria: 1) *hesC* transcript levels are down-regulated following forced mis-expression of Pmar1; 2) *hesC* transcripts disappear from the micromere territory during early development; and 3) MO-mediated inhibition of HesC translation results in an increase in mesenchymal cells and in the ectopic expression of *delta* (Revilla-i-Domingo et al., 2007). Based on these findings, *hesC* has been considered the linchpin of a double-repression gate, and the evolutionary invention of the *pmar1*/*hesC* gate has been put forward as a pivotal event during the evolution of skeletogenesis in sea urchins (Davidson and Levine, 2008; Gao and Davidson, 2008).

Our WMISH studies show that the activation of *alx1* and *delta* selectively in the large micromere territory occurs prior to the clearing of *hesC* mRNA from these cells. We considered the possibility that maternal *hesC* transcripts might be non-translatable, or could encode a non-functional form of the HesC protein, and that WMISH signal from maternal transcripts might prevent us from detecting a local repression of zygotic *hesC* transcription. QPCR studies, however, showed that levels of maternal hesC transcripts were low (see also Revilla-i-Domingo et al., 2007), and that at the developmental stages that were used for quantitative F-WMISH analysis, most *hesC* transcripts were zygotic in origin. Therefore, our combined QPCR and WMISH data indicate that 1) *hesC* is transiently transcribed in the large micromere territory, and 2) *alx1* and *delta* are activated selectively in these cells at a stage when zygotic *hesC* transcripts are ubiquitous. Our QPCR analysis also showed that the activation of *alx1* occurred at the same time as the activation of *hesC* **(Fig. 2.1.G,H)**. It is therefore difficult to envision how regional differences in *hesC* transcription, which would require some time to produce differences in HesC protein levels, could influence the early spatial pattern of *alx1* expression. These

considerations, however, do not preclude an essential role for *hesC* repression in the later maintenance phase of *alx1* expression (see below).

Considerable evidence indicates that *pmar1* is a pivotal regulator of the micromere-PMC GRN. Mis-expression of *pmar1* is sufficient to activate the skeletogenic GRN in non-micromere-derived cells (Oliveri et al., 2002; 2003; Nishimura et al., 2004; Yamazaki et al., 2005; 2009; this study). It has been more difficult to test directly the function of *pmar1* in the large micromere territory (where the gene is ordinarily expressed) due to the difficulty in blocking the expression of multiple, tandem *pmar1* genes using morpholinos. A VP16-Pmar1 fusion protein, which probably acts in a dominant negative fashion, blocks PMC formation and reduces the levels of several skeletogenic mRNAs, at least at late developmental stages (Yamazaki et al., 2005). This loss-of-function analysis supports the view that *pmar1* is required for the deployment of the skeletogenic GRN in the large micromere territory. Pmar1 (a known repressor) presumably mediates the activation of *alx1, delta*, and other early genes in the network by blocking the expression of a second repressor, as discussed by Oliveri et al., (2002). Our findings therefore point to one of two possibilities: 1) the existence of as-yet-undiscovered repressor downstream of *pmar1* but distinct from *hesC*, or 2) a *pmar1*-independent mechanism of GRN activation, which might be reinforced later in development by the *pmar1-hesC* de-repression system.

The conclusion that the skeletogenic GRN is activated by mechanisms that are independent of *hesC* repression seems at odds with evidence that inhibition of *hesC* function is sufficient to activate the GRN ectopically (Revilla-i-Domingo et al., 2007; Smith and Davidson, 2008). It should be noted that in a recent structure-function analysis of Pmar1, one mutant construct (N-HD-A-C) that lacked a portion of the C-terminal region of the protein was reported to down-regulate *hesC* mRNA levels throughout the embryo without expanding the expression of *alx1*, *tbr*, or *ets1* (Yamazaki et al., 2009). This observation suggests that down-regulation of *hesC* may not be sufficient to activate the skeletogenic GRN in non-micromere lineages. If, as the earlier data suggest, inhibition of *hesC* function is sufficient to activate the network, then one interpretation is that *alx1*, *delta* and other early genes can be activated by more than one regulatory mechanism. According to this view, the repression of *hesC* is sufficient to activate these genes in non-

micromere lineages, but during normal development (i.e., in the large micromere lineage), a separate regulatory pathway is utilized very early in development that activates the network, essentially by-passing *hesC* repression, which is relegated to a maintenance function. A prediction of this view is that genes such as *alx1* and *delta* will have multiple activation modules, any one of which can activate transcription once engaged. The cis-regulatory architecture of *alx1* has not been described, but *delta* has been analyzed extensively in this regard (Revilla-i-Domingo et al., 2004; 2007; Smith and Davidson, 2008). Consistent with the above model, two separate regulatory modules have been identified that are sufficient to drive expression of *delta* in the micromere territory; both modules are responsive to *pmar1* but only one contains putative HesC binding sites.

Our findings reinforce the view that the activation and the maintenance of *alx1* expression are controlled by very different mechanisms. Positive inputs into *alx1* from MAP kinase signaling and from *ets1* (inputs that may be related to one another) regulate the maintenance, but not the onset, of *alx1* expression. One essential, early input into *alx1* that we have identified is a cellular, rather than a molecular one; namely, the unequal cleavage of vegetal blastomeres. It was shown previously that PMC specification is influenced by the cleavage pattern (Langelan and Whiteley, 1985), but this work predated the elucidation of the skeletogenic GRN, and ours is the first effort to analyze the molecular step(s) at which unequal cell division impinges on the network. Surprisingly, although *pmar1* is ordinarily activated in the micromeres immediately they form, unequal cleavage is not required for the transcriptional activation of *pmar1*. Instead, a molecular step between *pmar1* expression and the activation of *alx1* and *delta* is linked to unequal cleavage. Whatever the regulatory connection, it is likely to be a novel feature of echinoid development. The embryos of a related group of echinoderms, the ophiuroids (brittle stars), exhibit equal cleavage, but nevertheless form PMCs and an embryonic skeleton (Tominaga et al., 2004 and references therein). Evolution has evidently experimented freely with the upstream regulation of the skeletogenic GRN (Gao and Davidson, 2008; Ettensohn, 2009).

A key, unanswered question is why the skeletogenic GRN is activated only in the large micromere territory, when *pmar1* mRNA is present in both the large and small micromeres (Oliveri et al., 2002). A variety of mechanisms can be envisioned that involve

the asymmetric segregation of polarized maternal determinants, differences in nucleus-to-cytoplasm ratio, and other mechanisms. Interestingly, during normal development, *hesC* expression persists in the small micromere territory after it is extinguished elsewhere in the vegetal plate (**Fig. 2.4;** Smith et al., 2008). This suggests that Pmar1 protein is not present (or is inactive) in the small micromeres. Other transcriptional regulators undergo polarized, proteolytic degradation along the animal-vegetal axis of the sea urchin embryo (Weitzel et el., 2004; Angerer et al., 2005). Our analysis of the expression of Pmar1-GFP argues against the hypothesis that this protein is selectively degraded in the small micromeres, but other modes of post-transcriptional regulation may be involved. Even if Pmar1 protein is present in the nuclei of both large and small micromeres, separate regulatory mechanisms may operate in the small micromeres that override the double-repression system and prevent the deployment of the skeletogenic GRN. The small micromeres express several germline markers (Juliano et al., 2006; Voronina et al., 2008) and in other animals the prospective germline is globally transcriptionally repressed during early development (Nakamura and Seydoux, 2008).

The regulative deployment of the skeletogenic GRN by NSM cells requires the ectopic activation of *alx1* via novel, *pmar1*-independent regulatory inputs (Ettensohn et al., 2007; Ettensohn, 2009). Several of the molecular conditions that might be envisioned to be required for the expression of *alx1* (viz., activation of MAPK, expression of Ets1, and down-regulation of *hesC*) appear to ordinarily be present in NSM cells, yet *alx1* is not expressed. Although it has not been tested directly, it seems unlikely that unequal cell division, which is essential for the activation of *alx1* in the micromere lineage and is a consequence of maternal cortical polarity, plays a role in the ectopic activation of *alx1* in transfating cells. Further analysis of the molecular mechanisms that activate the skeletogenic GRN, and the identification of additional inputs that are unique to the endogenous or to the regulative pathways, will shed light on this example of developmental plasticity.

Primer name	Primer sequence (5`-3`)
Spalx1 F	CACCCGTAGAGGGCGCTATA
Spalx1 R	TGCTGGAGTCTTGCGATTCG
Spdelta F	ACGGAGCTACATGCCTGAAC
Spdelta R	TCACAATGGACCGAATCAGA
SphesC F	AGAGGCGAGCTCGCATCAAC
SphesC R	CTGGGGTCTGGACGTCTTTC
Spz12 F	AGTCGTCCAGCCATGTCTTT
Spz12 R	AAGCACACCTCGCACCTATC
Lvalx1 F	TGGAGAAGGTTTTCCAAAGG
Lvalx1 R	CGTAACCAGATCCTGGTCCT
Lvdelta F	TTGCTCTGCATTGGATTAGC
Lvdelta R	GATATCCTTGGCTTGGTGGT
LvhesC F	AAGTACCACGCTGGCTTCAC
LvhesC R	GTGCTGCAACGATCAGCTAG
Lvpmar1 F	CTGCTCACCAACCAGTCATT
Lvpmar1 R	TGTCGTCTGGTTGACCTCAT
Lvubiquitin F	CACAGGCAAGACTATCACTC
Lvubiquitin R	GATAGAGTGCGGCCGTCCTC

Table 2.1. QPCR primer sequences (F=forward primer, R=reverse primer)

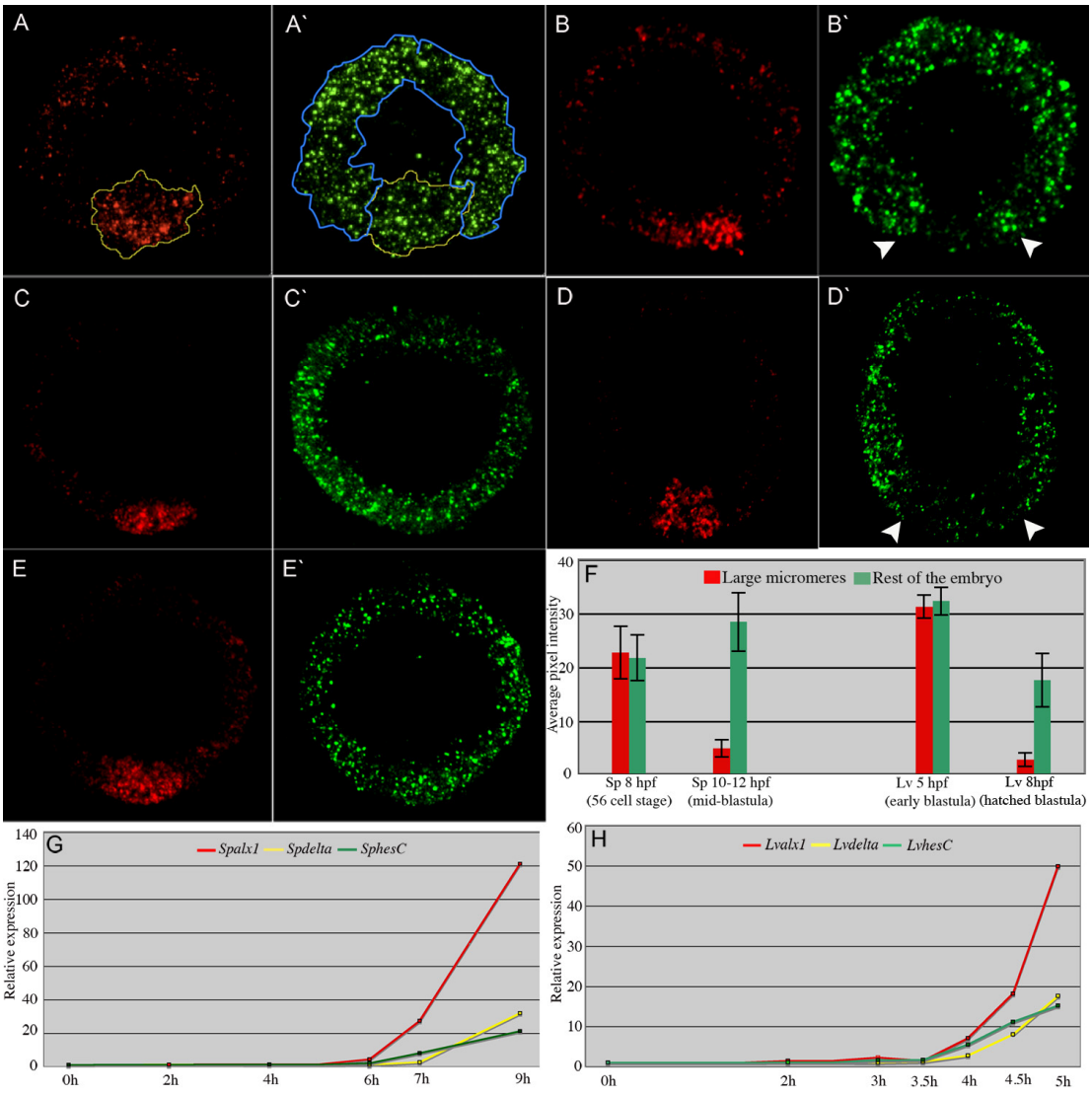

Fig. 2.1. Accumulation of *alx1* transcripts precedes the clearing of *hesC* mRNA from the large micromere territory. Two-color F-WMISH was performed using digoxigenin-labeled *hesC* probes (green channel) and fluorescein-labeled *alx1* or *delta* probes (red channel). Each image is a projection of 3-5 confocal sections. **(A-B')** *Spalx1* and *SphesC* expression in *S. purpuratus*, shown at 8 hpf (56-cell stage) (A,A') and 10-12 hpf (mid-blastula stage) (B,B'). **(C-D')** *Lvalx1* and *LvhesC* expression in *L. variegatus,* shown at 5 hpf (128 cell stage) (C,C') and 8 hpf (mid-blastula stage) (D,D'). **(E,E')** *Lvdelta* and *LvhesC* expression at 5 hpf (128-cell stage). Arrowheads in B' and D' indicate the vegetal region of *hesC* clearing. **(F)** Quantification of *hesC* F-WMISH signal. Average pixel intensities were determined for the large micromere territory (i.e., the *alx1*-expressing region) and for the remainder of the embryo, as illustrated in (A,A`) (see Methods). For

each species and time point analyzed, data from 6-12 different embryos were used to calculate mean, average pixel intensities for the two regions (red and green bars). Black bars show standard errors. **(G,H)** QPCR analysis of *alx1*, *delta*, and *hesC* expression in *L. variegatus* (G) and *S. purpuratus* (H). For each time point, the average C_t value for each gene was normalized against the average C_t value of an internal standard mRNA (*ubiquitin* for L. *variegatus* and *z12* for S. *purpuratus*). Values shown on the y-axis reflect relative numbers of *hesC* transcripts at the various stages, with the maternal expression level arbitrarily set to 1.

Fig. 2.2. ClustalW alignment of the nucleotide sequences of *LvhesC* and *SphesC*.

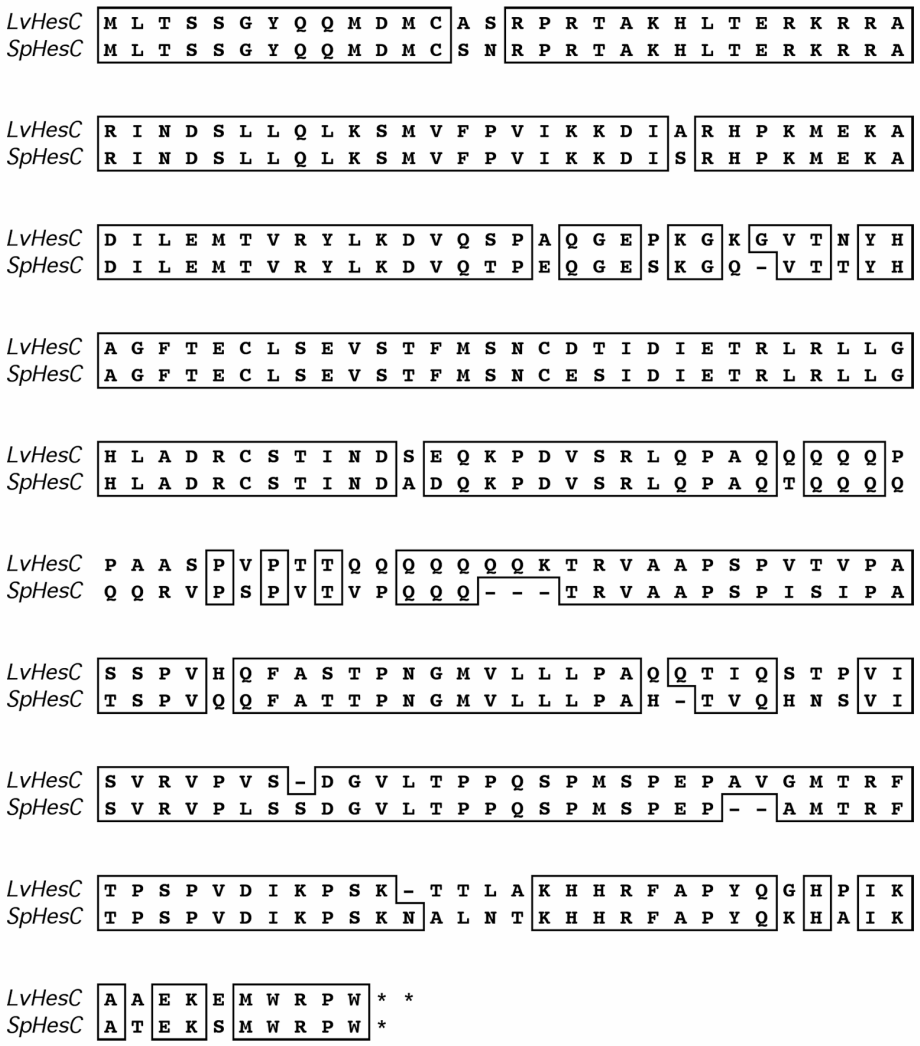

Fig. 2.3. ClustalW alignment of the predicted amino acid sequences of LvHesC and SpHesC.

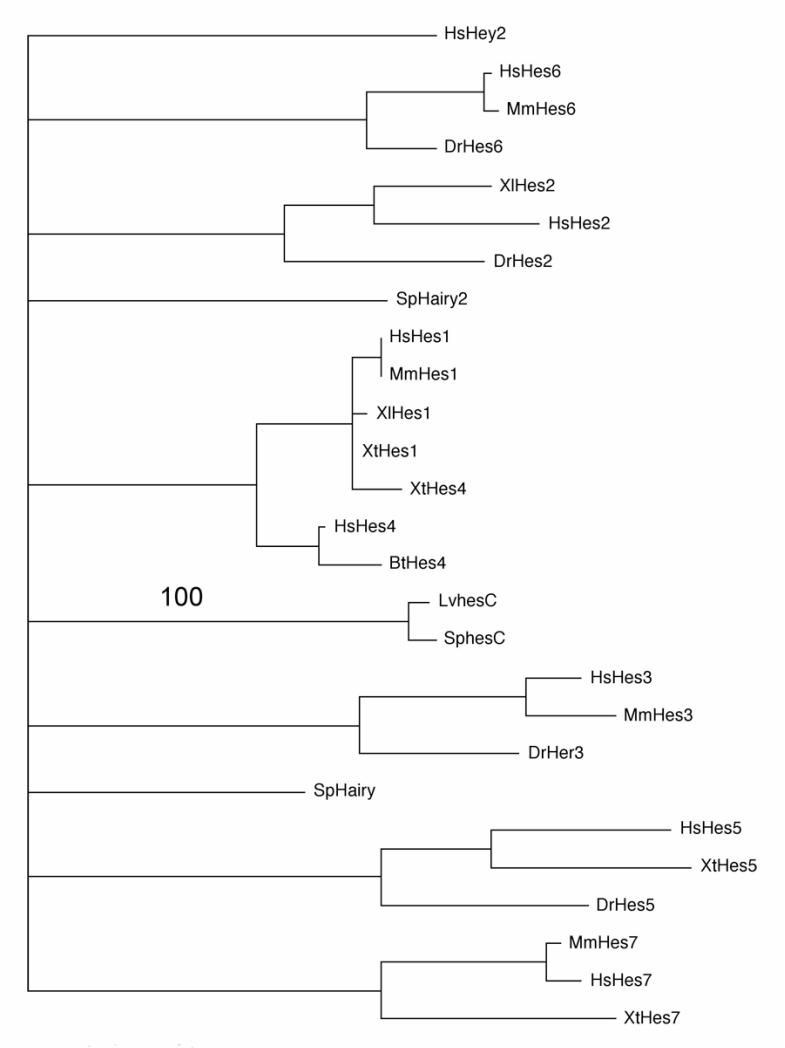

Fig. 2.4. Phylogenetic tree showing that LvhesC and SphesC are orthologous proteins. Amino acid sequences were aligned using ClustalW, BioEdit was used to remove gaps from the alignment, and a phylogenetic tree was constructed using PAUP. The HsHey protein sequence was treated as the outgroup. The number above the LvhesC and SphesC branch indicates the bootstrap support value generated from 1000 bootstrap replicates. Species abbreviations: Bt, B*os taurus*; Dr, *Danio rerio*; Hs, *Homo sapiens*; Lv, *Lytechinus variegatus*; Mm, *Mus musculus*; Sp, *Strongylocentrotous purpuratus*; Xl, *Xenopus laevis*; Xt, *Xenopus tropicalis*.

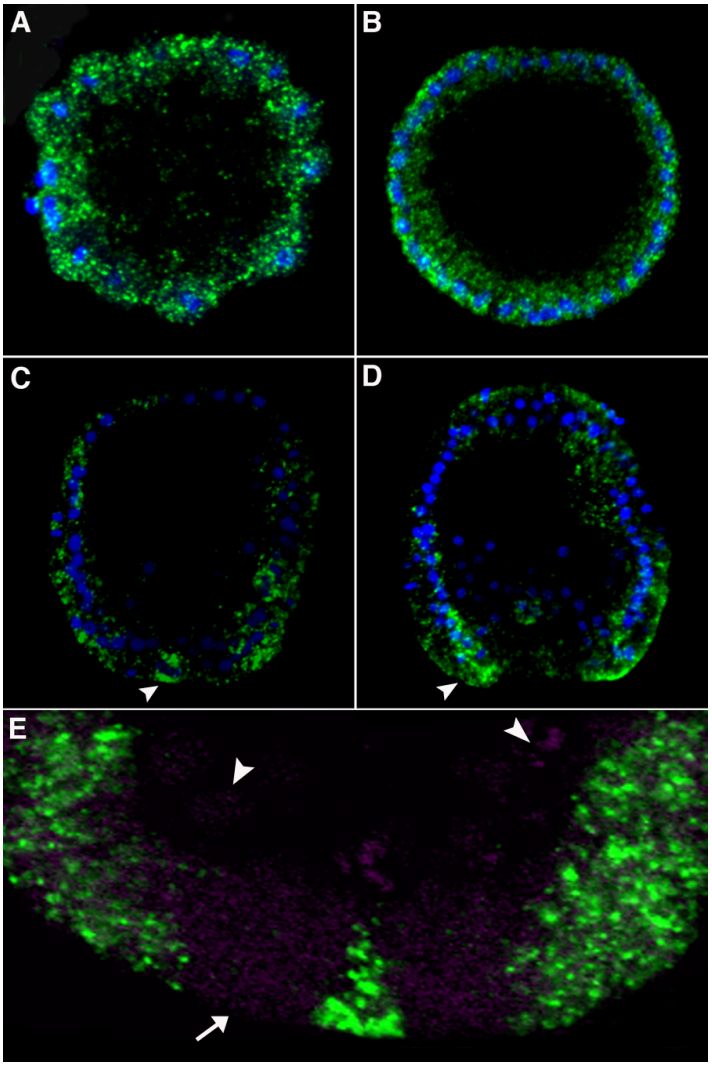

Fig. 2.5. WMISH analysis of *hesC* mRNA expression in *L. variegatus* (green = *LvHesC*, blue = Hoechst). (A,B) Zygotic expression of *LvhesC* mRNA is detectable in all cells of the embryo at 4 hpf (A) and 6 hpf (B). (C) A mesenchyme blastula stage embryo showing downregulation of *LvhesC* mRNA in the PMCs, the NSM territory, and the apical plate region, but expression in the small micromeres (arrowhead). (D) A mid-gastrula stage embryo showing downregulation of *LvhesC* mRNA in the invaginating endoderm and high levels of expression around the blastopore (arrowhead). (E) A high magnification view of the vegetal plate of a mesenchyme blastula stage embryo. *LvhesC* mRNA is not detectable in the presumptive PMCs (arrowheads).

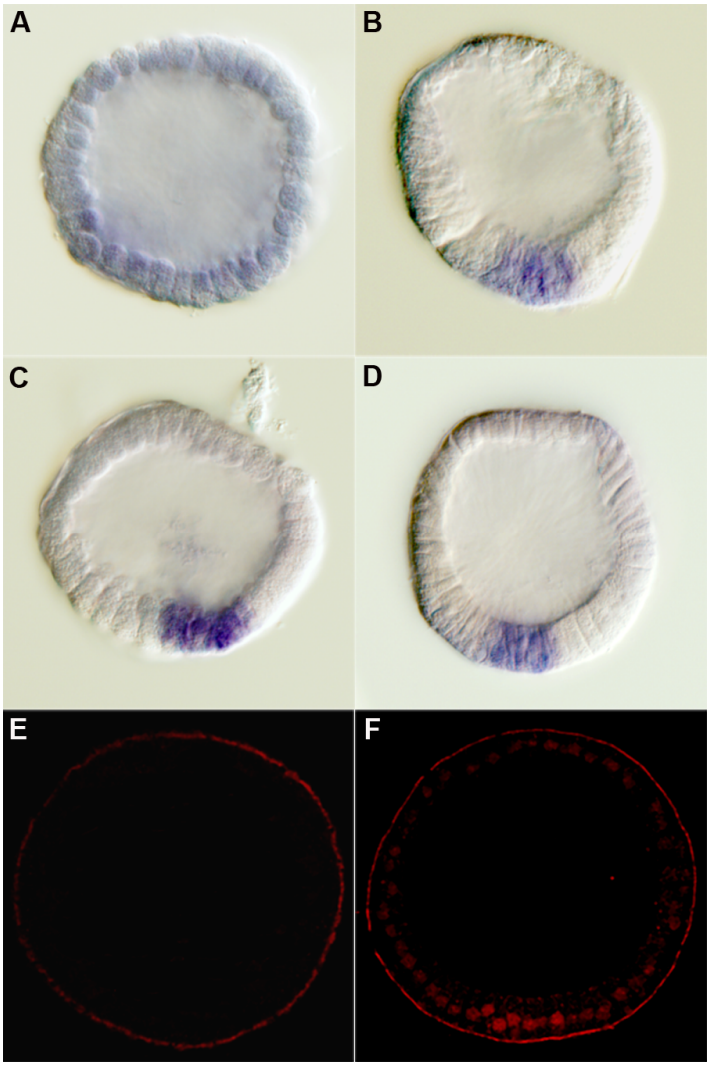

Fig. 2.6. *Lvalx1* mRNA expression precedes the nuclear localization of LvEts1 protein. (A-D) WMISH analysis of *Lvets1* (A,B) and *Lvalx1* (C,D) expression. Maternal *Lvets1* mRNA is present in all cells of the embryo until 6 hpf (mid-blastula stage) (A), but by 8 hpf (hatched blastula stage) maternal transcripts decline in most cells and the zygotic expression of *Lvets1* is restricted to the large micromere territory (B). In sibling embryos, strong expression of *Lvalx1* is seen in the large micromere territory at 6 hpf (C) and at 8 hpf (D). **(E,F)** Immunolocalization of LvEts1 protein. Nuclear LvEts1 protein is not detectable by immunostaining at 6 hpf, (E), a stage at which *Lvalx1* transcripts are already strongly expressed. At 8 hpf, LvEts1 protein is concentrated in the nuclei of all blastomeres, and is present at the highest levels in presumptive PMCs (F).

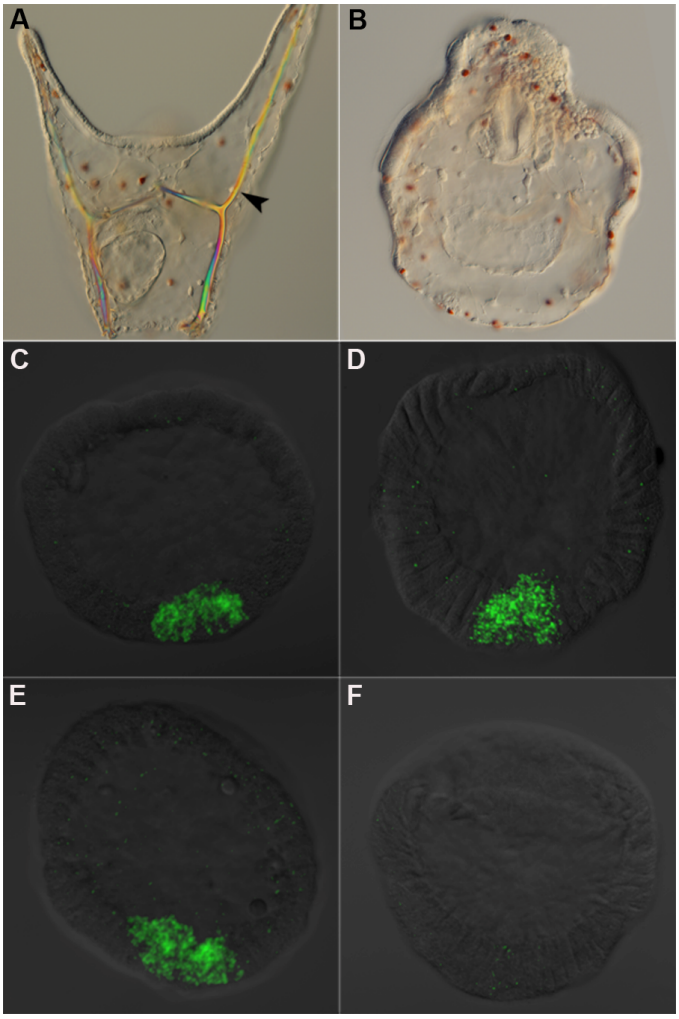

Fig. 2.7. LvEts1 is required for the maintenance, but not for the activation, of *Lvalx1* expression. (A) Control pluteus larva, 72 hpf. Arrowhead indicates skeletal rods. **(B)** Sibling embryo expressing *dnLvets1,* also at 72 hpf. *DnLvets1* mRNA-injected embryos fail to form skeletal elements even after prolonged periods in culture. **(C-F)** *Lvalx1* expression in embryos overexpressing *dnLvets1*. Panels C and D show control embryos injected with 20% glycerol alone and examined at 6 hpf (mid-blastula stage) (C) and 8 hpf (hatched blastula stage) (D). Panels E and F show embryos injected with *dnLvets1* mRNA and examined at 6 hpf (E) and 8 hpf (F). Each panel is a merged image of a z-projection of several confocal slices and a single DIC image taken at the mid point of the stack. *DnLvets1* mRNA-injected embryos exhibit normal levels of Lv*alx1* expression at 6 hpf (compare C with E), but by 8 hpf, *Lvalx1* expression is no longer detectable (compare D with F).

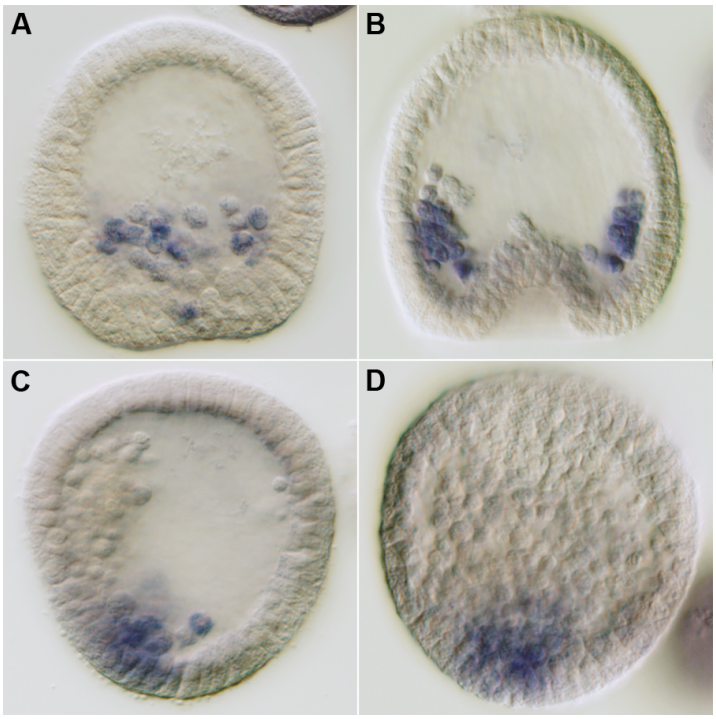

Fig. 2.8. Mis-expression of *Lvets1* mRNA converts many cells of the embryo to a mesenchymal fate, but *Lvalx1* expression remains restricted to the large micromere lineage. *Lvalx1* expression was examined in *Lvets1*-mRNA injected embryos when sibling control embryos were at the mesenchyme blastula (MB) or early gastrula (EG) stages. **(A,B)** Control embryos showing normal expression of *Lvalx1* at the MB stage (A) and the EG stage (B). **(C,D)** *Lvets1*-mRNA injected embryos showing that *Lvalx1* expression is restricted to the PMCs at the MB stage (C) and later in development, when additional mesenchymal cells form (D).

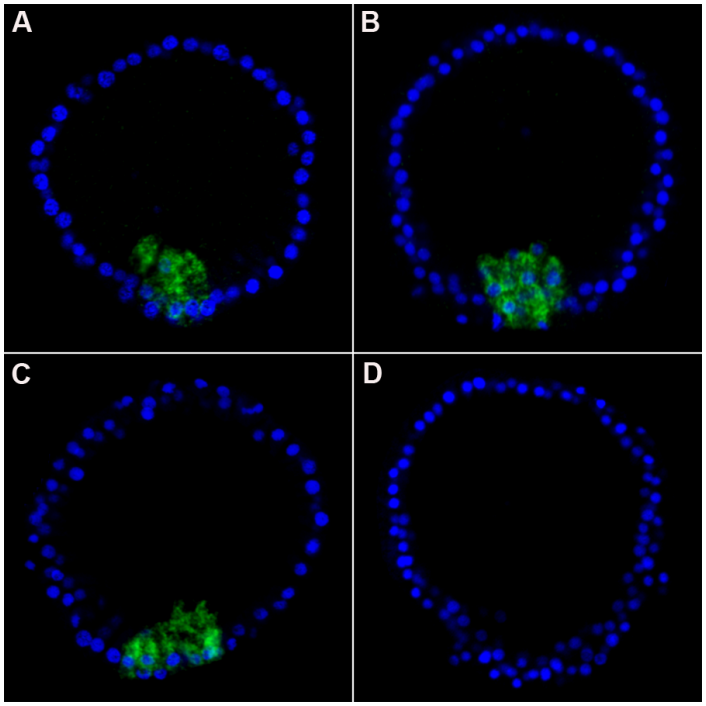

Fig. 2.9. The MAPK pathway is required for the maintenance of *Lvalx1* expression. Embryos were treated with 6 mm U0126 and *Lvalx1* expression was assayed at 7 hpf (hatched blastula stage) and 9 hpf (pre-ingression blastula stage). Each panel is a merged image of z-projections of confocal stacks (green = *Lvalx1*, blue = Hoechst). **(A,B)** DMSO-treated, control embryos showing normal *Lvalx1* expression (green) at 7 hpf (A) and 9 hpf (B). **(C,D)** U0126-treated embryos showing normal expression of *Lvalx1* at 7 hpf (C) but a striking loss of *Lvalx1* expression by 9 hpf (D).

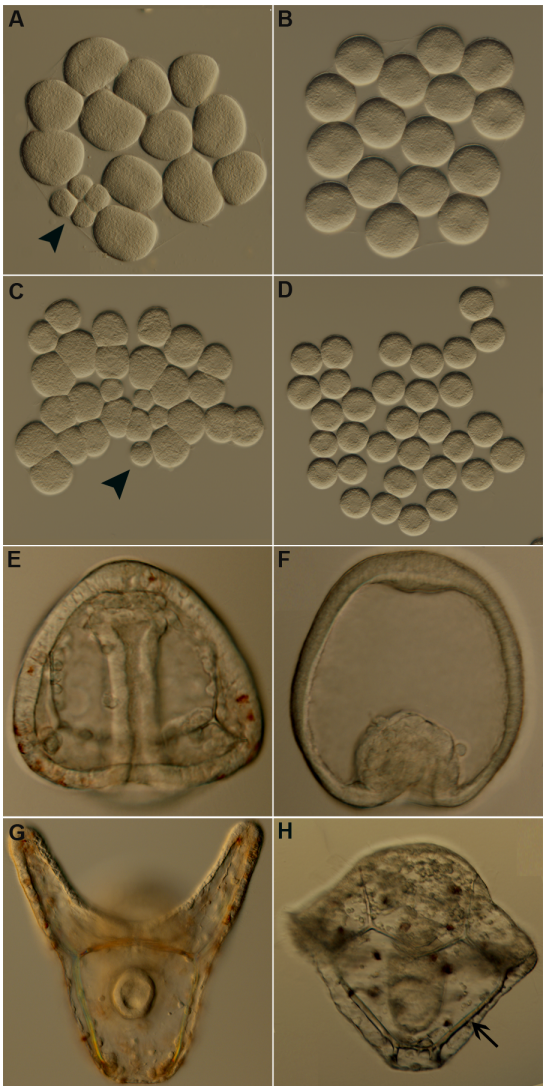

Fig. 2.10. SDS treatment equalizes the 4th and 5th cleavage divisions and blocks PMC formation in *L. variegatus*. Embryos were visualized using DIC optics; cleavage stage embryos shown in A-D were flattened with a coverslip. Left panels show control embryos at the 16-cell **(A)**, 28-cell **(B)**, late gastrula **(E)**, and pluteus stages **(G)**. Arrowheads indicate micromeres. Right panels show sibling, SDS-treated embryos at the same developmental stages. In most SDS-treated embryos, all cells are approximately equal in size after the 4th and 5th cleavage divisions **(B,D)**. These embryos lack PMCs **(F)** and form reduced skeletons **(H, arrow)**.

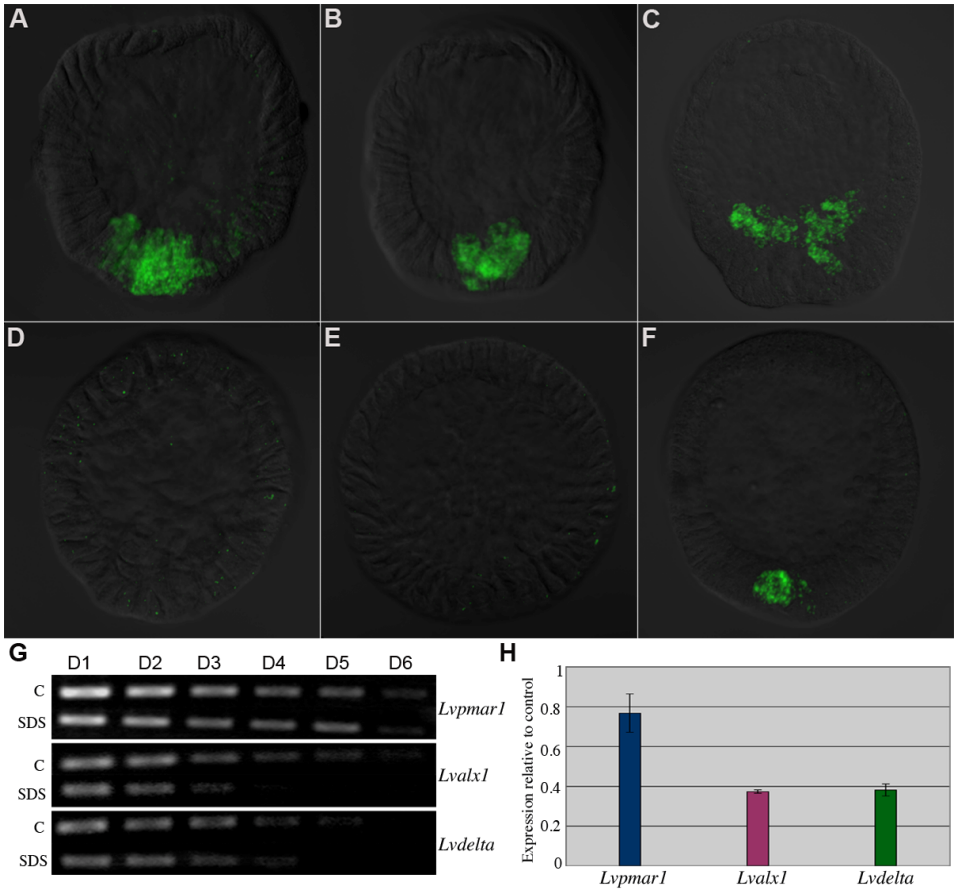

Fig. 2.11. The activation of *Lvalx1* and *Lvdelta,* but not that of *Lvpmar1,* is dependent on unequal cleavage division. (A-F) F-WMISH analysis of *Lvalx1* expression in SDS-treated embryos. Each photomicrograph is a merged image of a z-projection of a confocal stack and a single DIC section at the mid-point of the stack. (A-C) Control embryos showing normal *Lvalx1* expression at 8 hpf (hatched blastula) (A), 10 hpf (pre-ingression blastula) (B) and 12 hpf (mesenchyme blastula) (C). (D-F) Sibling SDS-treated embryos at 8 hpf (D), 10 hpf (E) and 12 hpf (F). *Lvalx1* expression is not detectable at 8 hpf or 10 hpf. At 12 hpf, ~50% of the SDS-treated embryos lack any *Lvalx1*-positive cells, while the remaining embryos have greatly reduced numbers of *Lvalx1*-positive cells (an example of such an embryo is shown in F). **(G,H)** Analysis of gene expression in equally-cleaving embryos. Total RNA was isolated from 200 SDS-treated embryos and 200 control embryos at 6 hpf. The expression of *Lvpmar1*, *Lvdelta*, and *Lvalx1* was analyzed by RT-PCR using serial dilutions (D1-D6) of the two cDNA samples (G), and by QPCR (H). SDS treatment had no effect on *Lvpmar1* expression, but levels of *Lvalx1* and *Lvdelta* mRNA were significantly reduced. The bars in (H) show levels of expression in SDS-treated embryos relative to sibling controls. Standard errors based on two independent trials are also indicated.

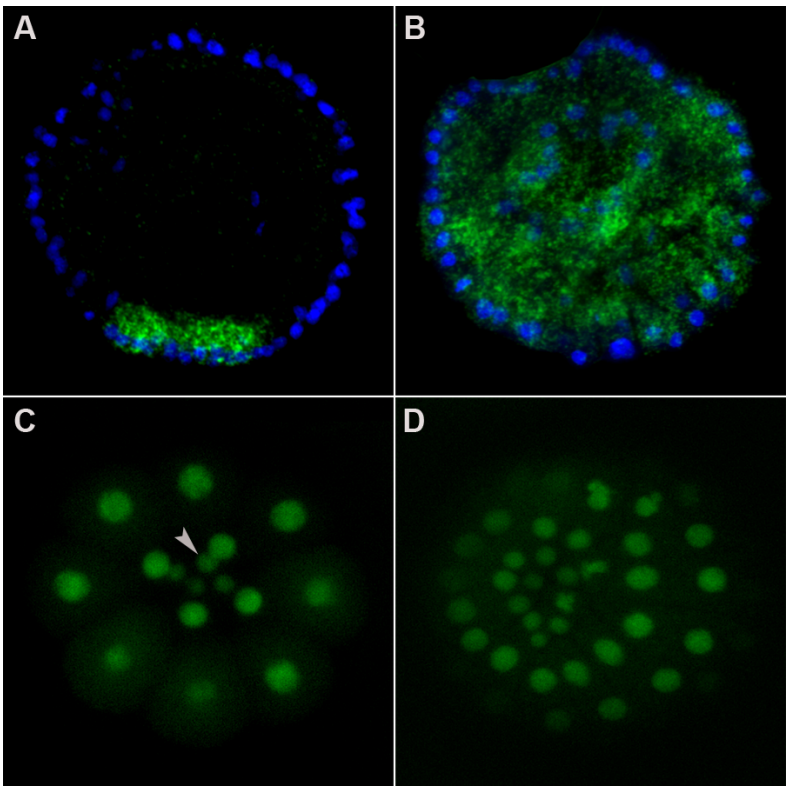

Fig. 2.12. (A,B) Mis-expression of LvPmar1 activates *Lvalx1* expression in all cells of the embryo. *Lvpmar1* mRNA was injected into fertilized eggs and *Lvalx1* expression was assessed by F-WMISH at 6 hpf (mid-blastula stage). Merged images of confocal stacks are shown (green = *Lvalx1*, blue = Hoechst*)*. Control embryos show expression of *Lvalx1* in the large micromere territory at 6 hpf (A), whereas mis-expression of LvPmar1 induces *Lvalx1* expression in all cells (B). **(C,D)** LvPmar1 protein is stable in both the large and small micromeres. Fertilized eggs were injected with mRNA encoding the coding region of LvPmar1 fused to GFP, and living embryos were examined by confocal microscopy. Projections of the vegetal hemisphere of a 32-cell stage embryo (D), and a ~128-cell stage embryo (E) are shown, viewed from the vegetal pole. LvPmar1-GFP is stable in all vegetal blastomeres, including the small micromeres (arrowhead in C).

Chapter 3

Regulative Deployment of the Skeletogenic Gene Regulatory Network During Sea Urchin Development

3.1 Abstract

The well-known regulative properties of the sea urchin embryo, coupled with the recent elucidation of gene regulatory networks (GRNs) that underlie cell specification, make this a valuable experimental model for analyzing developmental plasticity. In the sea urchin, the primary mesenchyme cell (PMC) GRN controls the development of the embryonic skeleton. Remarkably, experimental manipulations reveal that this GRN can be activated in almost any cell of the embryo. Here, we focus on the activation of the PMC GRN during gastrulation by non-skeletogenic mesoderm (NSM) cells and by endoderm cells. We show that most transfating NSM cells are prospective blastocoelar cells, not prospective pigment cells, as was previously believed. Earlier work showed that the regulative deployment of the GRN, unlike its deployment in the micromere-PMC lineage, is independent of the transcriptional repressor, Pmar1. In this work, we identify several additional differences in the upstream regulation of the GRN during normal and regulative development. We provide evidence that, despite these changes in the upstream regulation of the network, downstream regulatory genes and key morphoregulatory genes are deployed in transfating NSM cells in a fashion that recapitulates the normal deployment of the GRN, and which can account for the striking changes in migratory behavior that accompany NSM transfating. Finally, we report that mitotic cell division is not required for genomic reprogramming in this system, either within a germ layer (NSM transfating) or across a germ layer boundary (endoderm transfating).

3.2 Introduction

A fundamental question in development concerns the molecular mechanisms that underlie cellular plasticity. The plasticity of embryonic cells has been documented in almost all metazoan embryos that are used for developmental studies, challenging the view that cell fates are rigidly and immutably fixed. More recently, the finding that somatic cells can be reprogrammed to generate embryonic pluripotent stem cells, with potential uses in regenerative medicine, has led to an increased interest in understanding the process of cellular reprogramming. The sea urchin embryo is a valuable experimental model to study questions related to developmental plasticity because of its extensive and well-described regulative properties. In addition, in recent years, a systems biology approach has been used to generate detailed transcriptional GRNs for the different cell lineages of this embryo. This presents a unique opportunity to approach questions related to developmental plasticity in terms of the epigenetic regulation of GRNs.

During normal development, the skeletogenic cells are the descendants of the four large micromeres, cells that arise from unequal 4^{th} and 5^{th} cleavage divisions at the vegetal pole of the embryo. At the blastula stage, the descendants of the large micromeres occupy the central region of the vegetal plate and are surrounded by NSM cells. At the start of gastrulation, the large micromere descendants undergo an epithelial-mesenchymal transition (EMT) and migrate into the blastocoel; these cells are referred to thereafter as PMCs. The PMCs migrate to specific positions in the blastocoel and secrete the calcified endoskeleton of the larva. Later in gastrulation, two populations of NSM cells also undergo EMT; first pigment cells, and later a population of fibroblast-like cells known as blastocoelar cells (Gibson and Burke, 1985, Tamboline and Burke, 1992). Other NSM cells give rise to circumesophageal muscle cells and the cells of the coelomic pouches (Ruffins and Ettensohn, 1996).

The PMC GRN is currently one of the best-understood developmental GRNs (Oliveri et al., 2008; Ettensohn, 2009). The activation of this GRN is dependent on the stabilization of β-catenin in the vegetal region of the embryo (Wikramanayake et al., 1998; Logan et al., 1999; Ettensohn, 2006). A direct target of β-catenin is the transcriptional repressor *pmar1* (Kitamura et al., 2002; Oliveri et al., 2002). By a de-

repression mechanism, Pmar1 is believed to activate the signaling gene *delta* (Oliveri et al., 2002; Sweet et al., 2002), and a suite of early regulatory genes, which includes *alx1* (Ettensohn et al., 2003)*, tbrain* (Fuchikami et al., 2002; Oliveri et al., 2002), *ets1* (Kurokawa et al., 1999), specifically in the large micromere territory. These transcription factors activate other regulatory genes and, ultimately, genes that control PMC morphogenesis and biomineralization. The MAPK signaling pathway is required for PMC specification and ingression; this pathway plays a role in maintaining the expression of the key transcription factor, *alx1,* and other genes through the phosphorylation of Ets1 (Rottinger et al., 2004; Sharma and Ettensohn, 2010). The large micromeres also play an essential role in the induction of the NSM; elimination of Delta or Notch function results in embryos that lack pigment cells and have reduced numbers of blastocoelar and muscle cells (Sherwood and McClay, 1999; Sweet et al., 2002).

Surgical removal of PMCs at the mesenchyme blastula stage results in the activation of the skeletogenic GRN by NSM cells, a process referred to as NSM transfating **(Fig. 1.4).** NSM transfating is associated with the expression of *alx1* and several downstream biomineralization-related genes. Unlike normal development, the activation of *alx1* by transfating NSM cells occurs by a Pmar1- independent mechanism, a finding that points to the presence of novel upstream inputs into the network during regulative development (Ettensohn et al., 2007). In addition, the same study showed that regulative development requires active MAPK signaling for the synthesis of the larval skeleton, although the role of MAPK in the regulation of the skeletogenic GRN was not explored further. Other surgical manipulations result in the ectopic activation of the PMC GRN by other cell types; for example, the removal of both the PMCs and the NSM results in the activation of this network by presumptive endoderm cells (McClay and Logan, 1996).

The purpose of this study was to further dissect the molecular basis of developmental plasticity in the sea urchin embryo by analyzing the regulative deployment of the skeletogenic GRN. Our findings modify the current view of the population of NSM cells that transfate and, therefore, the nature and extent of the genomic reprogramming that occurs. We identify several differences in the upstream activation of the GRN in transfating cells as compared to the large micromere-PMC

lineage, but find that the faithful recapitulation of intermediate regulatory layers of the network and the activation of key morphoregulatory genes mediate the striking changes in cell behavior that are associated with transfating. To compare the mechanisms that activate the skeletogenic GRN in different embryonic lineages, we extend this approach to the deployment of the GRN by endoderm cells and provide evidence that this occurs by the re-specification of an NSM territory. Finally, we show that mitotic cell division is not required for the re-programming of NSM or endoderm cells to a skeletogenic phenotype.

3.3 Materials and Methods

Animals

Adult *Lytechinus variegatus* were obtained from Reeftopia Inc. (Key West, FL, USA). Gametes were obtained by intracoelomic injection of 0.5 M KCl and embryos were cultured at 23°C.

Fluorescent whole-mount in situ hybridization (F-WMISH)

Single and two-color F-WMISH were performed as described previously (Sharma and Ettensohn, 2010). Cell nuclei were stained by incubating embryos in 0.5 μg/ml Hoechst 33342 in PBST (0.1% Tween-20 in phosphate-buffered saline) for 5 minutes, followed by several rinses in PBST.

Microscopy and image processing

Z-stacks were collected at 1 μm intervals using a Zeiss LSM 510 metal/UV DuoScan spectral confocal microscope and a 40X oil immersion lens. Each image shown in the figures is a two-dimensional projection of ~10-20 digital sections obtained using the average intensity projection tool of ImageJ.

Morpholino microinjections

Lvdelta morpholino (MO) (Sweet et. al 2002) was obtained from Gene Tools, LLC. The injection solution consisted of 2 mM MO in 20% glycerol.

U0126 treatment

PMC(-) or PMC(-), arch(-) embryos were treated with U0126 at a concentration of 6 μM immediately after surgery until the desired developmental stage, when the embryos were fixed for F-WMISH analysis.

Microsurgery

PMCs removal and archenteron removal were carried out at the mesenchyme blastula and early gastrula stages, respectively, as described previously (Ettensohn and McClay, 1988; McClay and Logan, 1996).

Cell proliferation assay

EdU (5-ethynyl-2-deoxyuridine') labeling and detection by click chemistry was carried out using the Click-iT EdU cell proliferation kit (Invitrogen). Control experiments showed that EdU remained stable in seawater for at least 24 hours and was incorporated within 15 minutes by cells that were in S phase. Aphidicolin, an inhibitor of DNA polymerase I, effectively blocks DNA replication and cell division in the sea urchin embryo (Stephens et al., 1986). Control studies confirmed that 0.3 mg/ml aphidicolin blocked the incorporation of EdU within 15 minutes. For PMC-removal experiments, embryos were placed in 1 mM EdU 30-60 minutes prior to PMC removal and were incubated continuously in the presence of EdU. 7-11 hours after PMC removal, embryos were fixed and stained with monoclonal antibody (MAb) 6a9 (Ettensohn and McClay, 1988). For (PMC + archenteron) removal experiments, PMCs were removed at the mesenchyme blastula stage and the archenteron was removed 2-3 hours later, at the early gastrula stage. Embryos were transferred to 1 mM EdU 1 hour prior to the removal of the archenteron and were incubated continuously in the presence of the label. Embryos were fixed and immunostained with MAb 6a9 12 or 22 hours after removal of the archenteron. For all experiments that used aphidicolin, the inhibitor was added to the seawater 30 minutes prior to the addition of EdU.

3.4 Results

3.4.1 During transfating, the upstream regulation of the PMC GRN is modified but the downstream network is faithfully recapitulated

The transcription factor *alx1,* which in the micromere-PMC GRN is regulated by a de-repression system mediated by *pmar1*, is activated in NSM cells by novel, *pmar1*-independent input(s) (Ettensohn et al., 2007). To analyze the network in transfating cells in greater detail, we first focused on the activation of two other early genes in the network; *delta* and *tbr*. *Delta* is activated zygotically and is expressed in the large micromeres at the early blastula stage. *Delta* is subsequently downregulated in the micromeres and is expressed transiently in the NSM until the late mesenchyme blastula - early gastrula stage. The only known function of micromere-derived Delta is the induction of the NSM (Sweet et al., 2002), a function that is probably not required at the stage when NSM transfating occurs. To test whether *delta* is activated during transfating, two-color F-WMISH was performed on PMC(-) embryos at 2 and 5 hours post-depletion (hpd). F-WMISH showed that *delta* was not activated in the transfating cells, whereas *alx1* expression was clearly detectable in the same embryos **(Fig. 3.1.A-B`)**.

During normal development, *tbr* mRNA is provided maternally and zygotic activation of *tbr* occurs only in the large micromere territory (Fuchikami et al., 2002). The enrichment of *tbr* transcripts in the large micromere descendants was first detected by F-WMISH at the mid-blastula stage, 6-7 hours post fertilization, hpf **(Fig. 3.1.D`)** but *alx1* transcripts could be detected earlier, at the early blastula stage (5 hpf) **(Fig. 3.1.C).** Therefore, during normal development, the accumulation of *alx1* transcripts precedes the zygotic activation of *tbr*. We found by F-WMISH that *tbr* was activated in PMC(-) embryos as early as 2-3 hpd, similar to the time when we first began to detect *alx1* transcripts, suggesting that both *alx1* and *tbr* were activated quite early, and nearly simultaneously, during transfating. To test more directly whether *alx1* and *tbr* were activated simultaneously in the transfating cells, we performed two-color F-WMISH with *alx1* and *tbr* probes on PMC(-) embryos at 2 and 3 hpd. At 2 hpd, when the process of transfating was just being initiated, we could detect the expression of *alx1* in only 4/11 embryos, and every embryo that expressed *alx1* also expressed *tbr* **(Fig. 3.1.E,E`)**. By 3

hpd we could detect the activation of both *alx1* and *tbr* in every embryo (n=10) **(Fig. 3.1.F,F`)**. Our findings indicate that these early regulatory genes are activated in a different temporal sequence during normal and regulative development; i.e., they are activated nearly simultaneously in transfating NSM cells, whereas the activation of *alx1* precedes that of *tbr* in the large micromere-PMC lineage.

We next examined the expression in PMC(-) embryos of several downstream genes in the skeletogenic GRN. We focused on the expression of five genes; *dri* (Amore et al., 2003), *foxB* (Minokawa et al., 2004), *jun* (Oliveri et al., 2008), *vegfr-Ig-10* (Duloquin et al., 2007) and *fgfr-2* (Rottinger et al., 2008). *Dri*, *foxB* and *jun* are late regulatory genes; *dri* and *foxB* are downstream targets of *alx1* (Oliveri et al., 2008) but nothing is known about the upstream regulation of *jun*. *Vegfr-Ig-10* and *fgfr-2* are tyrosine kinase receptors that have recently been implicated in PMC guidance and differentiation. The orthologs of these genes in L. variegatus were cloned using degenerate RT-PCR and RACE. We asked (i) whether these genes were activated during transfating, (ii) whether they were co-expressed in precisely the same cells, and (iii) whether their timing of activation mimicked that seen during normal development. To address these questions, we performed two-color F-WMISH for each gene in combination with *alx1* at different times after PMC removal. These studies showed that each of the five genes was activated in the same cells that expressed *alx1* during transfating **(Fig. 3.2.A-E``)**. This analysis also suggested that the order of activation of these genes was similar to that observed during normal development. For example, *fgfr-2* and *vegfr-Ig-10* are ordinarily activated later than the upstream regulatory genes in the network (Duloquin et al., 2007; Oliveri et al., 2008; Rottinger et al., 2008). In PMC(-) embryos these genes were activated only when transfating NSM cells began to migrate away from the tip of the archenteron (10-11 hpd) **(Fig. 3.2.D-E``)**, whereas transfated cells that had still not acquired a mesenchymal character did not have detectable levels of these mRNAs **(arrowhead, in Fig. 3.2.D-E``)**.

3.4.2 Presumptive blastocoelar cells transfate following PMC removal

NSM cells occupy the central region of the vegetal plate at the mesenchyme blastula stage, and during gastrulation, these cells are located at the tip of the growing

archenteron (Ruffins and Ettensohn, 1996). PMC removal induces the activation of *alx1* in cells at the tip of the archenteron (Ettensohn et al., 2007), indicating that the transfating cells lie within the NSM territory. It is unclear, however, whether all cells within this territory activate the network, or whether it is deployed by a specific subpopulation of NSM cells.

Pigment cells are the first NSM cells to undergo EMT. By the mid-gastrula stage, most pigment cells have migrated into the aboral ectoderm (Gibson and Burke, 1985). We confirmed this pattern of migration in *L. variegatus* by F-WMISH with *pks*, a gene specifically expressed by pigment cells (Calestani et al., 2003) **(Fig. 3.3.A-D)**. During transfating, *alx1* expression was detected within 2-3 hpd in cells that were located near the tip of the archenteron. These cells were epithelial in origin and maintained their epithelial character until the late gastrula stage (10-11 hpd), when they became mesenchymal and migrated away from the tip of the archenteron**.** Based on their very different locations in the embryo, it appeared unlikely that pigment cells contributed to the population of alx1(+) cells. We considered the possibility, however, that microsurgical depletion of PMCs might alter the pattern of pigment cell migration. To test this possibility, we examined the specification and migration of pigment cells in PMC(-) embryos at 2, 4 and 6 hpd by F-WMISH with *pks*. We found that the number and pattern of migration of pigment cells in PMC(-) and control embryos were indistinguishable **(Fig. 3.4.A-G)**, confirming that pigment cells do not contribute significantly to the population of transfating NSM cells.

Inhibiting the Delta-Notch signaling pathway using a Delta MO*,* or mis-expressing a dominant negative form of Notch, leads to the development of embryos that completely lack pigment cells (Sherwood and McClay, 1999; Sweet at al., 2002). We assayed the expression of the pigment cell marker *pks* and the blastocoelar cell marker *scl* in Delta MO-injected embryos. We found that the expression of *pks* was completely blocked in such embryos, but the expression of *scl* was still detectable **(Fig. 3.5.A-D)**. These observations confirmed that the Delta MO blocked pigment cell specification but had little effect on blastocoelar cell specification. We next examined the effect of blocking Delta-Notch signaling on transfating. Delta MO-injected, PMC(-) embryos were immunostained with MAb 6a9, which recognizes a family of PMC-specific cell surface

proteins (MSP130 proteins). We observed large numbers of 6a9-positive cells at the tip of the archenteron at 10 hpd **(Fig. 3.5.F)**, indicating that NSM transfating was not significantly perturbed by the absence of Delta signaling. Also, as in PMC(-) embryos, *alx1* was activated between 2-3 hpd in cells that were located at the tip of the archenteron **(Fig. 3.5.E)**. These findings indicated that in the absence of Delta signaling (and in the absence of pigment cells) transfating was robust and occurred on schedule.

Blastocoelar cells leave the tip of the archenteron during gastrulation (Tamboline and Burke, 1992). Two-color F-WMISH analysis shows that *ets1* is ordinarily expressed by blastocoelar cells, but not by pigment cells (Sharma and Ettensohn, unpublished observations). In this study, we found that transfating cells co-expressed *alx1* and *ets1*, suggesting that they might be presumptive blastocoelar cells **(Fig**. **3.6.A-A``)**. To analyze this further, we cloned the blastocoelar cell markers *gata1/2/3* and *scl* in *L. variegatus*. *Gata1/2/3* and *scl* are expressed by presumptive blastocoelar cells at the early mesenchyme blastula stage (Duboc et al., 2010; Sharma and Ettensohn, unpublished observations). Because the transfating response begins remarkably quickly (2-3 hpd), we suspected that we might detect the co-expression of *alx1* and *gata1/2/3* (or *scl*) mRNAs in single cells. We performed two-color F-WMISH on PMC(-) embryos at 2.5 hpd using *alx1* and *gata1/2/3* (or *scl*) and, as a control, we examined the expression of *alx1* and *pks* in sibling PMC(-) embryos. We found that *alx1* was expressed by cells that also expressed *gata1/2/3* and *scl* **(Fig. 3.6.B-C")**, but not by *pks*-expressing cells **(Fig. 3.6.D-D``).** We randomly selected *alx1*-positive cells in these specimens and found that almost all (54/57, or 95%) also expressed *scl* or *gata1/2/3* (note that *scl* and *gata1/2/3* are co-expressed at this stage; therefore, the expression of either gene implies the expression of both.) These observations indicate that most transfating cells are presumptive blastocoelar cells.

3.4.3 Endoderm transfating involves the re-establishment of a blastocoelar cell-like state and a delayed activation of the PMC GRN

Endoderm cells are conditionally specified and have the capacity to activate the skeletogenic program following the microsurgical removal of the PMCs and the archenteron, which includes the NSM territory (McClay and Logan, 1996). We refer to

such embryos as PMC(-), arch(-) embryos. At present, nothing is known concerning the deployment of the PMC GRN in such embryos. To determine the timing of activation of the PMC GRN, we first assayed for the expression of *alx1* in PMC(-), arch(-) embryos at various times after archenteron removal. *Alx1* was first expressed 7-8 hours after surgery in cells that were located at the tip of the archenteron, **(Fig. 3.7.A)**. Thus, there is significant delay (~5 hours) in the deployment of the PMC GRN during endoderm transfating as compared to the activation of the network during NSM transfating.

We also examined the expression of *scl* and *ets1* in PMC(-), arch(-) embryos and found that the expression of these blastocoelar cell markers was also re-established at the tip of the archenteron **(Fig. 3.7.B,C)**. To test directly whether *scl*- and *ets1*-expressing cells were the cells that activated *alx1* during endodermal transfating, we performed two-color F-WMISH, and found that the *scl*- and *ets1*-positive cells also expressed *alx1* **(Fig. 3.7.D``,E``)**. We conclude that, during endoderm transfating, cells at the tip of the archenteron re-establish a blastocoelar cell-like regulatory state and these same cells activate the PMC GRN.

3.4.4 The role of MAPK signaling differs in regulative and normal development

During normal development, the MAPK signaling pathway is required for PMC ingression and for maintaining the expression of *alx1* in the large micromere-PMC lineage (Rottinger et al., 2004; Sharma and Ettensohn, 2010). We tested the role of MAPK signaling in controlling the expression of another early regulatory gene in the PMC GRN, *tbr*. We found that, as in the case of *alx1*, there was robust activation of *tbr* in embryos treated continuously from the two-cell stage with the MEK-inhibitor U0126, but by the pre-ingression blastula stage, *tbr* transcripts were no longer detectable by F-WMISH **(Fig. 3.8)**. We also observed that in the presence of U0126, downregulation of *alx1* transcripts occurred earlier than the downregulation of *tbr* transcripts; this difference might reflect a higher abundance or a greater stability of *tbr* transcripts.

Previous studies have shown that MAPK signaling is required for the process of transfating (Ettensohn et al., 2007). We looked more closely at the role of MAPK pathway during transfating, focusing on the initial phase of activation of *alx1* and *tbr*. In control PMC(-) embryos, *alx1* and *tbr* expression was detected by 2 hpd **(Fig. 3.9.A,A`)**

(6/6 embryos). In PMC(-), U0126-treated embryos, however, the activation of *alx1* and *tbr* was suppressed (4/5 embryos showed no detectable expression in any cell, 1/5 showed a greatly reduced number of positive cells) **(Fig. 3.9.B,B`)**. We also confirmed that *alx1* and *tbr* were not expressed at 4 hpd **(Fig. 3.9.D,D`)** (10/10 embryos lacked expression in any cell), indicating that the inhibitor did not simply delay the activation of these genes. These findings point to a significant difference in the role of MAPK signaling in the skeletogenic GRN as it is deployed in the large micromere-PMC lineage and in transfating NSM cells. During normal development, MAPK signaling is required for the maintenance, but not for the activation, of the GRN. In contrast, our inhibitor studies reveal no MAPK/ets-independent mechanisms of GRN activation in NSM cells; instead, MAPK signaling is required for the initial deployment of the network. We found that the expression of *ets1* itself was not affected in PMC(-), U0126-treated embryos **(Fig. 3.9.E,F)**.

To test whether the MAPK-signaling pathway is also essential for activating the PMC GRN during endoderm cell transfating, PMC(-), arch(-) embryos were treated with U0126 and the expression of *alx1* was analyzed. We found that *alx1* was not expressed in these embryos (4/5 embryos showed no expression, 1 embryo had a single labeled cell) **(Fig. 3.10.D),** whereas all control (sibling, DMSO-treated) PMC(-), arch(-) embryos showed robust expression **(Fig. 3.10.C).** U0126-treated PMC(-), arch(-) embryos also did not secrete a larval skeleton **(Fig. 3.10.B)**. These results indicate that the MAPK pathway is also required for the activation of the PMC GRN during endoderm transfating, in contrast to its role during normal development.

3.4.5 Cell division is not required for transfating by NSM or endoderm cells

We incubated embryos with EdU, a thymidine analogue, to determine whether NSM cells divide during transfating. Transfated NSM cells were identified 7-11 hours after PMC removal by immunostaining with MAb 6a9. Under these conditions, most 6a9-positive cells (150/229, or 66%) were not labeled with EdU, indicating that they had fully deployed the skeletogenic network in the absence of DNA synthesis and cell division **(Fig. 3.11.A,A')**. Some 6a9-positive, EdU-positive cells probably underwent mitosis during the course of the experiment; therefore, the actual fraction of NSM cells that were

present at the time of PMC removal and which activated the skeletogenic GRN without dividing was presumably greater than 66%. Because NSM cells and PMCs are both derived from mesoderm, we also asked whether cell division might be required for more extensive GRN reprogramming; i.e., across a germ layer boundary. EdU labeling of PMC(-), arch(-) embryos showed that the majority of endoderm cells that deployed the GRN under these conditions did not undergo DNA synthesis **(Fig. 3.11.B, B')**. 12 hours after NSM removal, 65/83 (78%) of 6a9-positive cells were not labeled with EdU. To confirm that cell division was not required for transfating, we treated embryos with aphidicolin, an inhibitor of DNA polymerase I that blocks DNA synthesis and cell division in sea urchin embryos (Stephens et al., 1986). We observed a robust transfating response in PMC(-) embryos **(Fig. 3.11.C)** and PMC(-), arch(-) embryos (data not shown), despite the inhibition of DNA synthesis (indicated by a lack of EdU labeling throughout the embryo).

3.5 Discussion

In the sea urchin embryo, maternal factors and differential zygotic gene expression partition the embryo into distinct transcriptional domains very early in development. The transcriptional networks that are deployed during early development are relatively shallow and lead rapidly to the regional expression of terminal differentiation genes in various embryonic territories. Despite these early patterning processes, genomic regulatory programs are not fixed and many cells remain developmentally labile, even quite late in development. In this study, we have taken advantage of the recent elucidation of GRNs in the sea urchin embryo (in particular, the well-defined micromere-PMC GRN) to address questions related to developmental plasticity and genomic reprogramming.

During normal development, the skeletogenic GRN is activated by maternally-entrained mechanisms that operate autonomously within the large micromere-PMC lineage **(Fig. 3.12)**. The local stabilization of β-catenin in the vegetal region of the embryo directly activates *pmar1* and, because Pmar1 is a repressor, it presumably activates the GRN by blocking the expression of a second repressor (Oliveri et. al., 2002). One target of Pmar1 is the repressor, *hesC* (Revilla-i-Domingo et al., 2007). The repression of *hesC* does not account for the initial activation of the PMC GRN, however, as the level of *hesC* mRNA does not decline in the large micromere territory until after the network has been activated there (Sharma and Ettensohn, 2010). It is likely, therefore, that additional local activators and/or repressors are involved. We have also shown that the expression of two early genes, *alx1* and *delta*, but not that of *pmar1*, is dependent on unequal cell division (Sharma and Ettensohn, 2010). These various inputs lead to the activation of a core set of early genes, which include *alx1*, *tbr*, *ets1*, and *delta.* Although these genes are usually considered to have a common mechanism of activation, it appears that they are not expressed synchronously in the large micromere territory; a variety of evidence indicates that the zygotic activation of *tbr* follows that of *alx1* and *delta* (Croce et al., 2001; Croce and McClay, 2010; Ettensohn et al., 2003; Fuchikama et al., 2002; Ochiai et al., 2008). Our multiplex F-WMISH analysis confirmed that, in *L.*

variegatus, the accumulation of *alx1* mRNA in the large micromere territory precedes that of *tbr* mRNA.

In striking contrast to the deployment of the network during normal development, the activation of the GRN in NSM cells (and endoderm cells) is tightly regulated by extrinsic signals and is independent of *pmar1* (Ettensohn et al., 2007). The present study has revealed several additional differences in the upstream regulation of the network in transfating NSM cells (**Fig. 3.12**). There is a shift in the relative timing of expression of *alx1* and *tbr*, a finding that points to possible changes in the upstream regulation of the network during transfating. Moreover, we find that *delta* is not activated by transfating NSM cells. The role of micromere-derived Delta is to specify the overlying NSM, a function that is likely to be irrelevant at the stage when the process of NSM transfating is initiated. One hypothesis is that the loss of *delta* expression in the NSM [which normally occurs by the early gastrula stage (Sweet et al., 2002)] occurs by mechanisms that are irreversible; therefore, *delta* might no longer respond to the same inputs that ordinarily activate this gene in the micromere-PMC lineage. An alternative hypothesis, however, is that some or all of the inputs that ordinarily coordinate the activation of *alx1*, *tbr*, *ets1*, and *delta* in the micromere territory are not employed during transfating, and therefore these genes are no longer subject to parallel regulation.

The MAPK signaling pathway provides essential inputs into the micromere/PMC GRN. This pathway is believed to result in the phosphorylation of Ets1, which is required for maintaining (but not for activating) the expression of *alx1* and *tbr* during normal development (Rottinger et al., 2004; Sharma and Ettensohn, 2010; this study). In contrast, we have found that MAPK signaling is required for the activation of both *alx1* and *tbr* in transfating NSM and endoderm cells. Inhibition of MAPK signaling does not affect the expression of *ets1,* either in the large micromere-PMC lineage (Rottinger et al., 2004) or in transfating NSM cells (this study), a finding which supports the view that MAPK signaling acts downstream of *ets1* transcription. Overall, our results suggest that phosphorylated Ets1 provides an essential, early input into *alx1* and *tbr* in transfating NSM cells, while its role during normal development is to provide a late input that maintains the expression of these genes.

Gene epistasis studies and/or cis-regulatory analyses of *alx1*, *tbr*, and *delta* have identified positive inputs from Ets1 and negative inputs from HesC (Ochiai et al., 2008; Revilla-i-Domingo et al., 2007; Smith and Davidson, 2008; Wahl et al., 2009). During gastrulation, *ets1* is expressed in the NSM territory and *hesC* is silent, yet *tbr* and *alx1* are not ordinarily expressed by NSM cells. Moreover, the Ets1 protein that is produced is concentrated in the nuclei of NSM cells (Ettensohn, unpublished observations) and is likely phosphorylated, as ERK is active in the NSM territory (Rottinger et al., 2004; Rizzo et al., 2006). Wahl and co-workers have suggested that, in NSM cells, Erg competes with Ets1 for binding to the same DNA target sites but lacks an activation function; this might not occur in PMCs if levels of Erg are too low (Wahl et al., 2009). Thus, the network might be activated in NSM cells via a double-repression mechanism, whereby Erg (or a different repressor) is inactivated following the loss of the PMC-derived signal. Many other models may be envisioned, however.

Whatever regulatory mechanisms are responsible for the activation of *alx1* and *tbr* in the NSM territory during transfating, it is evident that they are deployed quite rapidly. It was previously reported that *alx1* expression is detectable in NSM cells 3-4 hpd (Ettensohn et al., 2007). In this study, using a more sensitive method, we have documented the accumulation of *alx1* transcripts in NSM cells 2-3 hpd. *Alx1* is a relatively large gene (~37 kb) and, following the activation of *alx1* transcription, approximately 40 minutes would be required for the appearance of the first complete transcript, assuming a transcription rate of 900 nt/minute at 24°C (Ben-Tabou de-Leon and Davidson, 2009). Thus, *alx1* transcription is probably initiated less than 2 hours after PMC removal.

Analysis of a set of downstream genes in the PMC GRN, which included the late regulatory genes *dri*, *jun* and *foxB*, and the tyrosine kinase receptors *vegfr-Ig-10* and *fgfr-2*, reveals that these genes are activated in transfating NSM cells in a temporal sequence that resembles their order of activation during normal development. These findings support the view that, despite differences in the upstream inputs into the network, and differences in the regulatory states of PMCs and NSM cells at the time that the network is activated, the later regulatory layers of the skeletogenic GRN are fully recapitulated during NSM transfating. The faithful deployment of the downstream layers of the

network explains the remarkable extent to which the morphogenetic behaviors of transfated NSM cells mimic those of PMCs. For example, during transfating, NSM cells become competent to respond to PMC-specific migratory guidance cues. Our finding that transfating cells activate the expression of *vegfr-Ig-10* and *fgfr-2*, two receptors that have recently been implicated in PMC migration and guidance (Duloquin et al., 2007; Rottinger et al., 2008), partly explain these dramatic changes in cell behavior.

Pigment and blastocoelar cells are the two principal populations of migratory NSM cells. A previous study suggested that the subpopulation of NSM cells that transfate might be presumptive pigment cells (Ettensohn and Ruffins, 1993). Due to the lack of molecular markers at that time, this finding was based solely on a ~50% reduction in the numbers of pigment cells in PMC(-) embryos at the pluteus larva stage. In this study, using molecular markers for pigment and blastocoelar cells, and focusing specifically on the initial stages of transfating, we show that the great majority of cells that transfate following PMC removal are scl(+), gata1/2/3(+) cells that lie on the oral (ventral) side of the archenteron; i.e. cells that would otherwise give rise predominantly to blastocoelar cells. One possible explanation for the reduced numbers of pigment cells in PMC(-) larvae is that mitotic divisions of pigment cells that occur after ingression are perturbed in some way by PMC removal.

Blastocoelar cells and PMCs exhibit similar morphogenetic behaviors, including EMT, filopodia-based motility, and cell-cell fusion. Several regulatory genes of the PMC GRN are also ordinarily expressed by blastocoelar cells, including members of the *ets* family (*ets1*, *erg*, and *ese*) (Rizzo et al., 2006; Rottinger et al., 2004), the *forkhead* family (*foxN2/3* and *foxO*) (Tu et al., 2006), and *snail* (Wu and McClay, 2007). We have recently identified many extracellular matrix proteins and cytoskeletal proteins that are selectively co-expressed by these two cell types (Rafiq and Ettensohn, unpublished observations). These observations point to striking similarities in the molecular programs of PMCs and blastocoelar cells and suggest that they share elements of a common mesenchymal regulatory state. The regulatory states of the two cell types are distinct in other respects, however. For example, *foxa*, *gcm*, *scl*, and *gata1/2/3* are all expressed in presumptive blastocoelar cells prior to gastrulation, but these genes are never expressed in the large micromere territory.

McClay and Logan (1996) showed that presumptive endoderm cells have the capacity to activate the PMC GRN. We have confirmed that PMC removal, followed by removal of the NSM territory, induces the ectopic activation of the skeletogenic GRN in a subset of presumptive endoderm cells. *Alx1*, and early marker, accumulates in cells near the tip of the regenerated archenteron, but in a delayed fashion compared with PMC(-) embryos, a delay that may reflect a more extensive genomic reprogramming. Our findings show that activation of the GRN by endoderm cells occurs via the regeneration of an NSM territory, by mechanisms that are unknown. During the regeneration process, endoderm cells re-establish at least some elements of a blastocoelar cell regulatory state, as shown by the *de novo* activation of *scl* and *ets1*. The activation of *alx1* in transfating endoderm cells, as in transfating NSM, is dependent on MAPK signaling and likely acts via Ets1 phosphorylation. These findings highlight the fact that the same GRN circuitry can be fully deployed within the context of multiple, pre-existing cell regulatory states.

Cell division has been proposed to play an important role in facilitating genomic reprogramming. Many transcription factors, including RNA polymerase II, are released from chromatin during mitosis, which may promote reprogramming (Egli et al., 2008). Nuclear envelope disassembly/reassembly might allow global changes in nuclear architecture that alter patterns of gene expression (Reddy et al., 2008). An early step in the conversion of somatic cells into induced pluripotent stem (iPS) cells is the acquisition of a program of rapid division (Smith et al., 2010), and experimental manipulation of cell cycle regulators indicates that proliferation is required for iPS cell formation (Ruiz et al., 2011). On the other hand, substantial reprogramming of somatic cell nuclei occurs in heterokaryons in the absence of DNA synthesis and cell division (Bhutani et al., 2010).

Our findings show that most transfating cells do not undergo mitosis during their reprogramming to a PMC-like state. In the case of NSM cells, this finding is consistent with the rapid deployment of the GRN (this study), and the relatively long, average cell cycle time at the gastrula stage (>6 hours in *L. variegatus*) (Nislow and Morrill, 1988). Surprisingly, even in the case of the slower (and presumably more extensive) reprogramming of endoderm, a large majority of the cells do not undergo mitosis during the transfating process. These findings show that unequal cell division, which plays a pivotal role in activating the skeletogenic GRN in the micromere-PMC lineage during

normal development (Sharma and Ettensohn, 2010), is not required for the regulative activation of the GRN. This is consistent with the view that the unequal division of vegetal blastomeres, and the linkages between this pattern of division and GRN activation, are recent evolutionary inventions (Ettensohn, 2009). More generally, our findings show that, at least in the context of the reprogramming of developmental GRNs, the dissociation of transcription factors from DNA, or other changes in nuclear organization during mitosis, do not play a critical role in the reprogramming process.

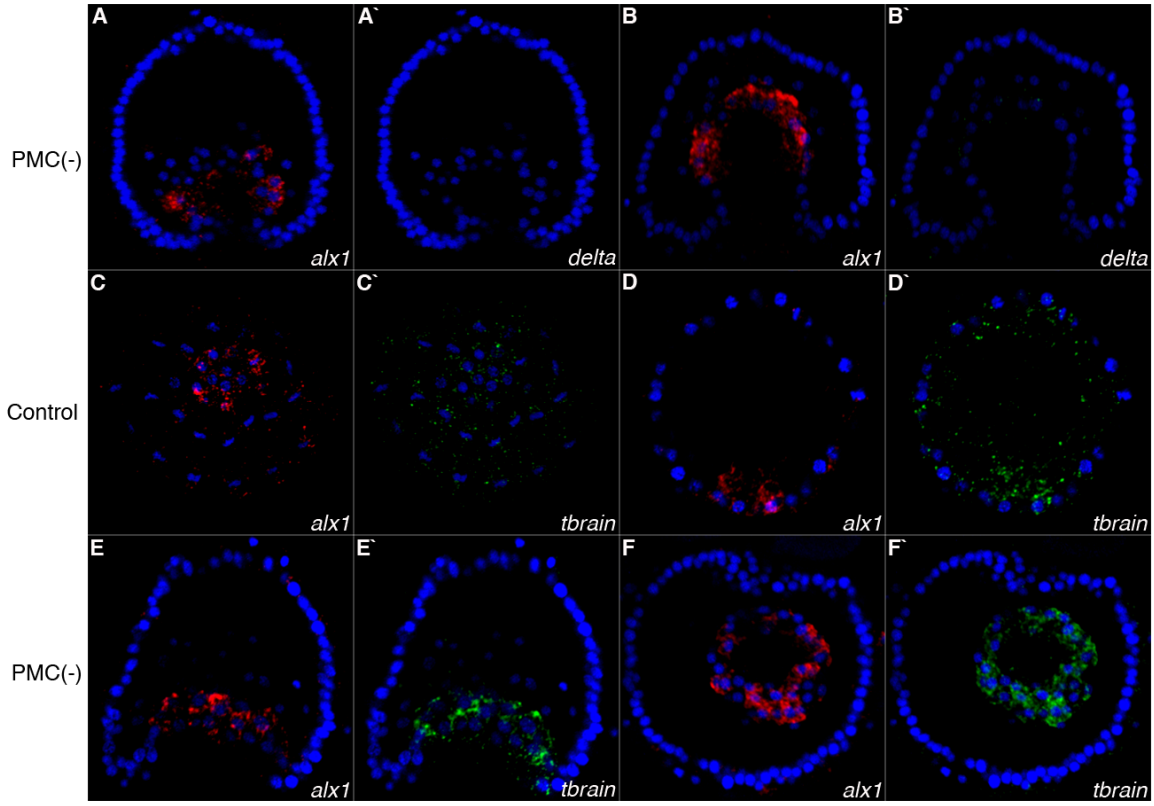

Fig. 3.1. The early skeletogenic GRN gene *tbr*, but not *delta*, is activated by transfating NSM cells. PMC(-) embryos were analyzed for the expression of *tbr* and *delta* at 2 and 5 hpd using two-color FWMISH in combination with *alx1*. **(A-B`)** The expression of *delta* is not detectable in the transfating cells (A`,B`), which are unambiguously identified by *alx1* expression (red, A,B). **(E-F`)** *Tbr* is activated in transfating cells, and its expression is detected as early as 2 hpd (C`), the earliest time at which *alx1* transcripts can be detected (C). **(C-D')** During normal development, *alx1* transcripts are detected at the early blastula stage (5hpf) (C, vegetal view), whereas *tbr* transcripts are detected at the mid-blastula stage (D'), showing that *alx1* expression precedes the expression of *tbr*.

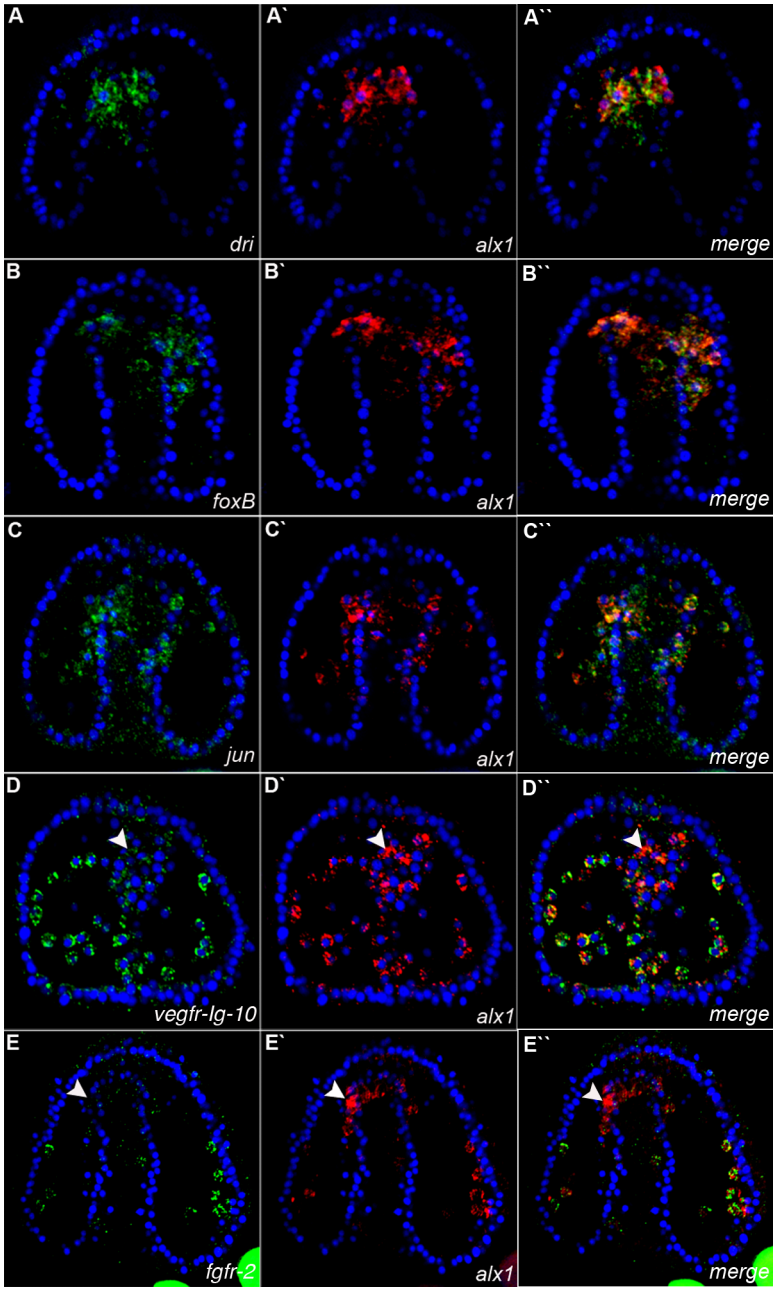

Fig. 3.2. The downstream PMC GRN is faithfully recapitulated during NSM transfating. The expression of *dri*, *foxB*, *jun, vegfr-Ig-10* and *fgfr2* (green) was analyzed by two-color F-WMISH in combination with *alx1* (red) in PMC(-) embryos at 5-11 hpd. Each image is a projection of several confocal sections. **(A-E``)** The regulatory genes *dri*, *foxB* and *jun* are expressed while transfating NSM cells are still associated with the archenteron (A-C``). Expression of *vegfr-Ig-10* and *fgfr2* is detectable only when the transfating cells begin to migrate away from the tip (D-E``); no expression is seen in cells that are still associated with the archenteron (arrowheads in D, D`, E, E`).

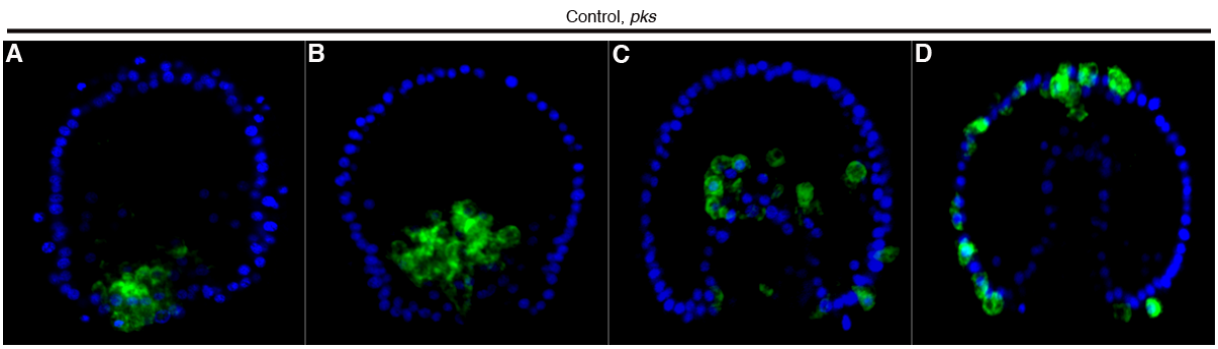

Fig. 3.3. Pattern of migration of pigment cells in *L. variegatus* embryos. (A-D) The expression of the pigment cell marker *pks* (green) was assayed by FWMISH at the mesenchyme blastula stage (A), early gastrula stage (B), mid gastrula stage (C), and late gastrula stage (D). Pigment cells ingress at the early gastrula stage (B) and by the late gastrula stage all pigment cells have migrated away from the tip of the archenteron (D).

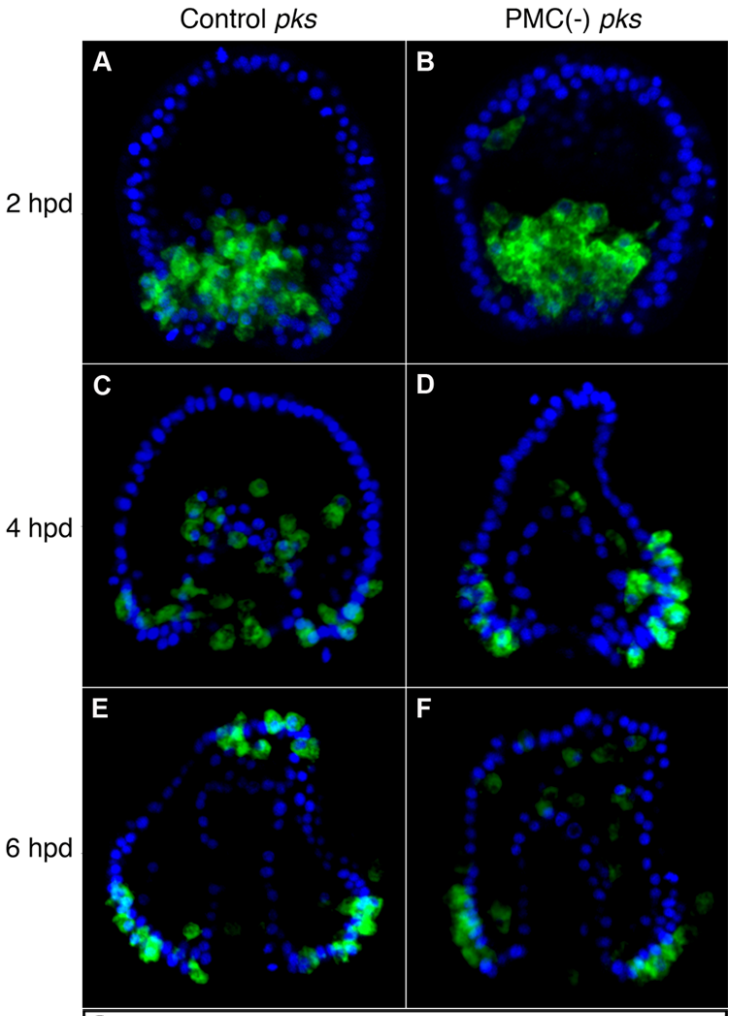

G	Average Number of Pigment Cells		
	2 hpd	4 hpd	6 hpd
Control Embryos	37 (n=4)	63 (n=3)	73 (n=3)
PMC(-) Embryos	44 (n=4)	66 (n=3)	61 (n=3)

Fig. 3.4. The specification and migration of pigment cells is unaffected by PMC removal. The migration pattern of pigment cells was examined in control and PMC(-) embryos by F-WMISH using *pks* as a marker. Each panel is a merged image of z-projections of confocal stacks (green, *pks*; blue, Hoechst). **(A,C,E)** Sibling control embryos at 2 hpd (A), 4 hpd (C) and 6 hpd (E) showing the normal pattern of pigment cell migration. **(B,D,F)** PMC(-) embryos at 2 hpd (B), 4 hpd (D) and 6 hpd (F). Depletion of PMCs at the mesenchyme blastula stage has no effect on the specification or migration of pigment cells. **(G)** Table showing the number of pigment cells in control and PMC(-) embryos at 2, 4 and 6 hpd. The number of pigment cells in PMC(-) embryos is comparable to the number of pigment cells in sibling control embryos.

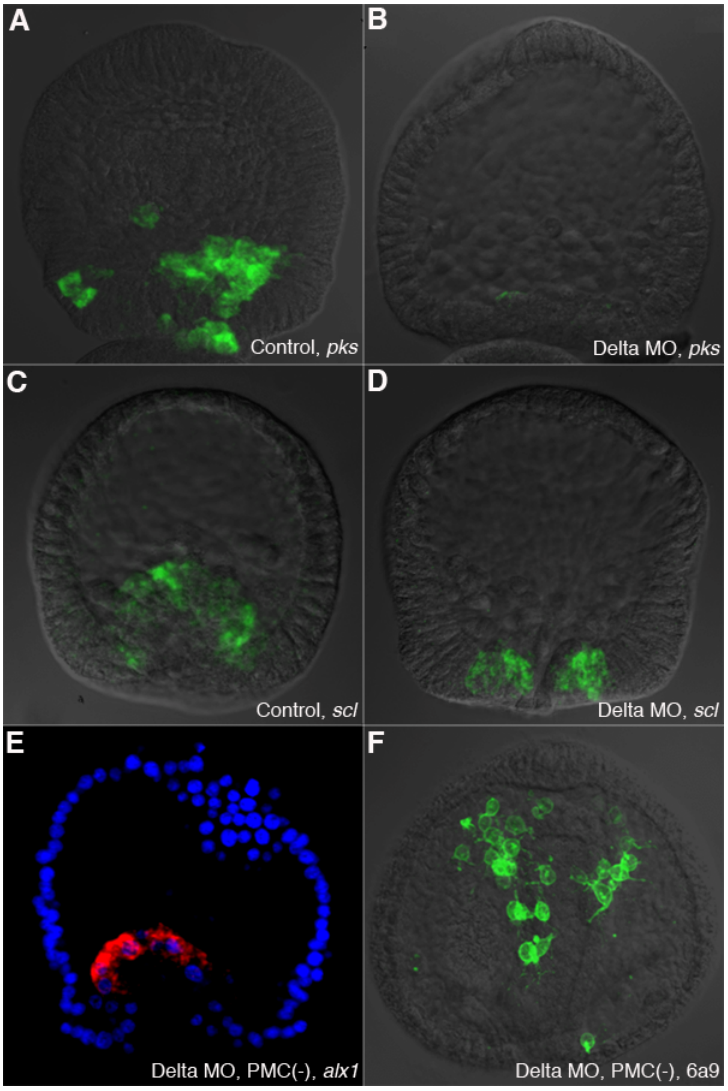

Fig. 3.5. Disruption of Notch-Delta signaling blocks pigment cell specification (but not blastocoelar cell specification) and does not affect transfating. The expression of *pks* and *scl* was examined by FWMISH in Delta MO-injected embryos. **(A-D)** *Pks* and *scl* expression in embryos injected with Delta MO. (A,C) Control embryos analyzed for *pks* expression (A), and *scl* expression (C). (B,D) Delta MO-injected embryos examined for the expression of *pks* (B), and *scl* (D). Each image is a z-projection of confocal slices and a single DIC image that was collected at the midpoint of the stack. Delta MO-injected embryos express *scl*, but not *pks*. The activation of the skeletogenic GRN in Delta morpholino, PMC(-) embryos was assessed by FWMISH using the *alx1* probe and by immunostaining with monoclonal antibody 6a9. **(E,F)** Delta MO-injected, PMC(-) embryos examined for *alx1* expression at 2 hpd (E) and for the presence of 6a9 positive cells at 10 hpd (F). The expression of *alx1* and the 6a9 antigen are unaffected by Delta knockdown.

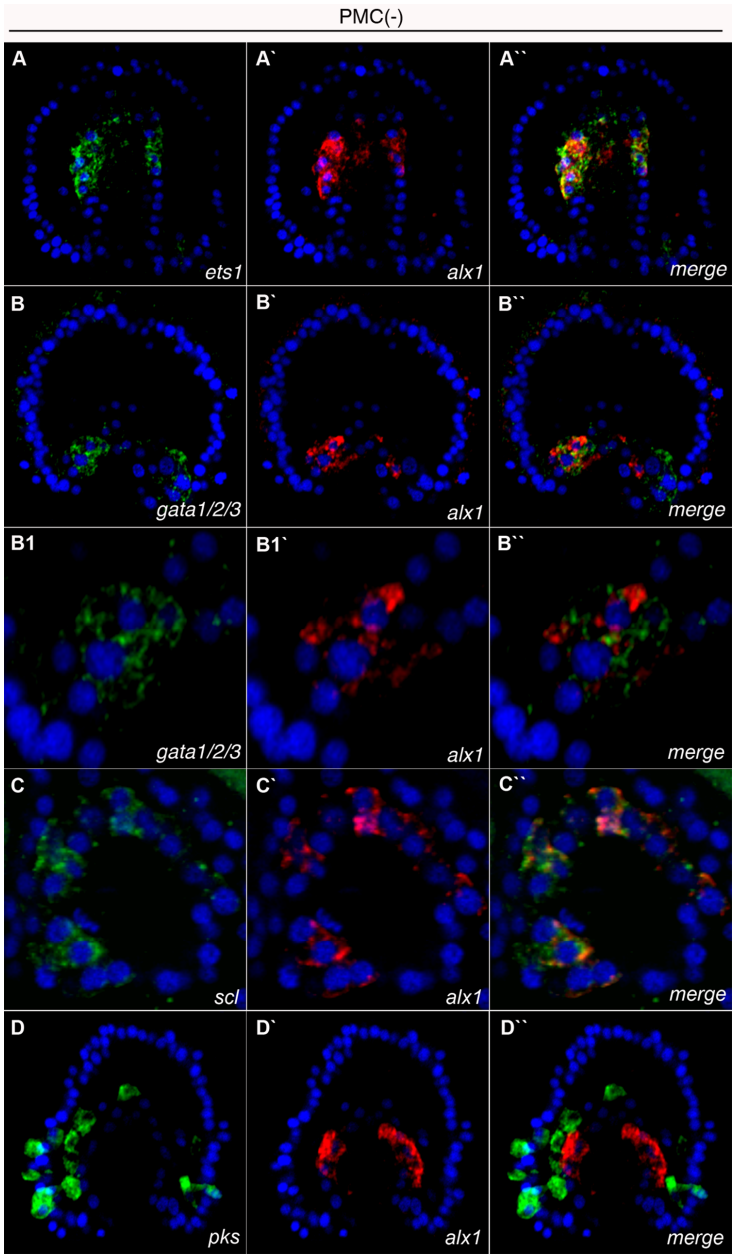

Fig. 3.6. Presumptive blastocoelar cells transfate following PMC removal. Two-color F-WMISH was performed on PMC(-) embryos using an *alx1* probe (red) and *ets1*, *gata1/2/3*, *scl* or *pks* probes (green). Embryos were counterstained with Hoechst dye (blue). Each panel is a projection of several confocal sections, except images B1-C``, which are digitally magnified views of a single section. **(A-A``)** Expression of *ets1* (A) and *alx1* (A`) in a PMC(-) embryo at 4 hpd. During transfating, *alx1* is activated in cells that also express *ets1*. **(B-B1``)** Expression of *gata1/2/3* (B,B1) and *alx1* (B`,B1`) in a PMC(-) embryo at 2.5 hpd. *Alx1* transcripts are detectable in cells that also express *gata1/2/3*. **(C-C``)** Expression of *scl* (C) and *alx1* (C`) in a PMC(-) embryo at 2.5 hpd. *Alx1* transcripts are detectable in cells that also express *scl*. **(D-D``)** *Pks* (C) and *alx1* (C`) expression in a PMC(-) embryo at 2.5 hpd. No *alx1* expression is detected in *pks*-positive cells.

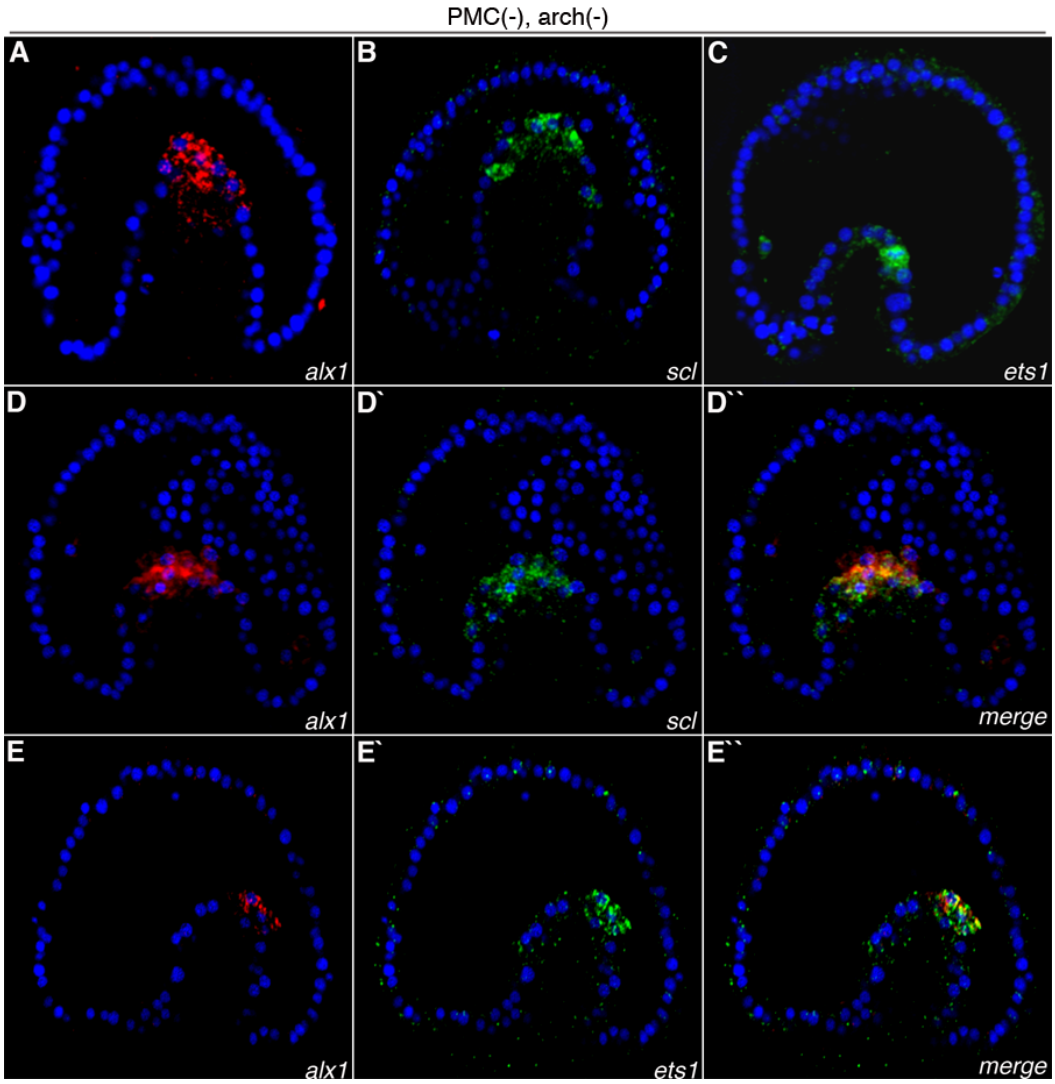

Fig. 3.7. In PMC(-), arch(-) embryos the skeletogenic GRN is activated in cells that re-establish a blastocoelar cell-like fate. (A) *Alx1* expression (green) in a PMC(-), arch(-) embryo. *Alx1* is activated 7-8 hours after archenteron removal, in cells at the tip of the regenerating archenteron. **(B,C)** *Scl* and *ets1* expression in a PMC(-) arch(-) embryo. The blastocoelar cell markers *scl* and *ets1* are also expressed in cells that are located at the tip of the archenteron. **(D-E``)** Two-color FWMISH using a fluorescein-labeled *alx1* probe (red) and digoxigenin-labeled *scl* or *ets1* probes (green) shows that *alx1* is expressed in cells that also express *scl* (D-D``) and *ets1* (E-E``).

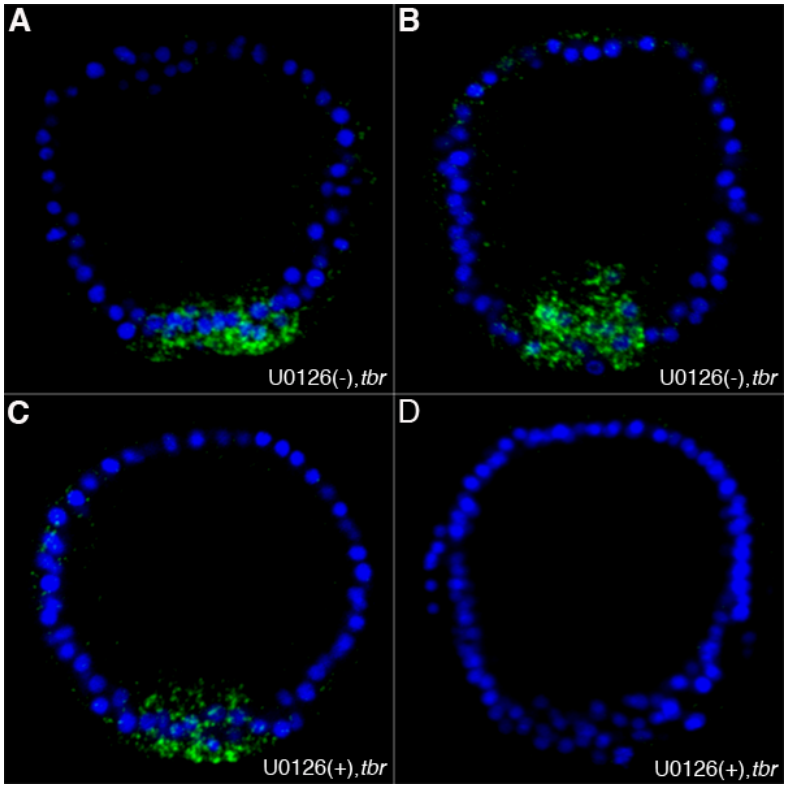

Fig. 3.8. The MAPK pathway is required for the maintenance of *Lvtbr* expression. Embryos were treated with 6 μM U0126 and *tbr* expression was assayed at 8 hpf (hatched blastula stage) and 10 hpf (pre-ingression blastula stage). **(A,B)** Control embryos showing normal *tbr* expression (green) at 8 hpf (A) and10 hpf (B). **(C,D)** U0126- treated embryos showing normal expression of *tbr* at 8 hpf (C), but a loss of *tbr* expression by 10 hpf

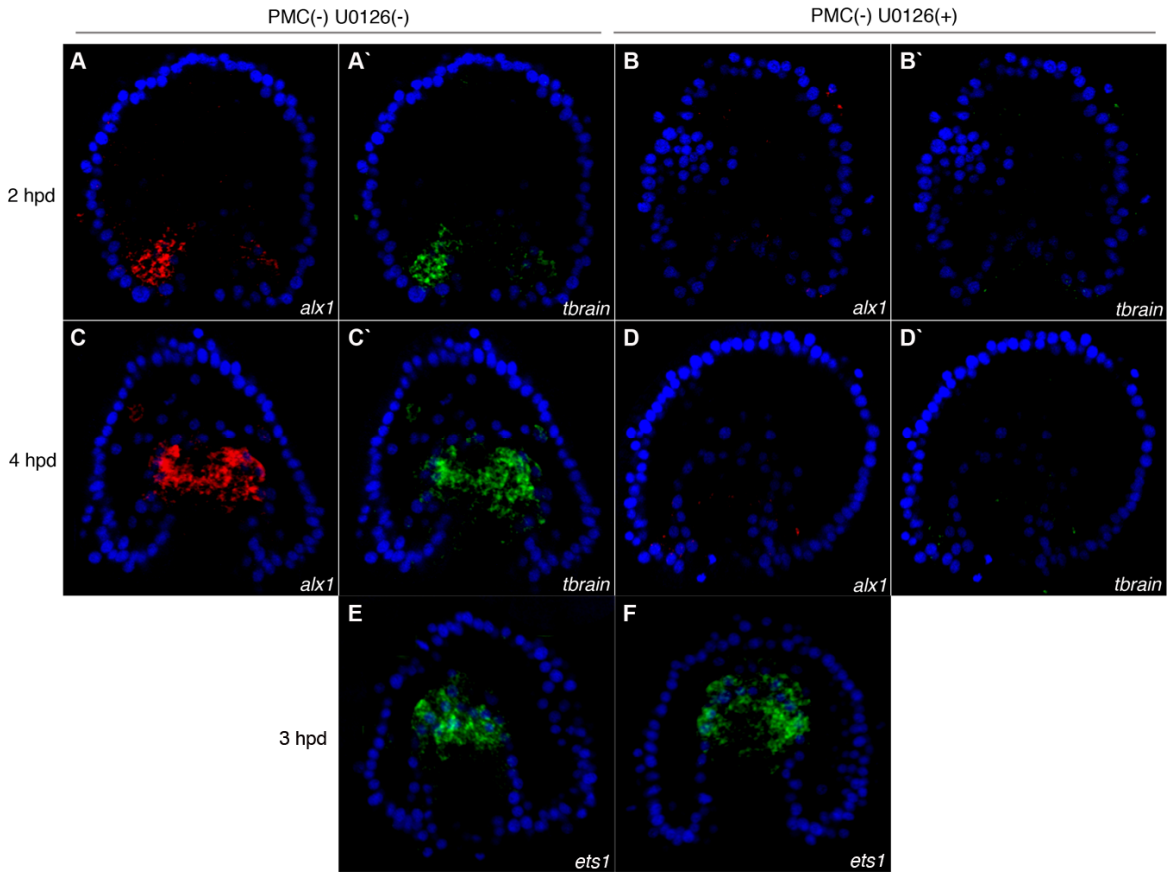

Fig. 3.9. The MAPK pathway is essential for activating the skeletogenic GRN during NSM transfating. The expression of *alx1* (red) and *tbr* (green) was assayed by two-color FWMISH in PMC(-) embryos that were treated with U0126 and in DMSO-treated, sibling PMC(-) embryos at 2 and 3 hpd. Each panel is a projection of several confocal slices. **(A,A`,C,C`)** Control PMC(-) embryos at 2 hpd (A,A`) and 3 hpd (C,C`) showing the activation of *alx1* and *tbr* during transfating. **(B,B`,D,D`)** PMC(-) embryos at 2 hpd (B,B`) and 3 hpd (D,D`) showing the absence of *alx1* and *tbr* activation in presence of U0126. **(E,F)** The expression of *ets1* in PMC(-) embryos that were treated with U0126 and in DMSO-treated, sibling PMC(-) embryos at 3 hpd. IN both PMC(-) control (E) and PMC(-), U0126-treated embryos, *ets1* is expressed by the transfating cells.

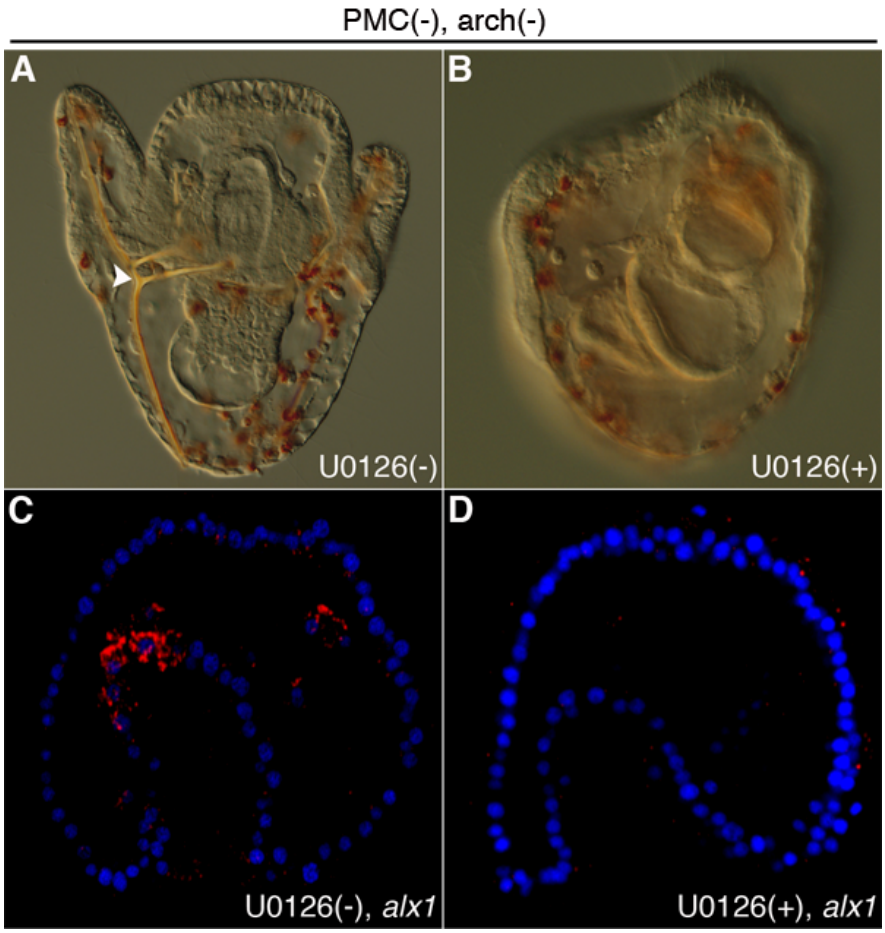

Fig. 3.10. Endodermal cell transfating requires MAPK signaling. (A) Control PMC(-), arch(-) embryo at 48 hpf. The arrowhead points to the skeleton. **(B)** Sibling PMC(-), arch(-) embryo treated with 6 μM U0126. Embryos treated with U0126 fail to form skeletal rods. **(C,D)** PMC(-), NSM(-) embryo were treated with U0126 and *alx1* expression was assayed 8 hours after archenteron removal. Embryos treated with DMSO alone show normal expression of *alx1* (C) but U0126-treated embryos fail to activate *alx1* (D).

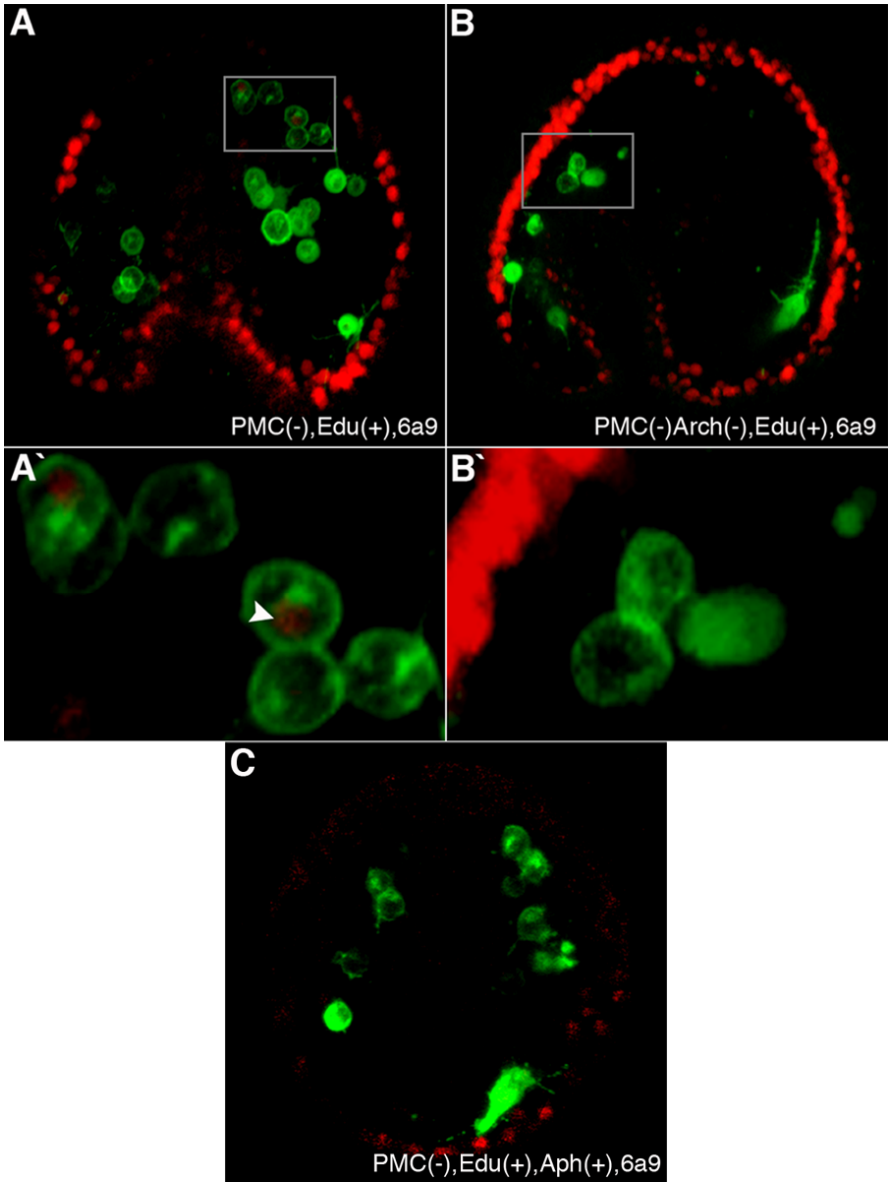

Fig. 3.11. Cell division is not required for NSM or endoderm transfating
MAb 6a9 immunostaining is shown in green. **(A)** An EdU treated, PMC(-) embryo at 9 hpd. Most transfated cells lack nuclear EdU label (red). **(A`)** Magnified view of the inset in panel A. The arrowhead points to a transfated cell that has incorporated EdU label (red). **(C)** An aphidicolin + EdU treated, PMC(-) embryo at 9 hpd. NSM cells transfate to a skeletogenic fate in the absence of DNA synthesis and cell division. **(B)** An EdU-treated PMC(-), arch(-) embryo at 12 hpd. Most transfated cells lack nuclear EdU label. **(B')** Magnified view of the inset in panel B.

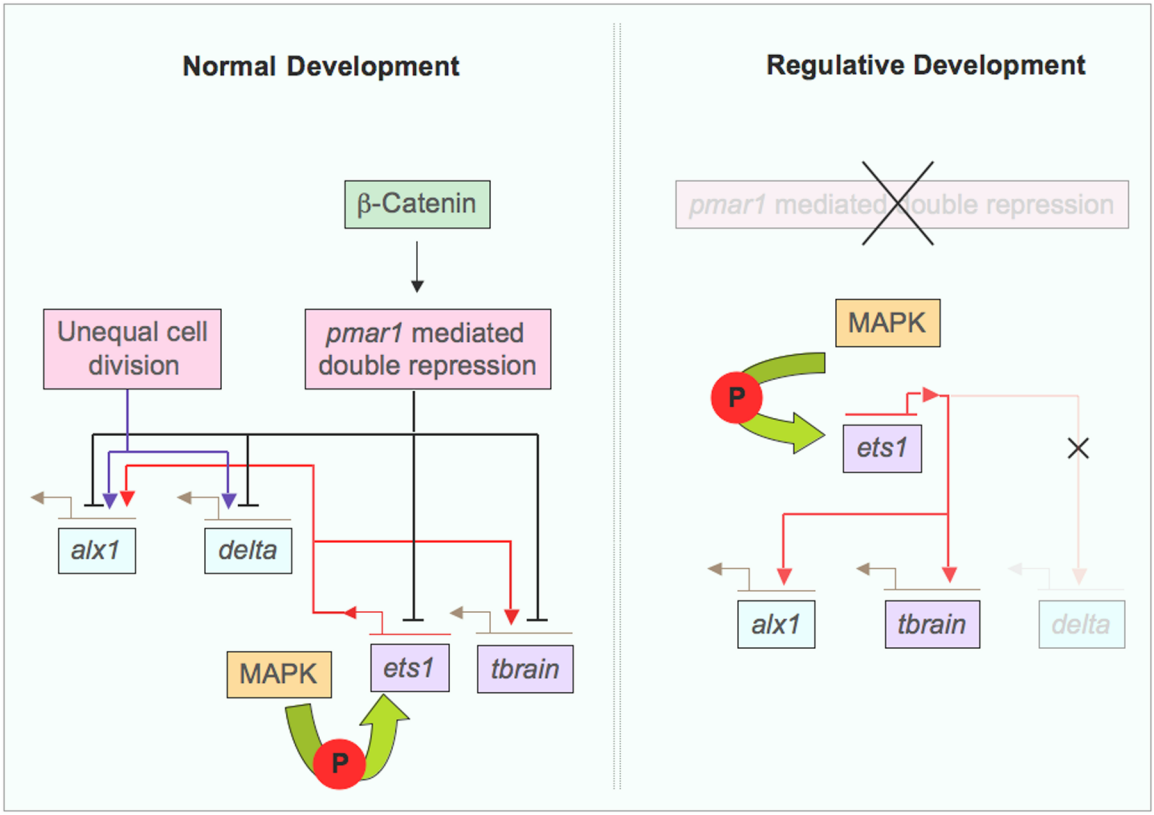

Fig. 3.12. Summary of known differences in the skeletogenic GRN during normal and regulative development.
The skeletogenic GRN during transfating is activated by *pmar1*-independent mechanisms. The regulative activation of the network (and not just its maintenance) is dependent on MAPK signaling, which likely mediates the phosphorylation of Ets1 (Rottinger et al., 2004). The transcription factors *alx1* and *tbr* are activated simultaneously in the transfating cells, whereas during normal development, the expression of *alx1* precedes that of *tbr*. *Delta* is not activated during transfating. Straight arrows and T-shaped bars represent activation and inhibition, respectively. Curved arrows represent phosphorylation.

Chapter 4

Conclusions and Future Directions

4.1 Conclusions and Future Directions

In this work we have studied the regulation of the skeletogenic GRN, focusing specifically upon the initial deployment of this network, during both normal and regulative development. We show that during normal development the activation of the early genes, *alx1* and *delta*, occurs prior to the transcriptional repression of *hesC* in the large micromeres. This finding argues against *hesC* repression being the only key event required to activate the skeletogenic GRN. Based on this finding we envision two possibilities. First, the presence of an additional unidentified repressor; second, the network might be activated by a Pmar1 independent mechanism. It is likely that Pmar1-HesC mediated double repression provides an input that is required only for maintaining the network. Our studies concerning the transcriptional regulation of *alx1* and *tbr* support the view that different inputs are responsible for activating and maintaining the expression of these genes.

The second possibility; i.e. the network is activated independent of Pmar1, can be tested experimentally by inhibiting Pmar1 protein function, and then assaying for the expression of *alx1* by FWMISH. In a preliminary study, we perturbed the function of Pmar1 (a repressor) by mis-expressing Pmar1 protein fused to the Vp16 activation domain. The Vp16 activation domain is known to activate *in-vivo* transcription (Triezenberg, et al., 1988; Sadowski et al., 1988). The Vp16-Pmar1 fusion protein has previously been reported to efficiently block Pmar1 function in the sea urchin species *H. pulcherrimus* (Yamaguchi et al., 2005). As in *H. pulcherrimus*, mis-expression of Vp16-Pmar1 protein in *L. variegatus* prevents PMC ingression, gastrulation and most embryos lack a skeleton (or some show a single mis-patterned skeletal rod) **(Appendix Fig. 1),** although the expression of *alx1* remains unaffected in these embryos **(Appendix Fig. 1)**. This result suggests that a Pmar1 independent mechanism might be responsible for activating the skeletogenic network. In the future, a more rigorous validation of this result is required, and in addition to *alx1* the activation of other genes like *delta*, *ets1*, and *tbr* can also be tested.

Our experiments also show that equalizing cell division by transiently treating embryos with SDS prevents the activation of *alx1*, but does not effect the expression of *pmar1*. This finding, however, lacks a molecular explanation. Otx mRNA and protein is maternally provided, and at the 16-cell stage this protein selectively translocates into the nuclei of the micromeres (Chuang et al., 1996). In the remainder of the embryo, the protein is retained in the cytoplasm by a binding interaction with alpha-actinin (this interaction was confirmed by a yeast-two hybrid study) (Chuang et al. 1996). The transient translocation of Otx into nuclei of the micromeres at the 16-cell stage, and the presence of an Otx binding *cis*-regulatory module (TAATCT) upstream of the *alx1* transcriptional start site, in a region that when fused to GFP gives an expression pattern that correlates with the endogenous *alx1* expression (Information provided by Sagar Damle, Davidson Lab), makes Otx an interesting and testable target that might play a role in directly activating the early transcription factors of the skeletogenic GRN.

The work presented in Chapter 3 takes advantage of the rich knowledge of the skeletogenic GRN, together with our findings presented in Chapter 2 to further dissect and understand questions related to developmental plasticity or lineage reprogramming. Our results uncover several upstream differences in the deployment of the skeletogenic GRN during transfating; (i) MAPK signaling is required for activating this network during regulative development, whereas during normal development the network is activated by MAPK independent inputs, (ii) *Delta*, one of the early genes in the skeletogenic network, is not expressed in the transfating cells, (iii) *Alx1* and *tbr* are activated simultaneously during transfating, however in normal development the expression of *alx1* precedes that of *tbr*, and (iv) Unequal cell division (or cell division) does not play a role in activating the network during regulative development. The downstream architecture of the network, however, is precisely recapitulated.

In addition, we show that the subpopulation of NSM cells that transfate are the presumptive blastocoelar cells and not the presumptive pigment cells as previously believed, and the transfating response occurs remarkably quickly (~2 hpd). Finally, we show that during endoderm transfating the endodermal cells acquire a blastocoelar cell like fate before activating the skeletogenic GRN.

Based on our finding that the transfating response occurs rapidly and in the absence of cell division it is tempting to speculate that the PMCs and the blastocoelar cells share several regulatory gene modules, and what makes them different is the expression of a few transcription factors that are responsible for directing lineage specific differentiation, like *alx1* and *tbr* in the skeletogenic cells and *scl* in the blastocoelar cells. In support of this hypothesis, we find that the two regulatory genes *ets1* and *erg* (that were previously categorized as being expressed by the PMCs and the NSM) are expressed by the PMCs and the blastocoelar cells, but not by the pigment cells **(Appendix Fig. 2 and 3)**. Currently, we are expanding this study by analyzing the spatial expression of other downstream genes that are expressed by both the PMCs and the NSM, which includes the cytoskeletal regulators and ECM proteins.

The fact that blastocoelar cells activate the skeletogenic GRN only in the absence of PMCs, suggests that during normal development some inhibitory mechanisms are in place that restricts their skeletogenic fate. Also, as the transfated cells make a complete phenotypic switch and differentiate into "true" PMCs, as evident by the activation of downstream differentiation genes, this suggests that additional inhibitory mechanisms are established that are responsible for repressing the blastocoelar cell fate. Therefore, two key events can be envisioned in the process of transfating; (i) the removal of one inhibitory mechanism to enable that activation of the skeletogenic GRN in the blastocoelar cells, (ii) the establishment of an inhibitory mechanism that represses the blastocoelar cell fate. Unfortunately, nothing is known about the molecular nature of these mechanisms.

In a previous study, chimeric embryos were generated by recombining micromeres from *alx1* MO treated embryos, and the animal cap from control embryos treated with a lineage dye. These chimeric embryos were capable of forming a normally patterned skeleton as a result of transfating (Ettensohn et. al., 2007). This result suggests that in the absence of *alx1* the micromeres can no longer suppress the skeletogenic potential of the NSM. This result also raises the possibility that the signal that prevents the NSM from adopting a skeletogenic fate might be downstream of *alx1*. Therefore, in the future identifying all downstream targets of *alx1* (focusing on genes that are known signaling molecules) using whole genome microarrays, which are now available for the

sea urchin embryo, might help in identifying the suppressive signal from the PMCs to the NSM.

Furthermore, with more data emerging regarding the *cis*-regulatory modules (CRMs) that are responsible for activating and restricting the expression of genes, which are specifically expressed in the skeletogenic cell lineage, like *alx1* (Damle and Davidson, unpublished data) and *tbr* (Wahl et. al., 2010), it is now possible to dissect the differences in the regulation of these genes at the *cis*-regulatory level during normal and regulative development. The experimental design would be to express a GFP tagged-CRM reporter construct in PMC(-) embryos that mimics the spatial and temporal expression of the gene in question, followed by analyzing GFP expression in live embryos. GFP expression will be detected in the transfating NSM cells only if the same CRMs are required for activating the gene during regulative development.

In evolutionary terms, it has been postulated that unequal cleavage division that leads to the formation of micromeres and the Pmar1-mediated double repression system are recent inventions. In the living cidaroids, which are believed to closely resemble the ancestors of the modern sea urchins, the skeleton forms from a group of late ingressing mesenchyme cells. The activation of the skeletogenic GRN in the NSM cells during transfating can be considered as a reminiscent of the ancestral mode of forming the skeleton. This hypothesis can be tested directly by elucidating the skeletogenic GRN in the "primitive" sea urchin species *E. tribuloides* (see introduction), focusing specifically on the initial deployment of the network. If the hypothesis that transfating represents an ancient mode of skeletogenesis is correct, then the upstream skeletogenic GRN in *E. tribuloides* should closely resemble the regulative skeletogenic GRN presented in Fig. 3.13.

In the future, answers to these and other related questions will not only provide insights into the molecular underpinnings that regulate developmental plasticity, but will also contribute to a more general understanding of how cell lineages evolve.

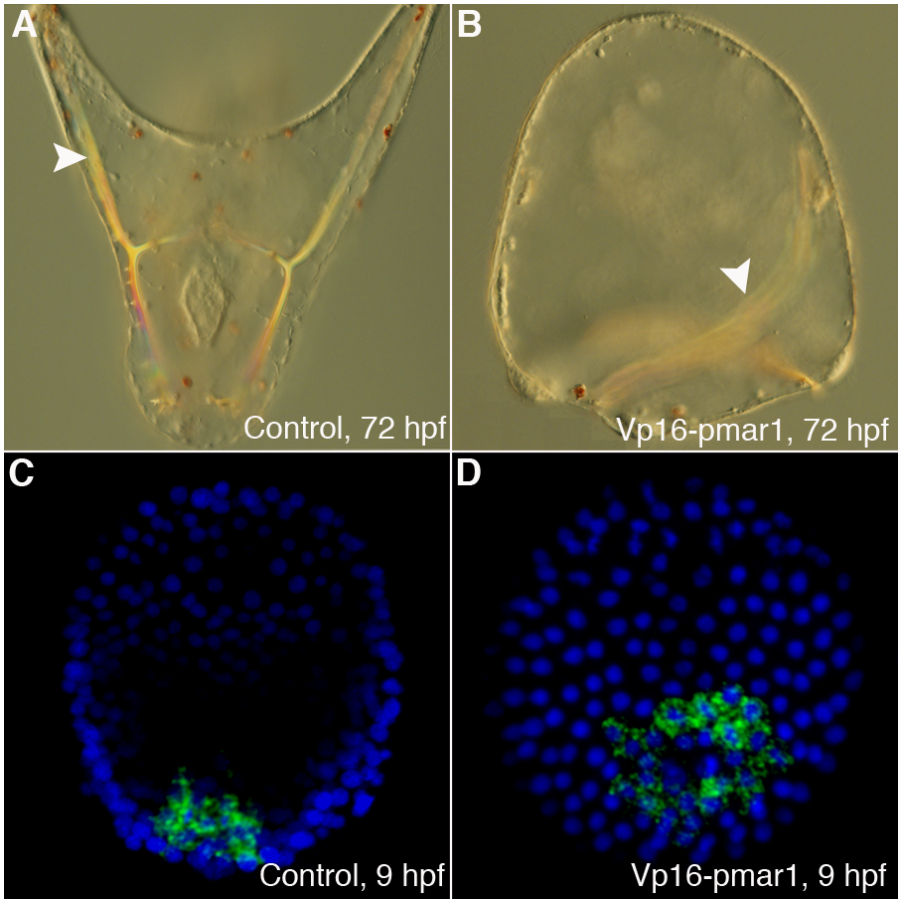

Appendix Fig. 1. (A) Control embryo, at 72 hpf. Arrowhead points to the skeleton. **(B)** Sibling Vp16-pmar1 overexpressing embryo at 72 hpf. Embryos overexpressing Vp16-Pmar1 do not gastrulate and lack correctly patterned skeletal elements, arrowhead in B. **(C, D)** Vp16-Pmar1 mRNA was injected at a concentration of 6 mg/ml and *alx1* expression was assayed 9 hpf. Both control (C) and Vp16-Pmar1 overexpressing embryos (D) show expression of *alx1*.

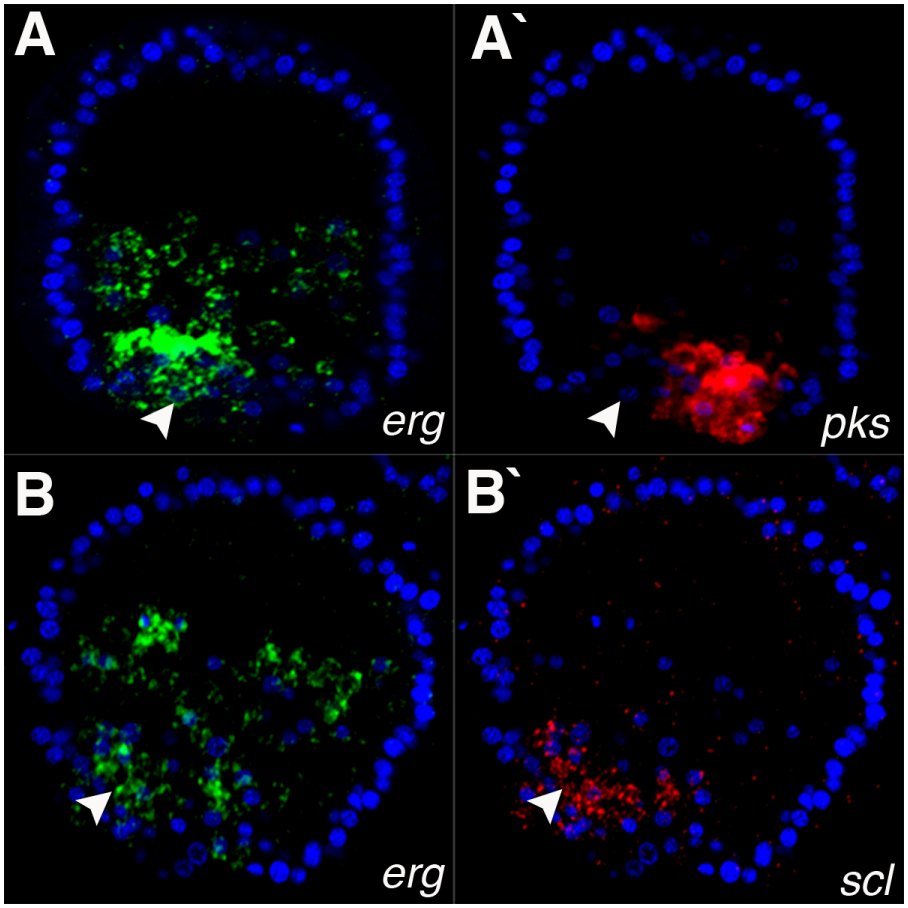

**Appendix Fig. 2. (A, A`)** A early gastrula stage embryo labeled with *erg* (green, A) and *pks* (red, A`). *Erg* is expressed in a subpopulation of NSM cells (arrowhead in A) and in the PMCs. *Pks* is expressed in the pigment cells on the opposite side of the vegetal plate. **(B, B`)** A early gastrula stage embryo labeled with *ets1* (green, B) and *scl* (red, B`). *Scl* is expressed in the presumptive blastocoelar cells and its expression overlaps with the expression of *erg* (arrowheads in B, B`).

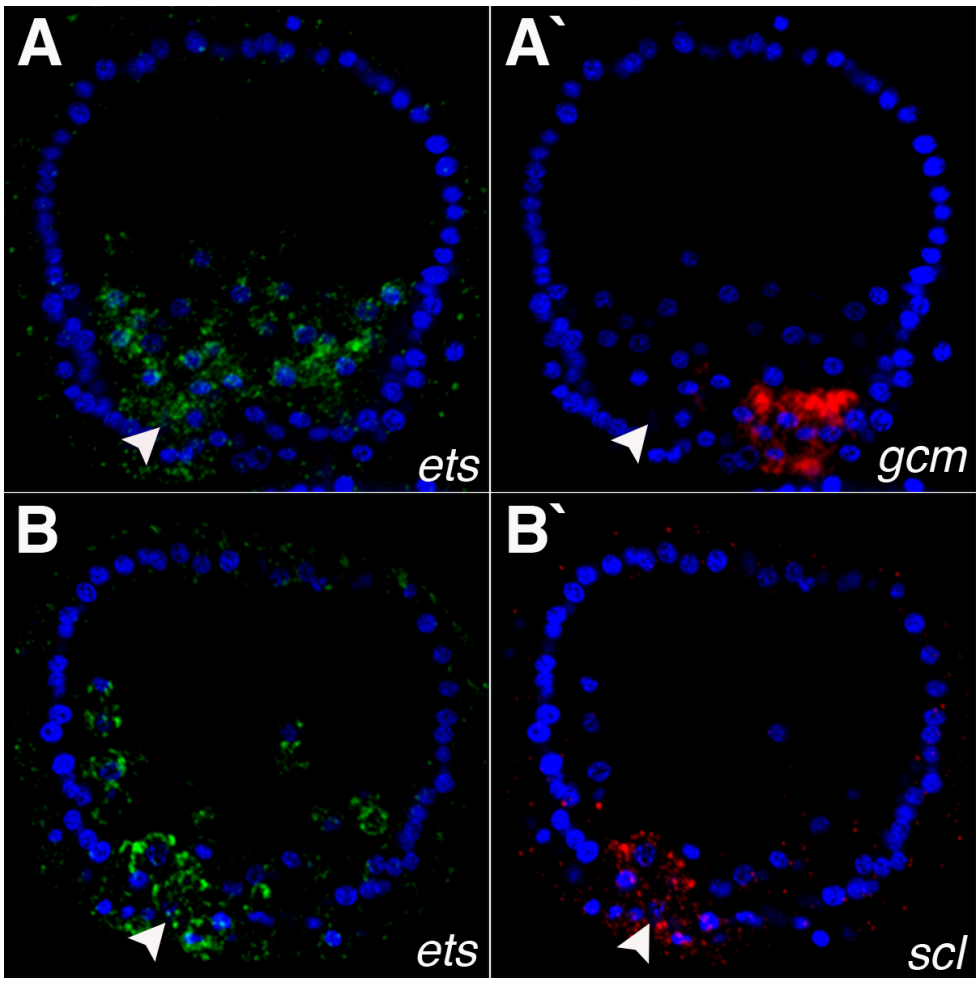

**Appendix Fig. 3. (A, A`)** A early gastrula stage embryo labeled with *ets1* (green, A) and *gcm* (red, A`). *Ets1* is expressed in a subpopulation of NSM cells (arrowhead in A) and in the PMCs. *Gcm* is expressed in the pigment cells on the opposite side of the vegetal plate. **(B, B`)** A early gastrula stage embryo labeled with *ets1* (green, B) and *scl* (red, B`). *Scl* is expressed in the presumptive blastocoelar cells and its expression overlaps with the expression of *ets1* (arrowheads in B, B`).

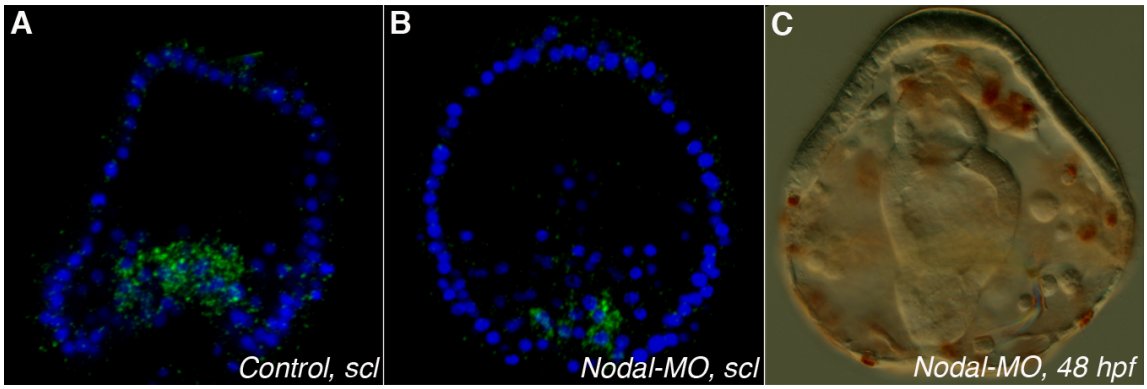

Appendix Fig. 4. Expression of *scl* is not completely abrogated in Nodal-MO injected embryos. (A, B) The expression of *scl* (green) in Nodal-MO injected embryos was analyzed by FWMISH when control embryos were at the early gastrula stage. Both control and Nodal-MO injected embryos show the expression of *scl* (in most Nodal-MO injected embryos the expression of *scl* was fainter in when compared to its expression in control embryos). **(C)** Phenotype of a Nodal-MO injected embryos at 48 hpf. These embryos have excess of pigment cells and do not form a skeleton. The nodal MO was injected at a concentration of 2 mM.

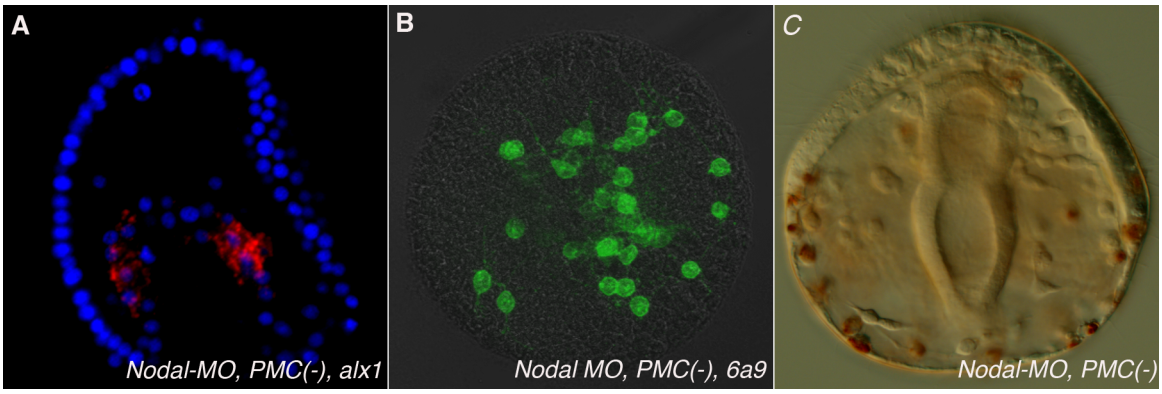

Appendix. Fig. 5. The disruption of Nodal signaling does not affect the activation of the skeletogenic GRN during transfating, but these embryos fail to form a skeleton. **(A, B)** PMC(-) nodal morphants examined for *alx1* expression at 2 hpd (A) and for the presence of 6a9-positive cells at 10 hpd (B). The expression of *alx1* and the 6a9 antigen are unaffected by Nodal knockdown. **(C)** Phenotype of a PMC(-) nodal morphant at 48 hours post PMC depletion. These embryos do not form a skeleton. The nodal MO was injected at a concentration of 2 mM.

Abbreviations

ECM	extracellular matrix
EdU	5-ethynyl-2-deoxyuridine
FWMISH	fluorescent whole mount in situ hybridization
GRN	gene regulatory network
Hpd	hours post depletion
Hpf	hours post fertilization
MAb	monoclonal antibody
MO	morpholino antisense oligonucleotide
NSM	non skeletogenic mesoderm
PBST	phosphate buffered saline containing Tween-20
PMC	primary mesenchyme cell
SDS	sodium dodecyl sulfate
WMISH	whole mount in situ hybridization

References

Adomako-Ankomah and Ettensohn. (2011). P58-A and P58-B: novel proteins that mediate skeletogenesis in the sea urchin embryo. *Dev. Biol.* (in submission).

Amore, G., Yavrouian, R. G., Peterson, K. J., Ransick, A., McClay, D. R. and Davidson, E. H. (2003). Spdeadringer, a sea urchin embryo gene required separately in skeletogenic and oral ectoderm gene regulatory networks. *Dev Biol* **261**, 55-81.

Angerer, L. M., Newman, L. A. and Angerer, R. C. (2005). SoxB1 downregulation in vegetal lineages of sea urchin embryos is achieved by both transcriptional repression and selective protein turnover. *Development* **132**, 999-1008.

Ben-Tabou de-Leon, S. and Davidson, E. H. (2009). Modeling the dynamics of transcriptional gene regulatory networks for animal development. *Dev Biol* **325**, 317-28.
Benson, S. C., Benson, N. C. and Wilt, F. (1986). The organic matrix of the skeletal spicule of sea urchin embryos. *J Cell Biol* **102**, 1878-86.

Bhutani, N,. Brady, J. J., Damian, M., Sacco, A., Corbel, S. Y., and Blau, H. M. (2010) Reprogramming towards pluripotency requires AID-dependent DNA demethylation. *Nature* **463**, 1042-7.

Calestani, C., Rast, J. P. and Davidson, E. H. (2003). Isolation of pigment cell specific genes in the sea urchin embryo by differential macroarray screening. *Development* **130**, 4587-96.

Cameron, R. A. and Davidson, E. H. (1991). Cell type specification during sea urchin development. *Trends Genet* **7**, 212-8.

Cheers, M. S. and Ettensohn, C. A. (2004). Rapid microinjection of fertilized eggs. *Methods Cell Biol* **74**, 287-310.

Cheers, M. S. and Ettensohn, C. A. (2005). P16 is an essential regulator of skeletogenesis in the sea urchin embryo. *Dev Biol* **283**, 384-96.

Chuang, C. K., Wikramanayake, A. H., Mao, C. A., Li, X. and Klein, W. H. (1996). Transient appearance of Strongylocentrotus purpuratus Otx in micromere nuclei: cytoplasmic retention of SpOtx possibly mediated through an alpha-actinin interaction. *Dev Genet* **19**, 231-7.

Croce, J., Lhomond, G., Lozano, J. C. and Gache, C. (2001). ske-T, a T-box gene expressed in the skeletogenic mesenchyme lineage of the sea urchin embryo. *Mech Dev* **107**, 159-62.

Croce, J. C. and McClay, D. R. (2010). Dynamics of Delta/Notch signaling on endomesoderm segregation in the sea urchin embryo. *Development* **137**, 83-91.

Dan, K. (1979). Studies on unequal cleavage in sea urchins. I. Migration of the nuclei to the vegetal pole. *Dev. Growth Differ.* **21**, 527-535.
Dan, K. and Tanaka, Y. (1990). Attachment of one spindle pole to the cortex in unequal cleavage. *Ann N Y Acad Sci* **582**, 108-19.

Dan K, Endo S, Uemura I (1983): Studies on unequal cleavage in sea urchins **11.** Surface differentiation **and** the direction of nuclear migration. Devel, Growth, Differ 25227-237.

Davidson, E. H. and Levine, M. S. (2008). Properties of developmental gene regulatory networks. *Proc Natl Acad Sci U S A* **105**, 20063-6.

Duboc, V., Lapraz, F., Saudemont, A., Bessodes, N., Mekpoh, F., Haillot, E., Quirin, M. and Lepage, T. (2010). Nodal and BMP2/4 pattern the mesoderm and endoderm during development of the sea urchin embryo. *Development* **137**, 223-35.

Duloquin, L., Lhomond, G. and Gache, C. (2007). Localized VEGF signaling from ectoderm to mesenchyme cells controls morphogenesis of the sea urchin embryo skeleton. *Development* **134**, 2293-302.

Egli D., Birkhoff, G. and Eggan, K. (2008). Mediators of reprogramming: transcription factors and transitions through mitosis. *Nat. Rev. Mol. Cell Biol.* **9**, 505-16.

Eilken, H. M., Nishikawa, S. and Schroeder, T. (2009). Continuous single-cell imaging of blood generation from haemogenic endothelium. *Nature* **457**, 896-900.

Erwin, D. H. and Davidson, E. H. (2009). The evolution of hierarchical gene regulatory networks. *Nat Rev Genet* **10**, 141-8.

Ettensohn, C. A. (1990). Cell interactions in the sea urchin embryo studied by fluorescence photoablation. *Science* **248**, 1115-8.

Ettensohn, C. A. (2006). The emergence of pattern in embryogenesis: regulation of beta-catenin localization during early sea urchin development. *Sci STKE* **2006**, pe48.

Ettensohn, C. A. (2009). Lessons from a gene regulatory network: echinoderm skeletogenesis provides insights into evolution, plasticity and morphogenesis. *Development* **136**, 11-21.

Ettensohn, C. A., Illies, M. R., Oliveri, P. and De Jong, D. L. (2003). Alx1, a member of the Cart1/Alx3/Alx4 subfamily of Paired-class homeodomain proteins, is an essential component of the gene network controlling skeletogenic fate specification in the sea urchin embryo. *Development* **130**, 2917-28.

Ettensohn, C. A., Kitazawa, C., Cheers, M. S., Leonard, J. D. and Sharma, T. (2007). Gene regulatory networks and developmental plasticity in the early sea urchin

embryo: alternative deployment of the skeletogenic gene regulatory network. *Development* **134**, 3077-87.
Ettensohn, C. A. and McClay, D. R. (1986). The regulation of primary mesenchyme cell migration in the sea urchin embryo: transplantations of cells and latex beads. *Dev Biol* **117**, 380-91.

Ettensohn, C. A. and McClay, D. R. (1988). Cell lineage conversion in the sea urchin embryo. *Dev Biol* **125**, 396-409.

Fuchikami, T., Mitsunaga-Nakatsubo, K., Amemiya, S., Hosomi, T., Watanabe, T., Kurokawa, D., Kataoka, M., Harada, Y., Satoh, N., Kusunoki, S. et al. (2002). T-brain homologue (HpTb) is involved in the archenteron induction signals of micromere descendant cells in the sea urchin embryo. *Development* **129**, 5205-16.

Gao, F. and Davidson, E. H. (2008). Transfer of a large gene regulatory apparatus to a new developmental address in echinoid evolution. *Proc Natl Acad Sci U S A* **105**, 6091-6.

Gibson, A. W. and Burke, R. D. (1985). The origin of pigment cells in embryos of the sea urchin Strongylocentrotus purpuratus. *Dev Biol* **107**, 414-9.

Gustafson, T. and Wolpert, L. (1967). Cellular movement and contact in sea urchin morphogenesis. *Biol Rev Camb Philos Soc* **42**, 442-98.

Hadorn, E. (1968). Transdetermination in cells. *Sci Am* **219**, 110-4 passim.

Hörstadius, S. (1939). The mechanics of sea urchin development studied by operative methods. *Biol. Rev.* **14**, 132-179.

Juliano, C. E., Voronina, E., Stack, C., Aldrich, M., Cameron, A. R. and Wessel, G. M. (2006). Germ line determinants are not localized early in sea urchin development, but do accumulate in the small micromere lineage. *Dev Biol* **300**, 406-15.

Kitamura, K., Nishimura, Y., Kubotera, N., Higuchi, Y. and Yamaguchi, M. (2002). Transient activation of the micro1 homeobox gene family in the sea urchin (Hemicentrotus pulcherrimus) micromere. *Dev Genes Evol* **212**, 1-10.

Koide, T., Hayata, T. and Cho, K. W. (2005). Xenopus as a model system to study transcriptional regulatory networks. *Proc Natl Acad Sci U S A* **102**, 4943-8.

Kurokawa, D., Kitajima, T., Mitsunaga-Nakatsubo, K., Amemiya, S., Shimada, H. and Akasaka, K. (1999). HpEts, an ets-related transcription factor implicated in primary mesenchyme cell differentiation in the sea urchin embryo. *Mech Dev* **80**, 41-52.

Kurokawa, D., Kitajima, T., Mitsunaga-Nakatsubo, K., Amemiya, S., Shimada, H. and Akasaka, K. (2000). HpEts implicated in primary mesenchyme cell differentiation of the sea urchin (Hemicentrotus pulcherrimus) embryo. *Zygote* **8 Suppl 1**, S33-4.

Langelan, R. E. and Whiteley, A. H. (1985). Unequal cleavage and the differentiation of echinoid primary mesenchyme. *Dev Biol* **109**, 464-75.

Livingston, B.T. and Wilt, F.H., 1989. Lithium evokes expression of vegetal-specific molecules in the animal blastomeres of sea urchin embryos. *Proc. Natl. Acad. Sci.* **86**, pp. 3669–3673.

Logan, C. Y., Miller, J. R., Ferkowicz, M. J. and McClay, D. R. (1999). Nuclear beta-catenin is required to specify vegetal cell fates in the sea urchin embryo. *Development* **126**, 345-57.

Maduro, M. F. (2009). Structure and evolution of the C. elegans embryonic endomesoderm network. *Biochim Biophys Acta* **1789**, 250-60.

Maves, L. and Schubiger, G. (1995). Wingless induces transdetermination in developing Drosophila imaginal discs. *Development* **121**, 1263-72.

McClay, D. R. and Logan, C. Y. (1996). Regulative capacity of the archenteron during gastrulation in the sea urchin. *Development* **122**, 607-16.

Minokawa, T., Hamaguchi, Y. and Amemiya, S. (1997). Skeletogenic potential of induced secondary mesenchyme cells derived from the presumptive ectoderm in echinoid embryos. *Dev. Genes Evol.* **206**, 472-476.

Minokawa, T., Rast, J. P., Arenas-Mena, C., Franco, C. B. and Davidson, E. H. (2004). Expression patterns of four different regulatory genes that function during sea urchin development. *Gene Expr Patterns* **4**, 449-56.

Morley, R. H., Lachani, K., Keefe, D., Gilchrist, M. J., Flicek, P., Smith, J. C. and Wardle, F. C. (2009). A gene regulatory network directed by zebrafish No tail accounts for its roles in mesoderm formation. *Proc Natl Acad Sci U S A* **106**, 3829-34.

Nakamura, A. and Seydoux, G. (2008). Less is more: specification of the germline by transcriptional repression. *Development* **135**, 3817-27.

Nishimura, Y., Sato, T., Morita, Y., Yamazaki, A., Akasaka, K. and Yamaguchi, M. (2004). Structure, regulation, and function of micro1 in the sea urchin *Hemicentrotus pulcherrimus*. *Dev. Genes Evol*. **214**, 525-536.

Yamazaki, A., Kawabata, R., Shiomi, K., Amemiya, S., Sawaguchi, M., Mitsunaga-Nakatsubo, K. and Yamaguchi, M. (2005). The micro1 gene is necessary and sufficient for micromere differentiation and mid/hindgut-inducing activity in the sea urchin embryo. *Dev. Genes Evol.* **215**, 450-459.

Yamazaki, A., Ki, S., Kokubo, T. and Yamaguchi, M. (2009). Structure-function

correlation of micro1 for micromere specification in sea urchin embryos. *Mech. Dev.* **126**, 611-623.

Ochiai, H., Sakamoto, N., Momiyama, A., Akasaka, K. and Yamamoto, T. (2008). Analysis of cis-regulatory elements controlling spatio-temporal expression of T-brain gene in sea urchin, Hemicentrotus pulcherrimus. *Mech Dev* **125**, 2-17.

Okazaki, K (1975). Normal development to metamorphosis. In "the sea urchin embryo. Biochemistry and Morphogenesis" (G. Czihak, Ed.) pp. 177-232. Springer-Verlag, New York.

Oliveri, P., Carrick, D. M. and Davidson, E. H. (2002). A regulatory gene network that directs micromere specification in the sea urchin embryo. *Dev Biol* **246**, 209-28.

Oliveri, P. and Davidson, E. H. (2004). Gene regulatory network analysis in sea urchin embryos. *Methods Cell Biol* **74**, 775-94.

Oliveri, P., Davidson, E. H. and McClay, D. R. (2003). Activation of pmar1 controls specification of micromeres in the sea urchin embryo. *Dev Biol* **258**, 32-43.

Oliveri, P., Tu, Q. and Davidson, E. H. (2008). Global regulatory logic for specification of an embryonic cell lineage. *Proc Natl Acad Sci U S A* **105**, 5955-62.

Pehrson, J. R. and Cohen, L. H. (1986). The fate of the small micromeres in sea urchin development. *Dev Biol* **113**, 522-6.

Range, R. C., Glenn, T. D., Miranda, E. and McClay, D. R. (2008). LvNumb works synergistically with Notch signaling to specify non-skeletal mesoderm cells in the sea urchin embryo. *Development* **135**, 2445-54.

Ransick, A. and Davidson, E. H. (1993). A complete second gut induced by transplanted micromeres in the sea urchin embryo. *Science* **259**, 1134-8.

Reddy, K. L., Zullo, J. M., Bertolino, E. and Singh, H. (2008) Transcriptional repression mediated by repositioning of genes to the nuclear lamina. *Nature* **452**, 243-7.

Revilla-i-Domingo, R., Minokawa, T. and Davidson, E. H. (2004). R11: a cis-regulatory node of the sea urchin embryo gene network that controls early expression of SpDelta in micromeres. *Dev Biol* **274**, 438-51.

Revilla-i-Domingo, R., Oliveri, P. and Davidson, E. H. (2007). A missing link in the sea urchin embryo gene regulatory network: hesC and the double-negative specification of micromeres. *Proc Natl Acad Sci U S A* **104**, 12383-8.

Rizzo, F., Fernandez-Serra, M., Squarzoni, P., Archimandritis, A. and Arnone, M. I. (2006). Identification and developmental expression of the ets gene family in the sea urchin (Strongylocentrotus purpuratus). *Dev Biol* **300**, 35-48.

Rottinger, E., Besnardeau, L. and Lepage, T. (2004). A Raf/MEK/ERK signaling pathway is required for development of the sea urchin embryo micromere lineage through phosphorylation of the transcription factor Ets. *Development* **131**, 1075-87.

Rottinger, E., Saudemont, A., Duboc, V., Besnardeau, L., McClay, D. and Lepage, T. (2008). FGF signals guide migration of mesenchymal cells, control skeletal morphogenesis [corrected] and regulate gastrulation during sea urchin development. *Development* **135**, 353-65.

Ruffins, S. W. and Ettensohn, C. A. (1996). A fate map of the vegetal plate of the sea urchin (Lytechinus variegatus) mesenchyme blastula. *Development* **122**, 253-63.

Ruiz, S., Panopoulos, A. D., Herrerías, A., Bissig, K. D., Lutz, M., Berggren, W. T., Verma, I. M. and Izpisua Belmonte, J. C. (2011). A high proliferation rate is required for cell reprogramming and maintenance of human embryonic stem cell identity. *Curr. Biol.* **11**, 45-52.

Sadowski, I., Ma, J., Triezenberg, S. and Ptashne, M. (1988). GAL4-VP16 is an unusually potent transcriptional activator. *Nature* **335**, 563-4.

Schroeder, T. E. (1981). The origin of cleavage forces in dividing eggs. A mechanism in two steps. *Exp Cell Res* **134**, 231-40.

Service, M. and Wardlaw, A.C. (1984). Echinochrome-A as a bactericidal substance in the coelomic fluid of Echinus esculentus (L.). *Comp. Biochem. Physiol.* **79B**: 161 – 165.

Sharma, T. and Ettensohn, C. A. (2010). Activation of the skeletogenic gene regulatory network in the early sea urchin embryo. *Development* **137**, 1149-57.

Sherwood, D. R. and McClay, D. R. (1999). LvNotch signaling mediates secondary mesenchyme specification in the sea urchin embryo. *Development* **126**, 1703-13.

Smith, J. and Davidson, E. H. (2008a). A new method, using cis-regulatory control, for blocking embryonic gene expression. *Dev Biol* **318**, 360-5.

Smith, J. and Davidson, E. H. (2008b). Gene regulatory network subcircuit controlling a dynamic spatial pattern of signaling in the sea urchin embryo. *Proc Natl Acad Sci U S A* **105**, 20089-94.

Smith, Z. D., Nachman, I., Regev, A., and Meissner, A. (2010) Dynamic single-cell imaging of direct reprogramming reveals an early specifying event. *Nat. Biotechnol*. **28**, 521-6.

Stathopoulos, A. and Levine, M. (2005). Genomic regulatory networks and animal development. *Dev Cell* **9**, 449-62.

Sweet, H. C., Gehring, M. and Ettensohn, C. A. (2002). LvDelta is a mesoderm-inducing signal in the sea urchin embryo and can endow blastomeres with organizer-like properties. *Development* **129**, 1945-55.

Tadros, W. and Lipshitz, H. D. (2009). The maternal-to-zygotic transition: a play in two acts. *Development* **136**, 3033-42.

Takahashi, K. and Yamanaka, S. (2006). Induction of pluripotent stem cells from mouse embryonic and adult fibroblast cultures by defined factors. *Cell* **126**, 663-76.

Tanaka, Y. (1976). Effects of surfactants on the cleavage and further development of the sea urchin embryo. I. The inhibition of micromere formation at the fourth cleavage. *Dev. Growth Differ.* **18**, 113-122.

Tanaka, Y. (1979). Effects of surfactants on the cleavage and further development of the sea urchin embryo. II. Disturbance in the arrangement of cortical vesicles and change in cortical appearance. *Dev. Growth Differ.* **21**, 331-342.

Tamboline, C. R. and Burke, R. D. (1992). Secondary mesenchyme of the sea urchin embryo: ontogeny of blastocoelar cells. *J Exp Zool* **262**, 51-60.

Tominaga, H., Nakamura, S. and KImatsu, M. (2004). Reproduction and development of the conspicuously dimorphic brittle star *Ophiodaphne formata* (Ophiuroidea). *Biol. Bull.* **206**, 25-34.

Triezenberg, S. J., Kingsbury, R. C. and McKnight, S. L. (1988). Functional dissection of VP16, the trans-activator of herpes simplex virus immediate early gene expression. *Genes Dev* **2**, 718-29.

Tsonis, P. A., Madhavan, M., Tancous, E. E. and Del Rio-Tsonis, K. (2004). A newt's eye view of lens regeneration. *Int J Dev Biol* **48**, 975-80.

Tu, Q., Brown, C. T., Davidson, E. H. and Oliveri, P. (2006). Sea urchin Forkhead gene family: phylogeny and embryonic expression. *Dev Biol* **300**, 49-62.

Voronina, E., Lopez, M., Juliano, C. E., Gustafson, E., Song, J. L., Extavour, C., George, S., Oliveri, P., McClay, D. and Wessel, G. (2008). Vasa protein expression is restricted to the small micromeres of the sea urchin, but is inducible in other lineages early in development. *Dev Biol* **314**, 276-86.

Wahl, M. E., Hahn, J., Gora, K., Davidson, E. H. and Oliveri, P. (2009). The cis-regulatory system of the tbrain gene: Alternative use of multiple modules to promote skeletogenic expression in the sea urchin embryo. *Dev Biol* **335**, 428-41.

Weber, W. and Dambach, M. (1974). Light-sensitivity of isolated pigment cells of the sea urchin Centrostephanus longispinus. *Cell Tissue Res* **148**, 437-40.

Weitzel, H. E., Illies, M. R., Byrum, C. A., Xu, R., Wikramanayake, A. H. and Ettensohn, C. A. (2004). Differential stability of beta-catenin along the animal-vegetal axis of the sea urchin embryo mediated by dishevelled. *Development* **131**, 2947-56.

Wikramanayake, A. H., Huang, L. and Klein, W. H. (1998). beta-Catenin is essential for patterning the maternally specified animal-vegetal axis in the sea urchin embryo. *Proc Natl Acad Sci U S A* **95**, 9343-8.

Wolff, G., 1985. Die regeneration der urodelenlines. Wilhelm Roux's Arch. Entw. Mech. Org. **1**, 380–390.

Wu, S. Y. and McClay, D. R. (2007). The Snail repressor is required for PMC ingression in the sea urchin embryo. *Development* **134**, 1061-70.

Yajima, M. and Wessel, G. M. (2011). Small micromeres contribute to the germline in the sea urchin. *Development* **138**, 237-43.

Yamada, T. and McDevitt, D. S. (1984). Conversion of iris epithelial cells as a model of differentiation control. *Differentiation* **27**, 1-12.

Yamazaki, A., Kawabata, R., Shiomi, K., Amemiya, S., Sawaguchi, M., Mitsunaga-Nakatsubo, K. and Yamaguchi, M. (2005). The micro1 gene is necessary and sufficient for micromere differentiation and mid/hindgut-inducing activity in the sea urchin embryo. *Dev Genes Evol* **215**, 450-59.

Yamazaki, A., Ki, S., Kokubo, T. and Yamaguchi, M. (2009). Structure-function correlation of micro1 for micromere specification in sea urchin embryos. *Mech Dev* **126**, 611-23.

Zhou, Q., Brown, J., Kanarek, A., Rajagopal, J. and Melton, D. A. (2008). In vivo reprogramming of adult pancreatic exocrine cells to beta-cells. *Nature* **455**, 627-32.